

REACTION DYNAMICS OF IRIDIUM BROMIDE COMPLEXES  
IN AQUEOUS SOLUTION

BY  
CRAIG M. HOAG

A DISSERTATION PRESENTED TO THE GRADUATE SCHOOL  
OF THE UNIVERSITY OF FLORIDA IN PARTIAL FULFILLMENT  
OF THE REQUIREMENTS FOR THE DEGREE OF  
DOCTOR OF PHILOSOPHY

UNIVERSITY OF FLORIDA

2000

## ACKNOWLEDGMENTS

The author would like to express his thanks to Dr. Robert J. Hanrahan for his advisement and for taking the time to make this endeavor possible. Thanks also go to Dr. M. Louis Muga, Dr. Basha Muga, and Mr. Larry L. Land for their continued friendship, and to Dr. Paul Chun for his help and for the use of his stopped-flow apparatus. The author would also like to express special thanks to his wife for her continued support and help during the time this work was completed.

## TABLE OF CONTENTS

	<u>page</u>
ACKNOWLEDGMENTS.....	ii
ABSTRACT .....	vi
INTRODUCTION .....	1
The Hexachloroiridate (III)/Hexachloroiridate (IV) System .....	1
The Analogous Hexabromoiridate (III)/Hexabromoiridate (IV) System ....	5
Mechanism for Pulse Radiolysis of $\text{IrBr}_6^{3-}$ in the Presence of $\text{Br}^-$ Ion .....	7
THE PULSE RADIOLYSIS METHOD .....	15
Pulse Radiolysis of Aqueous Solutions .....	15
The Febetron 706.....	20
Detection System.....	22
Light Sources .....	22
Xenon-arc Lamp .....	23
He-Ne Laser .....	23
Monochromator.....	24
Photo-Multiplier Tube.....	24
Computer Data-Acquisition System.....	25
Sample Cell and Reservoir.....	27
Applications of Pulse Radiolysis to Aqueous Solutions .....	31
Pulse Radiolysis of Aqueous Solution .....	31
Creating Totally Oxidizing or Totally Reducing Conditions .....	37
Totally oxidizing conditions.....	38
Totally reducing conditions.....	39
STOPPED-FLOW APPARATUS .....	40
Flow System.....	41
Measuring System .....	44
Data Acquisition System.....	44
Operation of the Computerized Durrum Stopped-Flow System .....	49

STABILITY OF AQUEOUS HEXABROMOIRIDATE .....	54
Chemical Dynamics of Solutions Containing $\text{Br}_2$ , $\text{Br}^-$ and $\text{IrBr}_6^{3-}$ .....	58
Solutions of $\text{Br}_2$ and $\text{Br}^-$ .....	58
Solutions of $\text{Br}_2$ , $\text{Br}^-$ , and $\text{IrBr}_6^{3-}$ .....	60
Experimental .....	64
Procedure One: Prompt Addition of $\text{Br}_2$ .....	68
Procedure Two: Delayed Addition of $\text{Br}_2$ .....	68
Procedure Three: Double-Delay Experiments .....	69
Results and Calculations .....	69
Procedure One: Prompt Addition of $\text{Br}_2$ .....	69
Procedure Two: Delayed Addition of $\text{Br}_2$ .....	79
Procedure Three: Double-Delay Experiments .....	85
REACTION OF HEXABROMOIRIDATE WITH OH RADICAL: ALTERNATIVE METHOD FOR COMPETITION KINETICS .....	93
Experimental .....	94
Results and Calculations .....	95
Reaction of OH Radical with $\text{IrBr}_6^{3-}$ : the Standard Competition Method .....	95
Reaction of OH Radical with $\text{IrBr}_6^{3-}$ : the Alternate Competition Method .....	99
REDUCTION OF HEXABROMOIRIDATE (IV) BY AQUEOUS ELECTRON .....	117
Experimental .....	118
Results and Calculations .....	120
STOPPED-FLOW INVESTIGATION OF REACTION OF HEXABROMOIRIDATE WITH BROMINE .....	134
Experimental .....	134
Results and Calculations .....	135
STOPPED-FLOW STUDIES OF THE REACTION OF AQUOPENTABROMOIRIDATE (III) WITH BROMINE .....	139
Experimental .....	139
Results and Calculations .....	141
CONCLUSION .....	149
APPENDIX A COMPUTER PROGRAM TO OPERATE THE STOPPED-FLOW APPARATUS COMPUTERIZED DATA- ACQUISITION SYSTEM .....	153

APPENDIX B	COMPUTER PROGRAM TO CALCULATE CONCENTRATIONS OF PRINCIPLE SPECIES PRODUCED DURING IRRADIATION OF WATER .....	173
BIBLIOGRAPHY .....		175
BIOGRAPHICAL SKETCH .....		182

Abstract of Thesis Presented to the Graduate School  
of the University of Florida in Partial Fulfillment of the  
Requirements for the Degree of Doctor of Philosophy

REACTION DYNAMICS OF IRIIDIUM BROMIDE COMPLEXES  
IN AQUEOUS SOLUTION

BY

CRAIG M. HOAG

August, 2000

Chair: Robert J. Hanrahan  
Major Department: Chemistry

A spectrophotometric study of aqueous solutions of  $\text{IrBr}_6^{3-}$  showed that  $\text{IrBr}_6^{3-}$  converts to  $\text{IrBr}_5\text{H}_2\text{O}^{2-}$  upon standing, and that  $\text{IrBr}_6^{3-}$  is also unstable when dissolved in aqueous 25 mM NaBr solution. The spectra taken periodically over time immediately after conversion of the iridium (III) complexes to the (IV) oxidation state changes from the three sharp peaks of  $\text{IrBr}_6^{2-}$  to a single broad peak characteristic of  $\text{IrBr}_5\text{H}_2\text{O}^-$ . The species  $\text{IrBr}_6^{3-}$  converted to  $\text{IrBr}_5\text{H}_2\text{O}^{2-}$  with a half-life consistent with the literature value of 19 minutes.

An alternate competition kinetic method was used to determine the rate constant for reaction of  $\text{IrBr}_6^{3-}$  with OH radical. The rate constant for the reaction of  $\text{IrBr}_6^{3-}$  with OH radical was determined to be  $2.8 \times 10^9 \text{ M}^{-1} \text{ s}^{-1}$ , assuming 50% conversion of  $\text{IrBr}_6^{3-}$  to  $\text{IrBr}_5\text{H}_2\text{O}^{2-}$ . Also, using the standard competition method, the rate constant was measured as  $2.6 \times 10^9 \text{ M}^{-1} \text{ s}^{-1}$ , based on the assumption of 50% conversion to  $\text{IrBr}_5\text{H}_2\text{O}^{2-}$ .

A mechanism for the pulse radiolysis of aqueous solutions of  $\text{IrBr}_6^{2-}$  was investigated using a Gear integrator. From computations of reactant and product concentrations, the simulated change in the absorbance at 634 nm over time was computed and compared to experimental measurements.

A stopped-flow apparatus was used to measure the rate of reaction  $\text{IrBr}_6^{3-}$  with  $\text{Br}_2$ . Using second order kinetics, it was found to be  $3.11 \times 10^6 \text{ M}^{-1} \text{ s}^{-1}$ .

The stopped-flow apparatus was used to study the reaction of  $\text{Br}_2$  with  $\text{IrBr}_5\text{H}_2\text{O}^{2-}$ ; both forward and reverse rate constants were determined by kinetic simulation using a Gear integrator. The values determined were  $k_{\text{forward}} = 4.1 \times 10^3 \text{ M}^{-1} \text{ s}^{-1}$  and  $k_{\text{reverse}} = 2.0 \times 10^7 \text{ M}^{-1} \text{ s}^{-1}$

## CHAPTER ONE INTRODUCTION

One of the central themes of study in the University of Florida Radiation Chemistry Laboratory is the study of solar energy. Some of the earlier work that was done in this laboratory was related to a method for the solar-assisted production of  $\text{H}_2$  and  $\text{Cl}_2$  in the presence of hexachloroiridate (III),  $\text{IrCl}_6^{3-}$ , and hexachloroiridate (IV),  $\text{IrCl}_6^{2-}$ . When the experiments on  $\text{IrCl}_6^{3-}$  and  $\text{IrCl}_6^{2-}$  were being carried out, it was thought that if the system was efficient, power utility companies would be able to use the method for the purpose of load leveling. Energy could be produced and stored during periods of low energy demand to be used later when demand exceeded the production capabilities of the utility companies. While studying the hexachloroiridate (III)/(IV) system, we began to look at the analogous hexabromoiridate (III)/(IV) system as an alternative and possibly more efficient system.

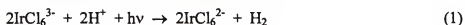
### **The Hexachloroiridate (III)/Hexachloroiridate (IV) System**

Harry B. Gray and his group studied the chemistry of iridium halide complexes and suggested that they could be used in solar photochemical systems [1, 2]. They proposed a system that was designed to produce hydrogen and chlorine from aqueous solution which also contained  $\text{HCl}$  and a small amount of dissolved  $\text{IrCl}_6^{3-}/\text{IrCl}_6^{2-}$ . In their studies of  $\text{IrCl}_6^{3-}$  in aqueous 12 M  $\text{HCl}$  solutions, production of  $\text{H}_2$  and  $\text{IrCl}_6^{2-}$  was

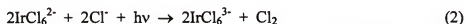


investigated when the solutions were irradiated with light at wavelengths of 254 nm. Irradiation at 313 nm and at 366 nm was also studied. But, the yield at 366 nm was essentially zero and the yield at 313 nm was negligible compared to the yield at 254 nm. Although the reaction proceeded negligibly at 313 nm and 366 nm, light at 254 nm caused a yield sufficient to warrant further study. They also found that  $\text{IrCl}_6^{2-}$  in aqueous 6 M HCl solution could be reduced photochemically to  $\text{IrCl}_6^{3-}$  when subjected to light of various specific wavelengths. Again, the wavelength that resulted in the highest yield was 254 nm, but the degree of difference of yield for the reduction reaction as a function of wavelength was not as striking as in the case of  $\text{H}_2$  yield. The quantum yields as a function of wavelength at 254 nm, 313 nm, 366nm, 420 nm and 488 nm were, respectively, 0.128, 0.107, 0.090, 0.0159, and 0.00361.

Dissolved chlorine gas was also a product of the reaction. They suggested that if the system could be made efficient enough, a substantial amount of chemical energy could be stored with a system using  $\text{IrCl}_6^{3-}$  and  $\text{IrCl}_6^{2-}$  in aqueous HCl solutions subjected to sunlight. The relevant reactions are as follows:



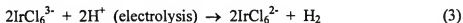
and



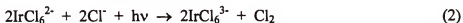
The problem with this system is that light of the wavelength necessary to drive Reaction (1) is essentially absent in the spectrum of sunlight at the surface of the earth, while light of the wavelength necessary to drive the second reaction is poorly represented in the solar spectrum.

Several studies were done in this laboratory that involved the second reaction of the system studied by Gray. The system investigated in this laboratory involved replacement of the first step of the system by an electrolysis step for the production of hydrogen gas [3-6]. In the new system as in the system studied by Gray, hexachloroiridate (IV) was reduced to hexachloroiridate (III) in a solution of hydrochloric acid during the solar-assisted reaction wherein chlorine gas was formed. As noted earlier, the best yield was produced when the system was exposed to light below about 400 nm. However, there was still a considerable yield at 420 nm. Although the solar flux at 420 nm is low, the reaction was driven by sunlight with moderate efficiency.

The second part of the system studied in this laboratory consisted of the electrolysis of hydrochloric acid solution to form hydrogen gas in the presence of hexachloroiridate (III), Reaction (3).



In this electrolysis step,  $\text{H}^+$  was converted to  $\text{H}_2$  gas from a solution of  $\text{HCl}$  with dissolved  $\text{IrCl}_6^{3-}$ . The conversion of  $\text{H}^+$  to  $\text{H}_2$  gas in this system required a lower voltage than the electrolysis of  $\text{HCl}$  solution with no dissolved  $\text{IrCl}_6^{3-}$ . As noted,  $\text{H}_2$  was produced in the electrolysis step while  $\text{Cl}_2$  was produced in the subsequent photolysis step, Reaction (2), as studied by Gray.



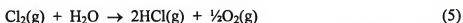
Reaction (4) represents the net reaction for the photolysis step and the electrolysis step.



The system as studied by Gray involved only the formation of  $\text{H}_2$  and  $\text{Cl}_2$ . At the University of Florida, the work was extended to consider systems based on the combined

electrochemical/photochemical decomposition of HCl. One type of system involved the recombination of H<sub>2</sub> and Cl<sub>2</sub> in a fuel cell, producing energy and reforming HCl. This essentially constitutes a cyclic process for energy storage in which HCl is dissociated in a combined electrolysis/photolysis step and recombined in a fuel cell in the production of electrochemical energy.

The second process studied at the University of Florida was designed for the net production of H<sub>2</sub>, a valuable industrial fuel. In this method, Cl<sub>2</sub> was reacted with steam either in a thermo or a photothermo process at moderately high temperature (approximately 600 °C) [7], Reaction (5).



This is the reverse of the Deacon Reaction, a well-known industrial process for the production of Cl<sub>2</sub> by oxidation of HCl, which occurs at about 450 °C.

In the presence of sunlight, it was determined that the "Reverse Deacon Reaction" was assisted by the photo-dissociation of Cl<sub>2</sub>, Reaction (6).



The chlorine atom then reacts with H<sub>2</sub>O to give HCl, Reaction (7).



Several additional mechanistic steps of the process are not listed here. The net effect of the photo-assisted Reverse Deacon Process is the conversion of Cl<sub>2</sub> and H<sub>2</sub>O to HCl and O<sub>2</sub>, Reaction (5). Combination of the Reverse Deacon Reaction with the photochemical/electrochemical decomposition of aqueous HCl solution provides for a cyclic process giving net production of H<sub>2</sub> and O<sub>2</sub>.

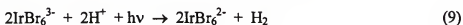
The complete cyclic process as described includes the reduction of  $\text{IrCl}_6^{2-}$  in the presence of HCl and sunlight to produce  $\text{Cl}_2$ , electrolysis of HCl solution in the presence of  $\text{IrCl}_6^{3-}$  to produce  $\text{H}_2$  plus  $\text{IrCl}_6^{2-}$ , and the Reverse Deacon Process to recycle  $\text{Cl}_2$  gas to HCl, is represented by Reaction (8).



Overall, this process is more practical than the method mentioned by Gray and his group for several reasons. Although the process is only partially driven by solar energy it is feasible because the wavelength necessary to drive the reactions is represented in the solar spectrum. Less electricity is required for the formation of  $\text{H}_2$  in this system than is required for the formation of  $\text{H}_2$  from sulfuric acid solution alone (the process presently used to produce  $\text{H}_2$ ). Combined with an  $\text{H}_2$ - $\text{Cl}_2$  fuel cell, the first part of the cycle, which results in the production of  $\text{H}_2$  and  $\text{Cl}_2$ , could be used for energy storage, as described. The Reverse Deacon Reaction part of the process could be used as needed, depending on the demand and commercial sales value of hydrogen.

### **The Analogous Hexabromoiridate (III)/Hexabromoiridate (IV) System**

Gray and his coworkers suggested that the production of  $\text{H}_2$  and  $\text{Br}_2$  in the related  $\text{IrBr}_6^{3-}/\text{IrBr}_6^{2-}$  system could occur with a greater efficiency than the production of  $\text{H}_2$  and  $\text{Cl}_2$  in the  $\text{IrCl}_6^{3-}/\text{IrCl}_6^{2-}$  system. They suggested that, because the ligand-to-metal charge transfer transitions for  $\text{IrBr}_6^{3-}/\text{IrBr}_6^{2-}$  complexes fall at lower energies than they do for the analogous chloride system, solutions of  $\text{IrBr}_6^{3-}$  exposed to sunlight could produce hydrogen at a wavelength well above 254 nm, Reaction (9).



The conversion should occur, they argued, in the 300 nm region. This is also indicated by theoretical calculation [8]. Energy at these wavelengths is still at best only marginally available from the solar spectrum. Based on this situation, however, it seemed possible that a combined photolysis/electrolysis process using a hexabromoiridate/bromide system would be more efficient than the solar-assisted hexachloroiridate/chloride system mentioned above. An added advantage of using the iridium bromide complexes is that the  $\text{Br}_2$  produced during stage one of the process would be more convenient to store than would  $\text{Cl}_2$  gas, since at room temperature  $\text{Br}_2$  is a liquid whereas  $\text{Cl}_2$  is a gas. Until the present time, no detailed account of the photochemical behavior of the hexabromoiridate complexes in aqueous  $\text{HBr}$  solution has appeared in the literature.

A detailed survey of the literature has shown some application of photolysis, pulse radiolysis, or steady-state radiation chemistry techniques to iridium bromide solutions [9-12]. Work by Broszkiewicz and by Mills and Henglein on pulse radiolysis of iridium bromide complexes [13, 14] has shown that  $\text{IrBr}_6^{3-}$  can be oxidized to  $\text{IrBr}_6^{2-}$ , or it can be reduced to  $\text{IrBr}_6^{4-}$ . Redox reactions of many similar transition metal halide complexes have also been studied using pulse radiolysis techniques [15-19].

As an extension of thermolysis, photolysis, and pulse radiolysis investigations of hexachloroiridate and related  $\text{H}_2$  and  $\text{Cl}_2$  systems by A. K. Gupta, M. R. Gholami and C. L. Crawford in this laboratory, a preliminary investigation of the hexabromoiridate system was undertaken [3-7, 20-22]. Using pulse radiolysis, Gholami and Crawford examined the reactions of  $\text{IrBr}_6^{2-}$  and  $\text{IrBr}_6^{3-}$  with aqueous electrons. They were able to show that  $\text{IrBr}_6^{2-}$  and  $\text{IrBr}_6^{3-}$  can be reduced by  $e_{aq}^-$  to form  $\text{IrBr}_6^{3-}$ , Reaction (10) and

$\text{IrBr}_6^{4-}$ , Reaction (11), respectively, under pulse radiolysis conditions.



They determined that the second order rate constants for Reactions (10) and (11) were  $1.6 \times 10^{10} \text{ M}^{-1} \text{ s}^{-1}$  and  $2.61 \times 10^9 \text{ M}^{-1} \text{ s}^{-1}$ , respectively.

Also, in a separate pulse radiolysis experiment, Gholami and Crawford were able to show that the reaction of  $\text{IrBr}_6^{3-}$  with OH radical formed  $\text{IrBr}_6^{2-}$ , Reaction (12).



They determined that the second order rate constant for Reaction (12) was equal to  $1.4 \times 10^9 \text{ M}^{-1} \text{ s}^{-1}$ .

Based on the considerations above, a more thorough investigation of the reaction chemistry of the bromide complexes of iridium in the +3 and +4 oxidation states appeared to be warranted. This would compliment some of the work previously done in this laboratory on the iridium chloride complexes [5-7, 20-22].

### **Mechanism for Pulse Radiolysis of $\text{IrBr}_6^{3-}$ in the Presence of $\text{Br}^-$ Ion**

The author of this work studied pulse radiolysis of aqueous  $\text{IrBr}_6^{3-}$  in the presence of  $\text{Br}^-$  as research conducted for a Master's Thesis [23]. The Master's research centered on the role of competition kinetics due to species produced when an aqueous solution of  $\text{IrBr}_6^{3-}$  which also contained  $\text{Br}^-$  was irradiated under pulse radiolysis. Many of the results and observations discussed in the thesis, as well as results from work of Gholami and Crawford for the  $\text{IrBr}_6^{3-}/\text{IrBr}_6^{2-}$  system, parallel the observations reported for the analogous hexachloroiridate system [13, 14].

The bulk of the work for the Master's thesis was on the investigation of the pulse radiolysis of aqueous solutions of hexabromoiridate (III) in the presence of bromide ions under totally oxidizing conditions. Under totally oxidizing conditions, the reductive species,  $e_{aq}^-$ , is converted to  $O^-$  in a solution saturated with  $N_2O$ . The  $O^-$  ion reacts with water to make OH radicals and hydroxide ion. Accordingly, under totally oxidizing conditions, the principal reactant formed as a result of the pulse radiolysis of aqueous solution is OH radical. The OH radical produced reacts very quickly with any oxidizable substrate dissolved in solution.

A mechanism was proposed for the pulse radiolysis of  $IrBr_6^{3-}$  in aqueous solution containing dissolved  $Br^-$ . The rate constant for the reaction of OH radical with  $IrBr_6^{3-}$ , Reaction (12), was determined using the proposed mechanism with the assistance of a Gear Integrator program. The Gear integrator program was written by R. L Brown, of the National Bureau of Standards in Washington, DC [24] and modified locally by R. J. Hanrahan. Gear integrator simulations of the concentrations of  $IrBr_6^{2-}$  produced by the reaction over time were compared to experimental values of  $IrBr_6^{2-}$  concentrations. The proposed mechanism and rate constants used to create the simulated concentrations of  $IrBr_6^{2-}$  are listed Table (1) in the Master's Thesis and reproduced here as Table (1). Using the Gear integrator, the rate constant for Reaction (12) was determined to be  $2 \times 10^9 \text{ M}^{-1} \text{ s}^{-1}$ .

Table (1): Mechanistic steps used for the simulation of the production of  $\text{IrBr}_6^{2-}$  for Figure (1) during pulse radiolysis of aqueous  $\text{Br}^-/\text{IrBr}_6^{3-}$  solution.

Reaction	Rate Const.	Ref.	
$e_{aq}^- + e_{aq}^- \rightarrow \text{H}_2 + 2\text{OH}^-$	$5.6 \times 10^9$	[25]	(13)
$e_{aq}^- + \cdot\text{OH} \rightarrow \text{OH}^-$	$3.0 \times 10^{10}$	[25]	(14)
$e_{aq}^- + \text{H}^+ \rightarrow \text{H}$	$2.3 \times 10^{10}$	[26]	(15)
$e_{aq}^- + \text{H} \rightarrow \text{H}_2 + \text{OH}^-$	$2.5 \times 10^{10}$	[25]	(16)
$e_{aq}^- + \text{HO}_2^- \rightarrow \cdot\text{OH} + 2\text{OH}^-$	$3.5 \times 10^9$	[27]	(17)
$e_{aq}^- + \text{O}^- \rightarrow 2\text{OH}^-$	$2.2 \times 10^{10}$	[25]	(18)
$e_{aq}^- + \text{H}_2\text{O}_2 \rightarrow \text{OH}^- + \cdot\text{OH}$	$1.1 \times 10^{10}$	[26]	(19)
$e_{aq}^- + \text{O}_2 \rightarrow \text{O}_2^-$	$1.9 \times 10^{10}$	[28]	(20)
$e_{aq}^- + \text{O}_2^- \rightarrow \text{O}_2^{2-}$	$1.3 \times 10^{10}$	[26]	(21)
$e_{aq}^- + \text{H}_2\text{O} \rightarrow \text{H} + \text{OH}^-$	$1.9 \times 10^1$	[26]	(22)
$\text{H} + \text{OH}^- \rightarrow e_{aq}^-$	$2.2 \times 10^7$	[26]	(23)
$\text{H} + \text{H} \rightarrow \text{H}_2$	$7.8 \times 10^9$	[29]	(24)
$\cdot\text{OH} + \cdot\text{OH} \rightarrow \text{H}_2\text{O}_2$	$5.5 \times 10^9$	[26]	(25)
$\text{H} + \cdot\text{OH} \rightarrow \text{H}_2\text{O}$	$7.0 \times 10^9$	[30]	(26)
$\text{H}^+ + \text{OH}^- \rightarrow \text{H}_2\text{O}$	$1.4 \times 10^{11}$	[31]	(27)
$\text{H}_2\text{O} \rightarrow \text{H}^+ + \text{OH}^-$	$2.6 \times 10^{-5}$	[31]	(28)
$\cdot\text{OH} + \text{H}_2 \rightarrow \text{H} + \text{H}_2\text{O}$	$4.2 \times 10^7$	[26]	(29)
$\cdot\text{OH} + \text{H}_2\text{O}_2 \rightarrow \text{HO}_2 + \text{H}_2\text{O}$	$2.7 \times 10^7$	[32]	(30)
$2\text{HO}_2 \rightarrow \text{H}_2\text{O}_2 + \text{O}_2$	$2.7 \times 10^6$	[26]	(31)
$\text{O}_2^- + \text{HO}_2 \rightarrow \text{HO}_2^- + \text{O}_2$	$4.4 \times 10^7$	[33]	(32)



Table (1) continued.

Reaction	Rate Const.	Ref.	
$\text{H} + \text{H}_2\text{O}_2 \rightarrow \cdot\text{OH} + \text{H}_2\text{O}$	$9 \times 10^7$	[34]	(33)
$\text{HO}_2 + \text{H} \rightarrow \text{H}_2\text{O}_2$	$1 \times 10^{10}$	[35]	(34)
$\text{HO}_2 + \cdot\text{OH} \rightarrow \text{H}_2\text{O} + \text{O}_2$	$6 \times 10^9$	[36]	(35)
$\text{H} + \text{O}_2 \rightarrow \text{HO}_2$	$2.1 \times 10^{10}$	[26]	(36)
$\text{O}_2^- + \text{H}^+ \rightarrow \text{HO}_2$	$4.7 \times 10^{10}$	[37]	(37)
$\text{HO}_2 \rightarrow \text{H}^+ + \text{O}_2^-$	$8 \times 10^5$	a	(38)
$\text{H}^+ + \text{HO}_2^- \rightarrow \text{H}_2\text{O}_2$	$3 \times 10^{10}$	b	(39)
$\text{H}_2\text{O}_2 \rightarrow \text{H}^+ + \text{HO}_2^-$	$3 \times 10^{-2}$	c	(40)
$\text{H}_2\text{O}_2 + \text{OH}^- \rightarrow \text{HO}_2^- + \text{H}_2\text{O}$	$5.0 \times 10^8$	[38]	(41)
$\text{HO}_2^- + \text{H}_2\text{O} \rightarrow \text{H}_2\text{O}_2 + \text{OH}^-$	$5.7 \times 10^4$	[38]	(42)
$\cdot\text{OH} + \text{OH}^- \rightarrow \text{O}^- + \text{H}_2\text{O}$	$1.2 \times 10^{10}$	[33]	(43)
$\text{O}^- + \text{H}_2\text{O} \rightarrow \cdot\text{OH} + \text{OH}^-$	$9.3 \times 10^7$	[33]	(44)
$\cdot\text{OH} + \text{HO}_2^- \rightarrow \text{OH}^- + \text{HO}_2$	$7.5 \times 10^9$	[32]	(45)
$\text{H} + \text{H}_2\text{O} \rightarrow \text{H}_2 + \cdot\text{OH}$	$1 \times 10$	[26]	(46)
$\cdot\text{OH} + \text{O}^- \rightarrow \text{HO}_2^-$	$2 \times 10^{10}$	[39]	(47)
$\cdot\text{OH} + \text{O}_2^- \rightarrow \text{OH}^- + \text{O}_2$	$1.0 \times 10^{10}$	[40]	(48)
$\text{O}^- + \text{H}_2 \rightarrow \text{H} + \text{OH}^-$	$8.0 \times 10^7$	[25]	(49)
$\text{O}^- + \text{H}_2\text{O}_2 \rightarrow \text{O}_2^- + \text{H}_2\text{O}$	$5 \times 10^8$	[26]	(50)
$\text{O}^- + \text{HO}_2^- \rightarrow \text{O}_2^- + \text{OH}^-$	$4 \times 10^8$	[26]	(51)
$\text{O}^- + \text{O}_2 \rightarrow \text{O}_3^-$	$3.6 \times 10^9$	[33]	(52)

Table (1) continued.

Reaction	Rate Const.	Ref.	
$O^- + O_2^- + H_2O \rightarrow 2OH^- + O_2$	$6.0 \times 10^8$	[41]	(53)
$N_2O + e_{aq}^- \rightarrow N_2 + OH^- + \cdot OH$	$9.1 \times 10^9$	[42]	(54)
$Br_2 + Br^- \rightarrow Br_3^-$	$1.5 \times 10^9$	d	(55)
$Br_3^- \rightarrow Br_2 + Br^-$	$8 \times 10^7$	d	(56)
$2Br_2^- \rightarrow Br_3^- + Br^-$	$1.7 \times 10^9$	[43]	(57)
$BrOH^- + H^+ \rightarrow H_2O + Br$	$4.4 \times 10^{10}$	[44]	(58)
$Br + Br^- \rightarrow Br_2^-$	$1 \times 10^{10}$	[44]	(59)
$BrOH^- + Br^- \rightarrow OH^- + Br_2^-$	$1.9 \times 10^8$	[44]	(60)
$BrOH^- \rightarrow Br + OH^-$	$4.2 \times 10^6$	[44]	(61)
$BrOH^- \rightarrow Br^- + \cdot OH$	$3.3 \times 10^7$	[44]	(62)
$\cdot OH + Br^- \rightarrow BrOH^-$	$1.06 \times 10^{10}$	[44]	(63)
$IrBr_6^{2-} + e_{aq}^- \rightarrow IrBr_6^{3-}$	$1.6 \times 10^{10}$	e	(10)
$IrBr_6^{2-} + H \rightarrow IrBr_6^{3-} + H^+$	$9.2 \times 10^9$	b	(64)
$IrBr_6^{3-} + H \rightarrow IrBr_6^{4-} + H^+$	$6 \times 10^9$	b	(65)
$IrBr_6^{4-} + IrBr_6^{2-} \rightarrow 2IrBr_6^{3-}$	$9.2 \times 10^8$	e	(66)
$IrBr_6^{3-} + e_{aq}^- \rightarrow IrBr_6^{4-}$	$2.61 \times 10^9$	e	(11)
$IrBr_6^{3-} + \cdot OH \rightarrow IrBr_6^{2-} + OH^-$	$2 \times 10^9$	f	(12)
$BrOH^- + IrBr_6^{3-} \rightarrow IrBr_6^{2-} + Br^- + OH^-$	$9.7 \times 10^6$	f	(67)
$Br_2^- + IrBr_6^{3-} \rightarrow IrBr_6^{2-} + 2Br^-$	$1.5 \times 10^8$	f	(68)

Table (1) continued.

Reaction	Rate Const.	Ref.	
$\text{Br}_2 + \text{IrBr}_6^{3-} \rightarrow \text{IrBr}_6^{2-} + \text{Br}_2^-$	$2.2 \times 10^4$	f	(69)
$\text{Br}_3^- + \text{IrBr}_6^{3-} \rightarrow \text{IrBr}_6^{2-} + \text{Br}_2^- + \text{Br}^-$	$6 \times 10$	f	(70)

- a. Calculated to give  $\text{pK} = 4.8$  with respect to Reaction (37).
- b. Estimated.
- c. Calculated to give  $\text{pK} = 11.8$  with respect to Reaction (39).
- d. The values for the rate constant for each of these reactions were taken from the literature [45]. However, the values have been adjusted because of an error in the reference, as explained later.
- e. Measured, this laboratory, previous work.
- f. Best fit, this laboratory, work for Master's thesis.

A graph of the simulated  $\text{IrBr}_6^{2-}$  concentration formed over time superimposed over the concentration of  $\text{IrBr}_6^{2-}$  produced experimentally is shown in Figure (1), reproduced from Figure (12) of the Master's Thesis. The concentrations of all species input in the Gear integrator to generate the  $\text{IrBr}_6^{2-}$  product concentrations used in Figure (1) are listed in Table (2) (page 14), given as Table (2) in the Master's Thesis. The concentrations of the aqueous intermediates were based on the OH radical concentration generated in the reaction and the G-values of the other intermediates.

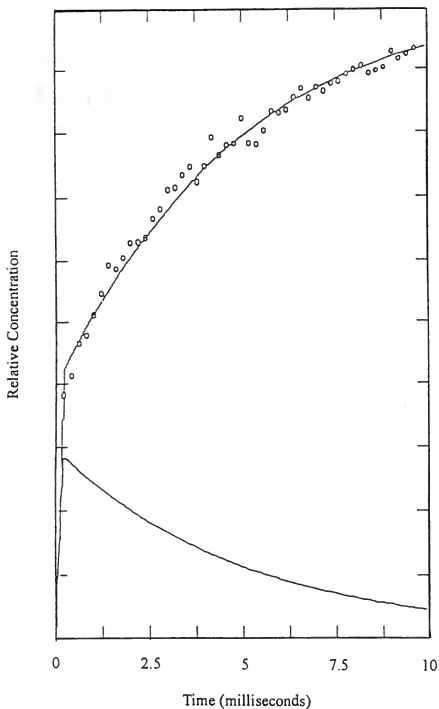


Figure (1). Plot of the simulated and experimental  $\text{IrBr}_6^{2-}$  concentrations due to the pulse radiolysis of a solution of  $\text{IrBr}_6^{3-}/\text{Br}^-$ . The points represent the experimental product concentration of  $\text{IrBr}_6^{2-}$ . The Upper curve is the simulated  $\text{IrBr}_6^{2-}$  concentration. The lower curve is the simulated  $\text{Br}_2$  concentration. The final concentration of  $\text{IrBr}_6^{2-}$  was 0.105 mM.

Table (2): Concentrations of all species input into the simulation program for the production of  $\text{IrBr}_6^{2-}$ .

Intermediate	Concentration
Species	(M)
$e_{aq}^-$	$7.75 \times 10^{-5}$
$\cdot\text{OH}$	$8.01 \times 10^{-5}$
$\text{H}^+$	$7.75 \times 10^{-5}$
$\text{H}_2$	$1.33 \times 10^{-5}$
$\text{H}_2\text{O}_2$	$2.00 \times 10^{-5}$
$\text{HO}_2^-$	$2.73 \times 10^{-6}$
$\text{HO}_2$	$7.66 \times 10^{-7}$
$\text{O}_2^-$	$1.03 \times 10^{-7}$
$\text{H}_2\text{O}$	55
$\text{Br}^-$	$2.5 \times 10^{-2}$
$\text{IrBr}_6^{3-}$	$1.02 \times 10^{-3}$
$\text{N}_2\text{O}$	$2.5 \times 10^{-2}$

$\text{Br}^-$ , and with the intermediate species in aqueous solution were especially intriguing with respect to the solar energy studies. The purpose of this work was to search for more information regarding these reactions and mechanisms, and specifically to measure rate constants for the individual steps of the proposed mechanism, and to offer new mechanistic pathways for the individual parts of the proposed mechanism, where applicable.

## CHAPTER TWO THE PULSE RADIOLYSIS METHOD

### **Pulse Radiolysis of Aqueous Solutions**

The radiolysis of chemical systems can be studied using either pulsed or steady state methods. Both methods, when applied to aqueous solution, involve the production of very reactive intermediates. The difference between the two methods is in the time scale of energy deposition. In the case of electron equivalent radiation (see below), the intermediates formed are the same, and are produced in the same yield with respect to the absorbed dose. A gamma emitter such as cobalt-60 is often used to study steady state radiolysis. Several types of electron accelerators are commonly used to study pulse radiolysis, including Linacs (linear electron accelerators), electron Van de Graaffs, and Febetrans as used in the present work.

During gamma radiolysis of water and aqueous solutions, the incident high-energy photons can interact with water or solute molecules through either the photoelectric effect, the Compton effect, or pair production, depending on the energy of the gamma and the atomic number of the absorber. The predominant pathway for the absorption of low-energy gamma radiation up to a few tens of thousands of electron volts is the photoelectric effect. The usual pathway for absorption of ionizing radiation in the range of about 50 keV to above 1 MeV is the Compton effect. At high-photon energies,

the incident radiation can interact with matter by pair formation; this is sometimes important with high  $Z$  absorbers, but less important with water [46].

In the case of the photoelectric effect, all of the energy of the photon is deposited in a single electron in a water molecule, causing ejection of the electron. This is generally the most tightly bound electron, a K electron of the oxygen atom. The energy required to eject this electron from the molecule is 532 eV. Any remaining energy of the photon is imparted to the electron in the form of kinetic energy. Because 532 eV is often a small fraction of the total energy of the gamma photon, the resulting electron carries considerable kinetic energy. The fast electron passes through the aqueous solution depositing portions of its energy to the water or solute molecules until it loses all of its energy.

The Compton effect is the predominant mechanism by which moderate-energy gamma radiation interacts with water. Compton absorption is an inelastic scattering process wherein an electron is ejected from the target molecule and the residual energy of the incident gamma appears as a scattered photon of lower energy. The secondary photon can then interact with another water molecule, causing another Compton electron and lower energy photon to be produced. This process continues until the energy of the original gamma is completely absorbed by the water or the lower energy gamma escapes from the solution. The fast secondary electrons travel in a scattered, frequently branched track, depositing portions of their energy to target molecules in the medium until they are thermalized.

Pair formation can occur when incident photons with energy of 1.02 MeV or higher interact with the intense electrical field near a target nucleus, producing two

product electrons, one positive and one negative. Any excess energy of the incoming photon appears as kinetic energy of the electrons produced. This process is of small importance for experiments using a cobalt-60 irradiator with gammas of ca. 1.25 MeV unless the target molecule contains a high Z element such as iodine.

In many cases (moderately high-photon energy, low Z absorbers) most of the energy deposition from a gamma field occurs by fast secondary electrons. Accordingly, moderate-energy gamma radiolysis in the case of water and dilute aqueous solution is referred to as "electron equivalent radiation," as mentioned to above.

In the present work, accelerated electrons pass through the solution under investigation, imparting energy to water or to solute molecules until they have lost all their energy and become thermalized. The University of Florida Pulse Radiolysis Facility makes use of a Febetron 706 manufactured by the Field Emission Corporation, which generates an electron beam with a maximum energy of about 600 keV. Electron accelerators are useful in the study of the effects of radiolysis because the energy deposition mechanism of both gamma and electron radiolysis are equivalent, in that ultimately the radiation damage is caused by fast secondary electrons.

When ionizing radiation interacts with aqueous solutions, the overall effect is the generation of short-lived, highly reactive intermediate species, many of which are radicals. These intermediates are produced through interactions of the ionizing radiation with water molecules in the irradiated solution [47]. Because ionizing radiation interacts with matter in proportion to the mass fraction of the substance present, the interaction of ionizing radiation with any dissolved solute is negligible if the solute is of low concentration. In consequence, damage to solutes present in low concentration is caused



by reaction with the reactive intermediates produced by direct irradiation of the solvent; this situation is described as the "indirect effect."

In the time range of about  $10^{-9}$  seconds to  $10^{-6}$  seconds, the most reactive of the intermediates that remain are the hydroxyl radicals,  $\cdot\text{OH}$ , and the aqueous electrons,  $e_{\text{aq}}^-$ . During or immediately after exposure to ionizing radiation, the intermediate species can react with any reactive solute present. The OH radicals and aqueous electrons are short-lived, and their reactions are often very fast.

Two conditions are necessary in order to measure the rates of the reactions of intermediates with dissolved solute. First, the radiation exposure time must be shorter than the reaction time of the intermediates with the solute. Ideally, the exposure time should be short enough compared to the time for the reaction to occur that the system can be treated as though the formation of the intermediates was instantaneous. The second condition is that the system used to monitor the reaction must be capable of collecting the data at a sufficiently fast rate over a short period of time.

The Febetron 706 at the University of Florida meets the first requirement. The pulse of the Febetron is short, approximately 3 nanoseconds. Hence, the exposure time is shorter than most of the reactions of the intermediates with the solute. Coupled with a fast detection and data acquisition system set up adjacent to the Febetron as peripheral instrumentation, the facility meets the second requirement. A diagram representing the pulse radiolysis system with the peripheral instrumentation as it is currently set up is shown in Figure (2).

The Febetron 706 was originally used in this laboratory to study gas phase reactions. But the facility was converted to a configuration that was suitable for the study

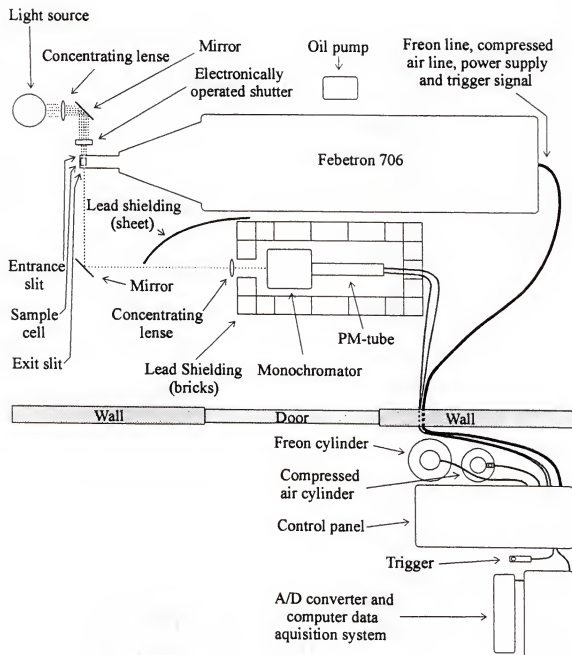


Figure (2). The general set-up of the Pulse Radiolysis Facility at the University of Florida. The Febetron 706 and peripheral instrumentation are in a separate room from the controls to minimize the operator from the excessive EMI effects from the Febetron.

of systems in solution. Conversion from gas phase to liquid phase studies involved modifying the beam window flange to accommodate the attachment of a small, 1 cm wide sample cell, with a thin Mylar window (200 microns) along the beam axis [48]. As it is currently configured, there are three major components of the pulse radiolysis system: the Febetron 706; a detection system composed of a light source, monochromator, and photo-multiplier tube with power source; and a data acquisition system composed of a fast 8-bit analog to digital converter (40 MHz) and computer, Figure (2). A more detailed description of the Febetron accelerator and the accessories is given below.

### **The Febetron 706**

The Febetron 706 electron accelerator operates using the Marx-surge principle. A block diagram of the Febetron 706 is shown in Figure (3). When triggered, the trigger pulse is shaped and amplified. The amplified output pulse then passes through the Trigger Transformer, which delivers a high voltage pulse to the Marx-surge circuitry.

The Marx-surge circuit consists of several high voltage capacitors stacked horizontally along the machine axis [49]. In preparation for triggering, the capacitors of this part of the Pulser are charged in parallel. When triggered, they are rapidly discharged in series. During discharge of a high voltage pulse, the energy stored in the capacitors is dumped in series, through spark gaps, into the Short Pulse Adapter. The Short Pulse Adapter then discharges an extremely short, 3-nanosecond high-current pulse into the field emission tube. This pulse generates electron emission from the cathode; the electrons are accelerated toward the exit window, the anode, at ground potential.

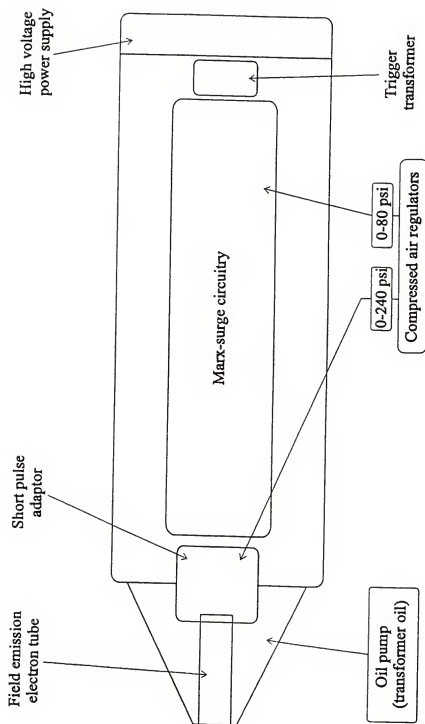


Figure (3). Block diagram of the Febetron 706 with the Marx-surge circuitry. The external case of the Febetron is filled with freon.

With the current arrangement, the electron beam is directed toward a small sample cell containing the solution under investigation. The field emission tube (beam tube) is somewhat deteriorated, and the Febetron 706 currently operates at an efficiency that is about 10 % of the original specifications, and the dose sometimes fluctuates ca. plus or minus 30% of the current signal. However, with carefully designed procedures, the consequences of the unreliability of the Febetron can be minimized.

### **Detection System**

The peripheral instrumentation used to monitor the activity in solution during experiments consists of a light source, a monochromator, and a photo-multiplier tube. Two different light sources were used for this work, a water-cooled xenon arc lamp housed in a PRA-Canada ALH 220 housing, powered by a PRA-Canada Model M301 DC power supply and igniter, and a Spectra Physics Model 155 helium-neon laser. The monochromator used in all experiments was made by Jarrell-Ash. It was a 0.25 meter Ebert Monochromator, model number 82-410. The photo-multiplier tube was from Hamamatsu, Model R928.

### **Light Sources**

Two different light sources were used for this work. A water-cooled xenon arc lamp was used in monitoring all of the experiments that required measurements of absorption at or below about 626 nm. A He-Ne laser, was used to monitor the aqueous electron,  $e_{aq}^-$ , at 632 nm.

## **Xenon-arc Lamp**

The xenon-arc system included a xenon-arc, high-pressure discharge lamp. The lamp housing was a PRA-Canada ALH 220 housing with dual water cooling loops. It was powered by a PRA-Canada Model M301 ignition-power supply. The power supply makes use of a continuous feedback, constant current mode of operation. The continuous feedback leads to greater current stability. The lamp electrodes, lamp housing and power supply were all water-cooled. The lamp housing and power supply were cooled by one continuous water line while a separate line cooled the lamp electrodes. The xenon-arc lamp gives a high output between ca. 300 nm to ca. 640 nm. It was used for most of the experiments.

## **He-Ne laser**

For some of the experiments, the aqueous electron was monitored. The aqueous electron absorbs strongly with a broad peak around 750 nm [33]. For these experiments, the output of the xenon-arc lamp was insufficient. The Spectra Physics Model 155 helium-neon(He-Ne) laser has a very high output with a sharp peak at 632.8 nm.

Although the absorption peak of the aqueous electron is centered at 750 nm, it absorbs enough light at 633 nm that the He-Ne laser with its intense output at that wavelength was useful in detecting and monitoring the aqueous electron. Characteristics of this laser, such as high collimation, low divergence and very intense, monochromatic light centered at 633 nm, make it ideal for studies which require monitoring the aqueous electron.

### Monochromator

All experiments utilized a Jarrell-Ash 0.25 meter Ebert Monochromator, model number 82-410. The photo-multiplier tube housing was attached to the exit slit of the monochromator through an adapting flange. The monochromator and photo-multiplier tube were situated behind and to the side of the Febetron, as shown in Figure (2). This arrangement created an appropriate angle that maximized the signal light input while at the same time minimizing the noise created by the excessive EMI effects from the Febetron. Additionally, a significant amount of lead shielding was used to protect the monochromator and photo-multiplier tube from both the EMI output and ionizing radiation output of the Febetron. Optimization of the geometry of the monochromator and photomultiplier tube increased the magnitude of the signal by a factor of approximately 5 and reduced the dead-time due to interference from the EMI noise and ionizing radiation output from about 5 to 10 microseconds to about 2 to 3 microseconds compared to a first-try arrangement.

### Photo-Multiplier Tube

A Hamamatsu Mode R928 photo-multiplier tube was used to monitor the analyzing light in all experiments. It is of the side-on type and was mounted in a Pacific Precision Instruments Model 3150 Housing. The Spectral response range was 185 nm to 900 nm. This range generally covered all wavelengths that needed to be measured, such as 512 nm, 584 nm and 626 nm for  $\text{IrBr}_6^{3-}$  reaction with OH radical, and 634 nm for  $\text{IrBr}_6^{2-}$  reaction with  $\text{e}_{\text{aq}}^-$ . A John Fluke, Inc. model 412A High Voltage DC power supply

used to power the photo-multiplier tube in earlier experiments was replaced with an Ortec Model 456 High Voltage DC power supply for the later experiments.

### **Computer Data-Acquisition System**

The signal from the PM-tube was measured as a voltage across a resistor, the value of which could be selected as required. The resistors used were typically between 25 ohm and 200 ohm. The signal from the PM-tube was analyzed using a Waag II Analog to Digital converter board plugged into a standard 8088 personal computer with a 10-megabyte hard drive. The Waag II was made by the Markenrich Corporation, 1812 Flower Ave., Duarte, CA, 91010. The Waag has the capability to monitor two channels, A and B. However, only channel A was used to monitor all of the experiments. Channel B was used as the trigger switch to initiate data acquisition. The Full-scale input jumpers were set to read from +0.635 V to -0.640 V. In this mode, the maximum sample frequency possible was 40 MHz (20 nanosecond time periods).

One of the special aspects of the Waag is its capability to give pre-trigger data. This is possible because the Waag, when set at the ready, successively reads and stores data (voltage across the resistor) in a predefined set of memory locations. In the one channel operational mode, the number of cells allocated to memory is 32768. When set at the ready, the Waag begins to successively read and store the voltage data in the memory locations. After the last (32768<sup>th</sup>) memory location has received an input, the Waag loops around and begins to place the new datum into the first cell again, replacing the old value with the new value. The cycle continues through the last cell, then loops around again in a continuous fashion.



At any point while set in the ready position, the Febetron can be triggered. The trigger signal goes to both the Febetron and the Waag board. When triggered, the Waag continues to read and input the data in the memory locations until a predetermined number of readings has been reached. The Waag was then capable of pulling up and using all of the data in the cells that were taken both before and after the Waag was triggered. This feature was particularly useful for this work because a predetermined number of data readings (usually 75 data points) taken before triggering the Febetron were read and used to calculate the light intensity before any reaction occurred, giving the full-light signal. The full-light signal was used later in the calculation of the absorbance.

In work done for the master's thesis [23], a program to control the Waag was written and compiled in QuickBasic. This program included subroutines from a previously written program, which had been written to interact with an entirely different data acquisition system. The function of the "borrowed" subroutines was to graph the data for manual selection of useful data points using software cursors. These subroutines could also be used to calculate from the selected data points the first, second and third order rate constants, and to save the data as optical densities or concentrations based on previously input extinction coefficients. However, the major aspects of the present pulse radiolysis program, including control features for the Waag, the graphical display during the operation of the Febetron, the features for determining the no-light and full-light signals, and the setting and utilization of the pre-trigger time delay, were written for the master's work and used in the current work. Certain parts of the pulse radiolysis data

acquisition software were used in a program for data collection during stopped-flow experiments described in a later section of this dissertation.

### **Sample Cell and Reservoir**

There are some difficulties associated with the application of the Febetron 706 to aqueous solution. The penetrating ability of 600 keV electrons in water is ca. 1.5 mm [50]. Charles Crawford checked the electron penetration depth of the Febetron in this laboratory using Fisher brand optical glass microscopic coverslides placed in the sample cell holder [22]. He determined the dose through each coverslide set in a series. His results showed that there was a uniform dose through the first three coverslides. There was a gradual falloff of dose to zero from between three and four coverslides to after about seven coverslides. The results showed that the maximum penetration in water is about 2.0 mm, assuming the glass density is two times the density of water. This agreed well with studies done elsewhere [51]. The sample cell to be used needed to be constructed with a thin window to allow for good electron penetration into the solution with minimal loss of the electron beam.

Two different sample cells were used in experiments applying the Febetron 706 to aqueous solutions. They were customized to accommodate the low penetrating ability of 600 keV electrons. They were constructed from existing 1-cm quartz cells to have an electron beam window made of a sheet of thin Mylar film (approximately 0.2 millimeters). The analyzing optical path was perpendicular to the electron beam, parallel and immediately adjacent to the e-beam Mylar window. The width of the analyzing light slit was adjustable. It was usually set at ca. 1 mm.

The first cell, cell A, as shown in Figure (4), was fashioned by making several modifications to a standard Ultraviolet-visible spectrophotometer cell. With respect to a cell oriented in a normal working position for a Ultraviolet-visible instrument, the bottom was sawed off with a glass saw and replaced with a thin Mylar film that served as the electron-beam window. The top was sealed. Of the remaining four sides, two opposite sides were fitted with glass tubing for filling and draining, and the other two sides functioned as windows for the incoming and outgoing analyzing light. When in use, the cell was placed horizontally so that the Mylar window faced the electron-beam exit window of the Febetron. The electron-beam path from the Febetron to the sample cell was enclosed in aluminum to prevent leakage of radio-frequency radiation into the room.

A second cell, cell B, was used in the later part of the pulse radiolysis work. The second cell was not constructed from a standard 1 x 1 cm Ultraviolet-visible spectrophotometer cell. It was fashioned from a custom cell that proved to be extraordinarily useful for this type of application. A conduit through the upper quartz wall allowed for addition of aliquots of solution to the front of the cell, near the added Mylar electron-beam entrance window. And a conduit for the drainage tube opened from the back of the cell. A quartz tubulation was attached to the top conduit for filling and a similar quartz tubulation was joined to the bottom conduit for drainage. The orientation described is with respect to use of the cell in the pulse radiolysis experiments and not the ordinary working position in a conventional Ultraviolet-visible spectrophotometer instrument. The new cell is shown in Figure (5). With this configuration, the new sample cell could stay in the experimentally ready position in the sample cell holder while being rinsed and filled with new aliquots of working solution.

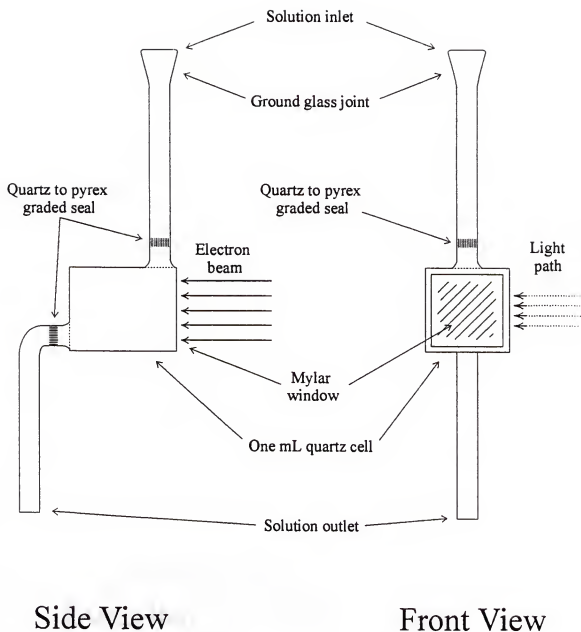


Figure (4). Sample cell (cell A) used in the earlier pulse radiolysis work. The sample cell was fabricated from a standard UV-vis spectrophotometer cell.

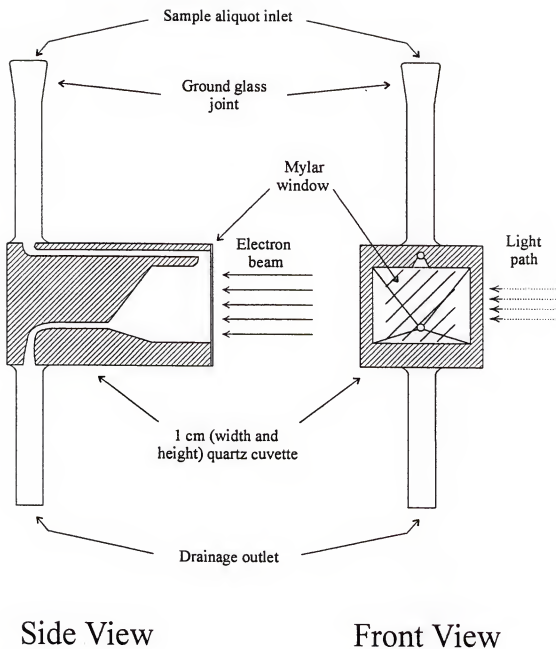


Figure (5) Sample cell (cell B) used for the later pulse radiolysis work. The cell was converted from a specialized spectrophotometer cell.

The arrangement of the new sample cell was a significant improvement over the arrangement of the old cell. It was much easier to rinse and add new aliquots without adding air. Also, less solution was required for rinsing and filling. The greatest advantage, however, was that the sample cell remained in the same position throughout the experiments. This reduced the risk of misalignment of the sample cell in the holder after each addition of a new aliquot, and eliminated a changing cell orientation as a possible source of error.

When used, each of the cells was connected to a separatory funnel, which functioned as a sample solution reservoir, Figure (6), and placed in the sample holder with the electron-beam window facing the beam exit window of the Febetron. The configuration of the sample cell in the cell holder can be seen in Figure (7). A separatory funnel was used as a sample reservoir from which aliquots of solution could be drawn without allowing air into the sample.

## **Applications of Pulse Radiolysis to Aqueous Solutions**

### **Pulse Radiolysis of Aqueous Solution**

Pulse radiolysis of aqueous solutions has been used extensively in the study of fast reactions in water. Many of the reactions studied using pulse radiolysis can be helpful in the understanding of processes that occur in biological systems, where the primary medium is water. Pulse radiolysis of aqueous solution shares basic mechanisms with steady state radiolysis; however, the time scale is much shorter (picoseconds and nanoseconds versus hours and days). There is usually a difference with respect to the source of the ionizing radiation. A cobalt-60 source, for example is often used for steady

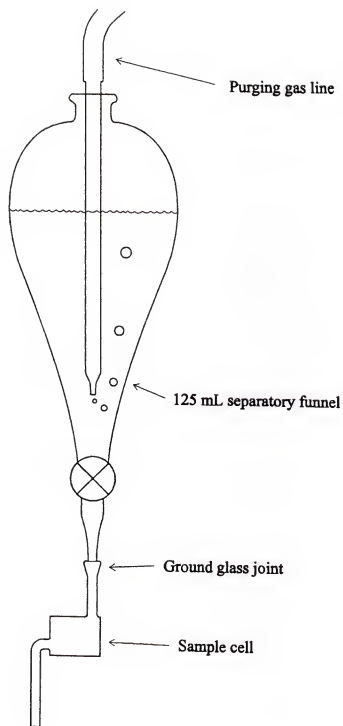


Figure (6) Sample reservoir with sample cell. The purging gas line outlet is also shown. The sample reservoir was made by attaching a ground glass joint to a standard 125 mL separatory funnel.

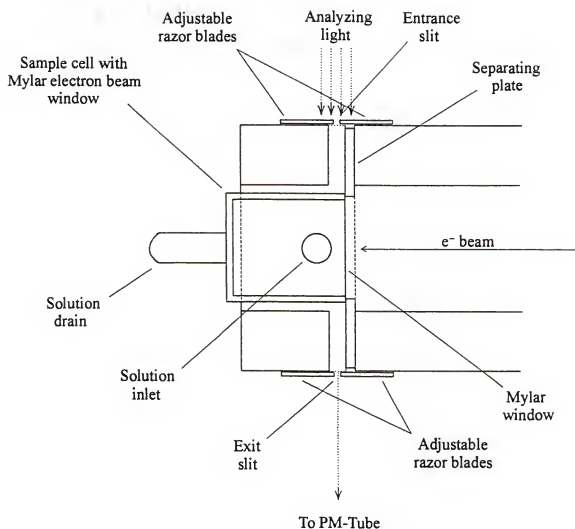


Figure (7). A top view of the sample cell holder is shown with the sample cell in place. The adjustable razor blades were used to allow the slit width to be adjusted if necessary.



state studies whereas a pulsed electron source is commonly used for pulse radiolysis studies. With the pulse radiolysis studies done for this work, the ionizing radiation consisted of a "beam" of electrons created electro-statically by application of a very short but intense electrical pulse generated in an electron accelerator.

The ionizing particles pass through a solution randomly depositing energy along their track until they have either deposited all of their energy or passed completely out of the solution. Energy deposition sites along a track are referred to as spurs [52]. The radicals created in the spurs by the ionizing radiation can initially react with other water molecules, react with other radicals, or diffuse out of the spurs. The "dry" electrons (electrons not yet hydrated) initially created in the spurs can either interact with water to create more radicals, react with the radicals, or solvate to become hydrated electrons,  $e_{aq}^-$ . A diagram representing the process of the irradiation of water solution and the subsequent events that follow is shown in Figure (8). The diagram is redrawn from "Basic radiation chemistry of liquid water," by G. V. Buxton, chapter 16 from "The study of fast processes and transient species by electron pulse radiolysis" [53]. A notable characteristic of the hydrated electron is that it can react by tunneling [54]. The result of this process is well-documented [47].

Within approximately  $10^{-7}$  seconds following interaction of the primary electron or photon with water, essentially all of the radical intermediates have diffused out of the spurs and tracks. At this time, there are very few radical-radical reactions still occurring within the spurs. The remaining radicals and other species created by the incident radiation can react with each other or with any reactive solute present. Reaction with the solute can be treated by steady-state reaction kinetics, as in a homogeneous solution.

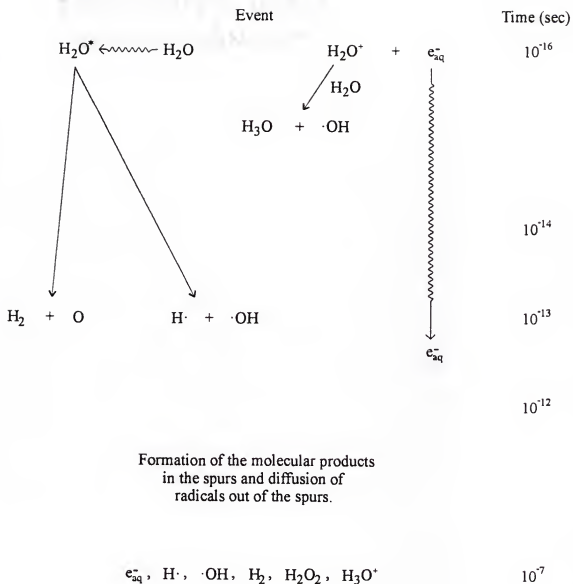


Figure (8) Representation of the events and time scale for the irradiation of water.

In the case of radiolysis, the extent of decomposition of water is measured in G-values,  $G(x)$ , where  $x$  represents a species either produced or consumed during the irradiation process per 100 eV of energy absorbed. The G-values for irradiation of water from high-energy accelerators are well established. Also, with low linear energy transfer, LET, and at medium pH (between ca. 3 and 11), the G-values are relatively constant. The term LET describes the characteristic value of the linear energy transfer parameter of the target substance along the length of the radiation path of a given projectile. Gamma rays and fast electrons have low LET values. Alpha particles have high LET values and fission fragments have very high LET values. The G-values for water radiolysis, given by Dragonic [55] are as follows:  $e_{aq}^-$ , 2.63;  $\cdot OH$ , 2.72;  $H$ , 0.55;  $H^+$ , 2.63;  $H_2$ , 0.45;  $H_2O_2$ , 0.68; and  $HO_2$ , 0.026 (in units of molecules/100eV).

A major feature that must be considered when performing pulse radiolysis experiments on aqueous solutions using the Febetron 706 is the consequence of the indirect effect. The incoming electron from the irradiation process causes the formation of ions and highly excited molecules in isolated pockets along the track of the radiation [52]. These pockets are referred to as spurs, as mentioned above. Although radical-solute reactions can occur in the spurs at higher concentrations, the G-values given above can be considered accurate enough for solutions that have solute concentrations at or below about 0.01 molar and are near neutral in pH [47]. Reaction of substrate is a secondary process involving reaction with the intermediate species (radicals) after diffusion from the spurs and tracks.

## Creating Totally Oxidizing or Totally Reducing Conditions

Based on G-values of the transient species produced in pulse radiolysis of water, the resulting solution will have approximately equal quantities of aqueous electron and OH radical. G-values for both are approximately equal,  $e_{aq}^- = 2.63$  molecules/100eV and  $\cdot OH = 2.72$  molecules/100eV; as noted above. It is a mistake however, to assume that an aerated solution has relatively equal oxidizing and reducing capacities because dissolved oxygen reacts very fast with the aqueous electron. The resulting  $O_2^-$  ion lowers the reducing ability of the solution, and often increases the oxidizing ability of the solution.

An initially air saturated solution can be made approximately equally oxidizing and reducing by purging the oxygen from the system by bubbling gaseous nitrogen or argon through the aqueous solution for about 20 minutes prior to subjecting the sample to pulse radiolysis. When subjected to the pulse, a solution with no dissolved oxygen will be approximately as strongly oxidizing as it is reducing. Although the primary yields of aqueous electron and OH radical are the same for an air saturated solution and for a degassed solution, the effective yield for the oxidation or reduction of a solute can be greatly influenced by deaerating. The net yield for the aqueous electron in the case of the air-saturated solution is essentially zero relative to the case of a degassed solution due to reaction of aqueous electron with oxygen in the initial stages of the process.

Pulse radiolysis of aqueous solution also produces hydrogen atom. When studying fast reactions, reaction of substrate with hydrogen atoms can usually be neglected. This is partially because the G-value of the OH radical and the aqueous electron are both about 5 times greater than the G-value for the hydrogen atom. But, more importantly, H atoms are much less reactive than the OH radical. Rate constants

for reactions of H atom are often 3 to 4 orders of magnitude smaller than rate constants for reactions of OH radical [33].

Most of the studies done for this work required either strictly oxidizing or strictly reducing conditions. For a solution to be either strictly oxidizing or strictly reducing, it must contain either OH radicals or aqueous electrons, but not both. There are several procedures that can be used to render an aqueous solution either totally oxidizing or totally reducing. These procedures must be done prior to exposure to the incident radiation.

### **Totally oxidizing conditions**

Totally oxidizing conditions can be accomplished by bubbling nitrous oxide through the solution for ca. 15 to 20 minutes. After passing  $N_2O$  through the solution for this time period at 1 atmosphere, the solution is saturated, with an  $N_2O$  concentration of 0.025 molar [33]. Nitrous oxide reacts with  $e_{aq}^-$  via Reactions (71) and (44) [26].



The overall reaction, the sum of Reactions (71) and (44), gives Reaction (54).



At first glance it appears that this method doubles the G-value for  $\cdot OH$ . The method, however, actually increases the G-value slightly more than double due to a change in the interactions that take place within the spurs [26]. At low concentrations of substrate (below 0.01 M), the difference is about two percent more than the sum of the G-values of  $e_{aq}^-$  and OH radical [56].

### Totally reducing conditions

A common and very convenient method to create effectively reducing conditions in solution is to convert the OH radicals to a less reactive species. This can be accomplished by adding a species to the solution prior to pulsing that will react quickly with OH radical, forming a secondary, less reactive radical. There are many additives that can be used to accomplish this. However, lower molecular weight alcohols function very well for this purpose; they are both cheap and effective. A particularly good reagent for creating totally reducing conditions is tert-Butanol (2-Methyl-2-propanol), which reacts with OH radical via Reaction (72), with a rate constant  $k = 6 \times 10^8 \text{ M}^{-1} \text{ s}^{-1}$  [55].



The rate constant for reaction of the t-butanol with  $e_{\text{aq}}^-$  is small as required.

Due to a moderately fast rate constant, coupled with a relatively high additive concentration (0.10 M), reaction of tert-butanol with OH radical will predominate in the early stages of the pulse radiolysis process. This causes the consumption of OH radical without affecting the G-value for aqueous electron. Thus, reaction of OH radical with a second dissolved substrate at a millimolar concentration can be neglected. Since the OH radical is eliminated on a short time scale while the concentration of  $e_{\text{aq}}^-$  is left essentially untouched in the presence of the solute and the less reactive tert-butanol radical, reaction of  $e_{\text{aq}}^-$  with the solute can be studied without the interference by OH radical.

### CHAPTER THREE STOPPED-FLOW APPARATUS

A Durrum Stopped-Flow Spectrophotometer, Model D-110, Durrum Instrument Corporation, 3950 Fabian Way, Palo Alto, California, 94303, was used for all of the stopped-flow experiments. The components of the stopped-flow apparatus can be separated into three major classifications. The solution flow system consists of a pneumatic plunger, two reaction solution reservoirs, two reaction solution injectors, and reaction chamber which doubles as a cuvette, and a stop syringe that also triggers the computer to start storing data. This system is used for the rapid mixing of reacting liquids or solutions. The light source, monochromator and photo-multiplier tube are used collectively to measure the time dependent optical absorption data and, combined, constitute the measuring system. And the third component consists of a computer system with an analog to digital converter, which function as the data acquisition system. The computer and analog to digital converter plug-in board was used to measure the signal from the photo-multiplier tube and process the data into a digital format for further analysis.

The original computer system and the triggering mechanism associated with the stopped-flow apparatus were both inoperable at the time the system was acquired. The original computer, a North Star system, that accompanied the stopped-flow apparatus was equipped with a Zilog Z-80 chip, and had a plug-in type analog to digital converter on the

S-100 bus. The computer was successfully repaired, but the trigger mechanism could not be made to work, lacking adequate circuit diagrams and instructions.

The original computer was replaced by an updated PC with a 12-bit analog to digital converter installed on the system bus. The computer was an IBM compatible PC/XT computer equipped with an Intel Inboard 80386-80387 CPU board, made available for the purpose of this work by Dr. Robert J. Hanrahan. The analog to digital converter system was a no-brand IBM PC compatible card with little documentation except programming notes. However, it is quite similar to a model 5500MF, 8-channel, 12 bit A/D I/O board with counter/timer made by the American Data Acquisition Corporation of Woburn, Maryland. A new electromechanical trigger mechanism based on a standard microswitch was fabricated and installed on the stopped-flow apparatus. The computer system and the triggering mechanism, constructed and fitted to the instrument, are discussed in detail below.

### **Flow System**

The primary objective of the flow system section of the Durrum Stopped-Flow apparatus is to accomplish rapid mixing of two reacting liquids or solutions. With rapid mixing, the solutions reach a state that is essentially homogeneous within a short period of time, about 1 to 2 milliseconds. The flow system is principally composed of a pneumatically operated plunger, reservoir syringes, injector syringes, mixing jets, a reaction chamber that also functioned as a cuvette, a stop syringe, and all of the necessary valves to allow filling and draining. The stop syringe functions so as to trip the triggering mechanism. The flow system is shown in detail in Figure (9).



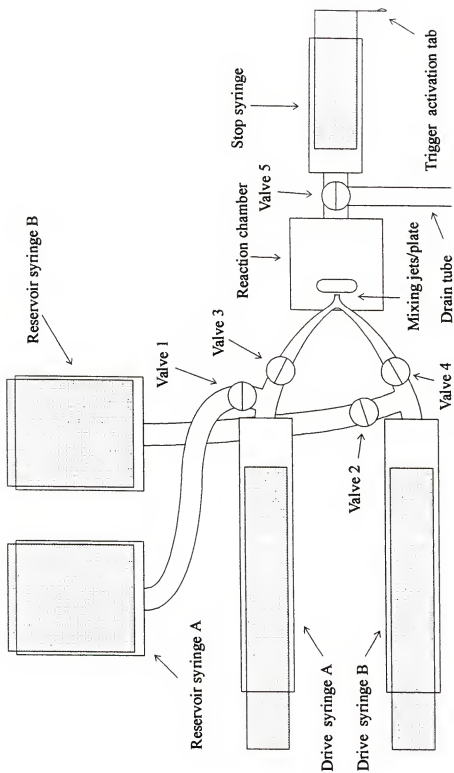


Figure (9). Flow system of the Durrum stopped-flow apparatus. For clarity, the drive piston and other components are not shown.

Two reservoir syringes supply the reacting solutions to the injector syringes A and B separately during the preparation procedure before each experimental run. Each reservoir syringe has a capacity of 20 mL.

The flow actuator drive unit is pneumatically operated and works under pressure of 60 psi. It drives the plunger, which drives both injector syringes at equal rates. With the present set-up, the injector syringe drive rate is 30 mL/second [49]. At this drive rate, solutions with a relative viscosity of 1.0, such as most aqueous solutions, mix to an extent of approximately 99.5 percent completion within two milliseconds. Therefore, the reaction can be monitored accurately starting 2 ms after the plunger has driven the solutions into the reaction chamber. The unavailable time period after activating the plunger is called the dead time.

When operated by the pneumatic plunger, the filled injector syringes force the two reacting solutions into a single conduit, which is immediately directed against a "plate" as a liquid jet. The majority of the mixing takes place in the reaction chamber, which also functions as a cuvette. The reaction chamber currently in use has a path length of 20 mm which is perpendicular to the flow axis, and in line with the analyzing light beam. It is possible to use injector syringes with different inner diameter barrels to give different relative amounts of reacting solutions in the reaction chamber. The barrels used in this laboratory were of the same inner diameter.

The last sub-component of the flow system is the stop syringe. It is also a part of the triggering system and is activated by the outgoing solution from the reaction chamber. Before activating the pneumatic plunger, the reaction chamber is typically filled with one of the reacting solutions. When the plunger is activated, the solution occupying the

reaction chamber is forced out of the chamber by the incoming solutions from the injector syringes, and goes directly into the stop syringe. This causes the rapid filling of the stop syringe, and the extension of the stop syringe plunger. The stop syringe plunger activates the trigger when fully extended.

### **Measuring System**

The system used to measure absorption by reactants or products in the reaction chamber is composed of a light source, a monochromator, a photo-multiplier tube and the electronics associated with the amplification of the PM-tube signal. A diagram representing the stopped-flow apparatus in its entirety is shown in Figure (10).

The optical absorbance subsystem of the stopped-flow apparatus was in working order when the equipment was brought into this laboratory and was used as is. The analyzing range of the combination of the appropriate analyzing light (tungsten or deuterium lamp), the monochromator, and the photo-multiplier tube is from 180 nm to 1000 nm. All measurements made in the present study were made at 584 nm, well within the working range of the system.

### **Data Acquisition System**

An analog to digital converter and computer system was connected to the output for the photo-multiplier tube and associated electronics for the purpose of data acquisition and analysis. The analog to digital converter was an IBM compatible 12-bit AD/DA card capable of monitoring 16 channels. It is an IBM PC bus compatible card that is very similar to the model 5500MF, 8 channel 12 bit A/D 16 digital I/O, counter/timer made by

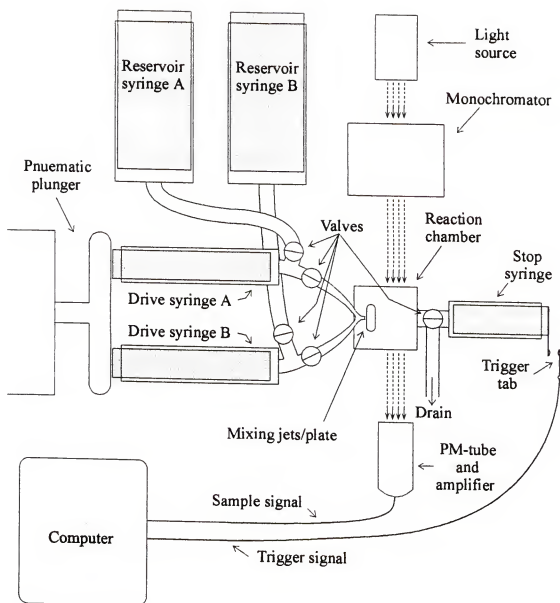


Figure (10). Representation of the Durrum stopped-flow apparatus.

the American Data Acquisition Corporation, Woburn, Maryland, available for \$195. One channel of the analog to digital converter was assigned as the trigger channel and a second channel was used to monitor the optical signal. The other channels were not used.

The time base of the AD/DA board was derived from the CPU clock of the data acquisition computer. The computer used was a standard IBM-compatible PC that had originally been equipped with an Intel 8088 CPU chip, but had been fitted with an Intel Inboard 80386-80387 CPU board. With this system, the modified computer, and the AD/DA converter, the shortest measurable time increment was 0.310 milliseconds. This time period is shorter than the stopped-flow dead time mentioned earlier.

The locally modified triggering mechanism of the stopped-flow apparatus was equipped with a micro-switch and a battery pack. The micro-switch was mounted on a bracket, which was fabricated from aluminum and attached to the wall of the base of the stopped-flow apparatus, Figure (11). An extended tab was added to the stop syringe to aid in activating the micro-switch. A 6-volt battery pack consisting four AA batteries was used to supply the trigger signal power to the analog to digital board when the stopped-flow was activated. The trigger circuit design is shown in Figure (12). Note that the arrangement included both the automatically activated trigger as well as a manually activated trigger used for calibration purposes. The computer was set to store data when the manual trigger was closed momentarily.

A data acquisition computer program was written and compiled in Microsoft QuickBasic to control the analog to digital converter and the computer system for data acquisition in the stopped-flow experiments. The source program is given in Appendix A. The program had several subroutines. The subroutines were designed for calibration

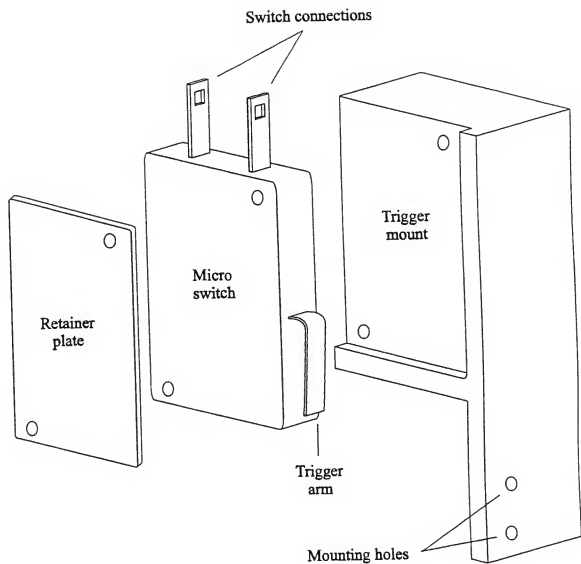


Figure (11). Trigger mounting block. The micro-switch was set between the mounting block and plate aluminum for added stability.

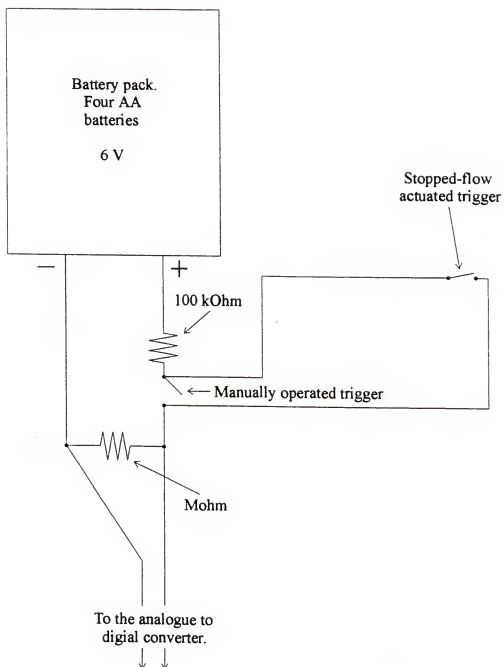


Figure (12). Wiring diagram of the trigger circuit devised for the Durrum stopped-flow apparatus.

of the system, data acquisition, graphing, storing data files to disk, and loading previously taken data sets from disk to computer memory. Some of the subroutines were borrowed from the data acquisition program written for pulse radiolysis work using the WAAG II analog to digital converter and earlier data acquisition systems of the Febetron 706.

Further details will be given in the next section.

### **Operation of the Computerized Durrum Stopped-Flow System**

The routine operation of the stopped-flow apparatus required several steps. A representation of the entire stopped-flow apparatus is shown in detail in Figure (10). Solutions to be used for reactions were prepared and stored in the reservoir syringes. In the rinsing the flow system in preparation for use, all appropriate valves were opened or closed as needed. Aliquots of each solution, call them solution A and solution B, were used to rinse and fill the injector syringes. The reaction chamber was left full of either solution A or solution B. Full-light and no-light signals were measured. The full-light signal is the voltage on the PM-tube with a sample blank in the sample holder, and the no-light signal is the signal with the light path blocked with opaque paper. The full-light signal and no-light signal were used in later calculations to determine the intensity of the light. The computer program was set in a stand-by loop, alternately measuring the optical signal and the trigger signal. A kinetic run was initiated by activating the pneumatic plunger, driving the injector syringes delivering reactant solutions to the reaction chamber. The computer monitored the signal for 512 data points at predetermined time periods, then terminated. The data set was automatically stored in computer memory.



The action of rinsing the injector syringes also rinsed the reaction chamber because the output of the injector syringes flowed through the reaction chamber. The rinse was done with alternate the solutions, rinsing first with one reactant solution, then the other reactant solution. This left the reaction chamber containing only one solution after the rinse procedure was complete. The stop syringe was set in the closed position (the ready position) containing no liquid before the rinse procedure. After rinsing, the reaction chamber and all of the flow system from the plunger up to but not including the stop syringe were filled with solution.

From the main menu of the computer program, the calibration mode was entered in order to set the no-light and full-light signal intensities. While in this mode, the program displayed a graphical box on the screen. The program then entered a loop in which it repeatedly measured the signal from the photo-multiplier tube, displayed the result on the screen as a dot on a graph, and checked the trigger signal. Every time the computer went through the loop, it added a new data point to the graph and checked for the trigger signal. The program began the display at the far left of the graphical box, and continued across the screen toward the right hand side. When the graphical box was full, the program cleared the screen and began the display process again.

While in this mode, the voltage applied to the photo-multiplier tube was adjusted manually. The light intensity signal was displayed at the bottom of the screen when the light-path to the photo-multiplier tube was not blocked (full-light signal) and the signal was displayed at the top of the screen when the light path was blocked (no-light signal). The maximum optical intensity was thereby adjusted to give the full-light signal at the bottom of the screen while the no-light signal was displayed at the top of the screen.

After adjusting the PM-tube voltage as described, the light path was blocked and a manually operated trigger activated. The program then read and stored in computer memory 512 data points as the no-light signal. The light path was then unblocked and 512 data points were measured and stored as the full-light signal. The program also calculated and displayed the average no-light and full-light signals, and waited for a prompt from the operator to either re-determine the full-light and no-light signals or to accept the values and return to the main menu. After acceptance of the full-light and no-light signals, the apparatus was ready for initiation of a stopped-flow run. A typical figure representing the full-light and no-light signals and the signal from the absorption of a product species while an experiment was in progress is shown in Figure (13). This is not seen in practice since the calibration and data acquisition experiments are performed separately.

Once the flow system was filled with solutions to be studied and the no-light and full-light signals had been measured, the system was ready for an experimental run. The data acquisition subroutine was entered from the main menu of the program. When the actuate button on the stopped-flow apparatus was pushed, the pneumatic plunger drove both injector syringes A and B simultaneously, injecting the reactants into the reaction chamber. Solutions A and B mixed at the mixing jet/plate in the reaction chamber. The solution that had previously occupied the reaction chamber was driven into the stop syringe by the incoming solutions, forcing the stop syringe plunger to the rear, full position. An extension tab attached to the stop syringe plunger activated the stationary micro-switch, closing the trigger circuit, thereby signaling the computer to measure and store 512 data points at the predetermined time increments. The computer then displayed

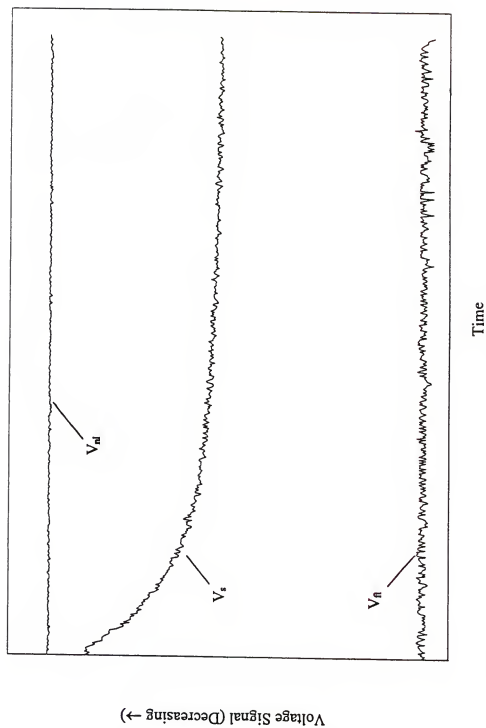


Figure (13) Representative screen display for a stopped-flow experiment. The upper line,  $V_{nl}$ , is the no-light signal, the lower line,  $V_n$ , is the full-light signal, and the curve,  $V_s$ , represents the product formation during a typical reaction.

a graph of the voltage versus time and waited for a prompt to accept or reject the data. A typical data acquisition graph is shown in the Figure (13),

After taking the data set, the main menu was accessed. From the main menu the data could be saved as a file and the data acquisition subroutine could be brought up again to do another experiment using the previously measured no-light and full-light values, or the no-light and full-light signals could be measured again. Other options available at the main menu were plotting of the data set and routine data manipulations based on zero, first, or second order kinetics. For kinetic analysis, any desired portion of the data set could be selected using software cursors. After several data sets were measured, the solutions in the reservoir syringes were changed and the whole process was started over again.

## CHAPTER FOUR

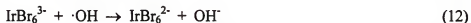
### STABILITY OF AQUEOUS HEXABROMOIRIDATE

There have been several previous studies regarding the first step of aquation reaction of  $\text{IrBr}_6^{3-}$  in aqueous solution, Reaction (73) [57-61].



However, there is considerable disagreement in the literature regarding the details of the aquation reaction and the relative stability of  $\text{IrBr}_6^{3-}$  dissolved with and without additional  $\text{Br}^-$  in aqueous solution.

In connection with their studies in this laboratory on the application of  $\text{IrCl}_6^{3-}$  and  $\text{IrCl}_6^{2-}$  to collection of solar energy, M. R. Gholami and C. L. Crawford conducted a preliminary investigation on aqueous solutions of  $\text{IrBr}_6^{3-}$  and  $\text{IrBr}_6^{2-}$ . In their studies, Gholami and Crawford looked at the possible reduction of  $\text{IrBr}_6^{3-}$  to  $\text{IrBr}_6^{4-}$  and oxidation of  $\text{IrBr}_6^{3-}$  to  $\text{IrBr}_6^{2-}$  during pulse radiolysis experiments. The respective processes are represented by Reactions (11) and (12).



In one of the pulse radiolysis experiments conducted by Gholami and Crawford, an increase of absorbance caused by reaction of OH radical with  $\text{IrBr}_6^{3-}$  under totally oxidizing conditions was observed at several wavelengths. A 350 Watt Xenon arc lamp was used to observe the process from 470 nm to 630 nm, while a 100-Watt Halogen lamp

was used for range from 500 nm to 730 nm. As seen in Figure (14), the product spectrum is very similar to the spectrum of a known sample  $\text{IrBr}_6^{2-}$ .

Gholami and Crawford estimated from their pulse radiolysis experiments that the rate constant for the reaction of  $\text{IrBr}_6^{3-}$  with  $e_{aq}^-$ , Reaction (11), was  $2.6 \times 10^9 \text{ M}^{-1} \text{ s}^{-1}$  and the rate constant for reaction of  $\text{IrBr}_6^{3-}$  with OH radical, Reaction (12), was  $1.4 \times 10^9 \text{ M}^{-1} \text{ s}^{-1}$ .

Zuoquian Li, while working in this laboratory as a visiting scientist from China, studied the stability of  $\text{IrCl}_6^{3-}$  and  $\text{IrCl}_6^{2-}$  complexes in aqueous solutions [20]. Mr. Li determined that the plus four state of the iridium chloride complex was considerable more stable than the iridium chloride complex in the plus three state. Based on these observations, it was provisionally assumed that both of the iridium bromide complexes were stable for a long enough period of time to perform all of the experiments connected with the pulse radiolysis studies. Certain published studies, however, contradicted that assumption, but the amount of information about the aquation reaction of  $\text{IrBr}_6^{3-}$  aqueous solution was limited and inconsistent.

The best data concerning conversion of  $\text{IrBr}_6^{3-}$  to  $\text{IrBr}_5\text{H}_2\text{O}^{2-}$  comes from Melvin and Haim [59]. Their studies were concerned with reactions of hexabromoiridate (IV) with chromium (II) and with pentacyanocobaltate (II). However, part of their investigation involved the kinetics of the conversion of  $\text{IrBr}_6^{3-}$  in aqueous solution to  $\text{IrBr}_5\text{H}_2\text{O}^{2-}$ , Reaction (73). They determined that the value for the forward rate constant of Reaction (73), at 25 °C and in the presence of 1.00 M  $\text{HClO}_4$ , was  $6.2 \times 10^{-4} \text{ s}^{-1}$ . The half-life for  $\text{IrBr}_6^{3-}$  based on the rate constant is about 19 minutes at 25 °C. The

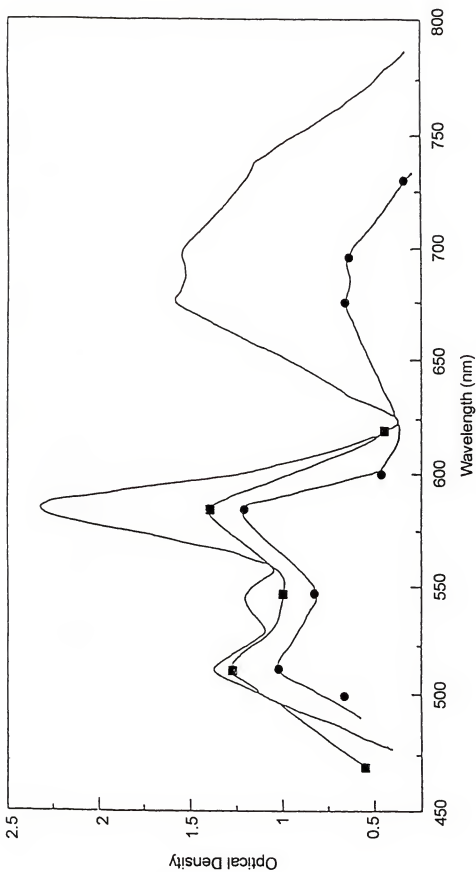


Figure (14). Comparison of the absorption spectra of  $\text{IrBr}_6^{2-}$  in 0.1 M aqueous KBr solution (—), pulse irradiated  $\text{N}_2\text{O}$  saturated solution of 0.1 mM  $\text{IrBr}_6^{3-}$  using a 350 W Xenon arc lamp (■), and a 100 W Halogen lamp (●). This work was done by Mr. Charles Crawford in this laboratory.

researchers made no reference to the rate constant for the reverse reaction, Reaction (74), or to the equilibrium constant for Reaction (73).



Kravtsov and his group found that the presence of the doubly charged cations,  $\text{Ca}^{2+}$ ,  $\text{Ba}^{2+}$ , and  $\text{Cd}^{2+}$ , slowed the aquation reactions of  $\text{IrBr}_6^{3-}$  [57] and of  $\text{IrBr}_6^{2-}$  [62] considerably. They also found that the presence of singly charged cations at concentrations equal to or greater than 0.1 M decreased the rate for the aquation reaction of  $\text{IrBr}_6^{3-}$ . They also made no mention of the reverse rate constant or equilibrium constant.

DeFelippis, et al. stated that the  $\text{IrBr}_6^{3-}$  ion can be stabilized by the presence of 0.1 M  $\text{Br}^-$  ion [60]. However, they were using the iridium complex as a competing reagent to help in the determination of the rate constant for an entirely different reaction, and their study was not centered on the stability of  $\text{IrBr}_6^{3-}$ . They made no statements regarding the identity of the counter cation or cations that were co-dissolved with  $\text{IrBr}_6^{3-}$ . It is conceivable that the use of 0.1 molar or somewhat lower concentrations of  $\text{NaBr}$  in solution would have a stabilizing effect due to both the sodium ion as studied by Kravtsov, et al., and the bromide ion, based on Le Chatlier's Principle and the common ion effect.

Consideration of the above review of the available literature on the stability of  $\text{IrBr}_6^{3-}$  made it obvious that it was necessary to initiate studies of the stability of  $\text{IrBr}_6^{3-}$  solutions as described below. However, a brief study of the stability of  $\text{IrBr}_6^{2-}$  was also carried out. During this experiment, the stability of  $\text{IrBr}_6^{2-}$  was verified using a solution that was approximately 0.25 mM in  $\text{K}_2\text{IrBr}_6$ . Ultraviolet-visible spectra of the solution



were measured over a period of 10 days. The spectrum showed some deterioration over time, but the degradation of the spectrum was very slow and did not deteriorate more than about 3 or 4 percent per day. Based on this experiment,  $\text{IrBr}_6^{2-}$  was determined to be relatively stable over a time period of several days.

### **Chemical Dynamics of Solutions Containing $\text{Br}_2$ , $\text{Br}^-$ and $\text{IrBr}_6^{3-}$**

An investigation was carried out to determine the stability of  $\text{IrBr}_6^{3-}$  in the presence of a 0.025 M NaBr solution, a somewhat smaller concentration of NaBr than used by DeFelippis et al. [60]. A bromide concentration as high as 0.1 M would have interfered with the desired studies of the reactions of  $\text{IrBr}_6^{3-}$  with OH radicals and with  $\text{Br}_2$ . It was thought that if conversion of  $\text{IrBr}_6^{3-}$  to  $\text{IrBr}_5\text{H}_2\text{O}^{2-}$ , Reaction (73), displayed adequate equilibrium characteristics, it may be possible to stabilize a solution of  $\text{IrBr}_6^{3-}$  by the addition of bromide ion at a concentration slightly smaller the 0.1 M concentration studied by DeFelippis, et al. It was thought that the added stabilizing effect of the bromide and sodium ions would possibly be sufficient for our purposes. In the application of bromide ion to the pulse radiolysis experiments, a 25/1  $\text{Br}^-/\text{IrBr}_6^{3-}$  ratio was the maximum ratio that could have been tolerated due to potential reaction of OH radical with  $\text{Br}^-$  rather than  $\text{IrBr}_6^{3-}$ .

### **Solutions of $\text{Br}_2$ and $\text{Br}^-$**

To understand the kinetic basis of the system used to study the stability of  $\text{IrBr}_6^{3-}$ , it is first necessary to consider the dynamics of a solution of  $\text{Br}_2$  in the presence of  $\text{Br}^-$  ion. The mixing of a solution containing  $\text{Br}_2$  with a solution containing  $\text{Br}^-$  ion results in

the reversible formation of tribromide ion, Reactions (55) and (56).

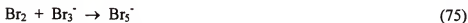


Ramette and Palmer determined the formation constant of tribromide according to Reaction (55) as 16.73 [63]. A slightly higher value of 16.85 was published in "Halogen Chemistry" [64]. An intermediate value of 16.8 was used in the present work. The rate constant for the forward reaction, Reaction (55), is reported by Marie-Françoise Ruasse et al. as  $1.5 \times 10^9 \text{ M}^{-1} \text{ s}^{-1}$  [45]. Using the standard relation  $k_f/k_r = K_{eq}$ , with  $K_{eq}$  of 16.8 and  $k_r$  of  $1.5 \times 10^9 \text{ M}^{-1} \text{ s}^{-1}$ , the rate constant for the reverse reaction, Reaction (56), was found to be  $8 \times 10^7 \text{ s}^{-1}$ .

There was a discrepancy in the rate constant for Reaction (56) reported by Marie-Françoise Ruasse et al. Through personal correspondence with Marie-Françoise Ruasse, it was realized that the reported value of  $5 \times 10^7 \text{ s}^{-1}$  for Reaction (56) was incorrect. This was a preliminary value which their group measured early in research program and was not intended for publication. The value they intended to publish was  $8 \times 10^7 \text{ s}^{-1}$ , as we had also concluded. From this value, they obtained their value of  $1.5 \times 10^9 \text{ M}^{-1} \text{ s}^{-1}$ , as mentioned above.

The Reaction pair (55) and (56) constitute an equilibrium system which favors production of  $\text{Br}_3^-$  because the rate constant for the formation of  $\text{Br}_3^-$ , Reaction (55), is 16.8 times the rate constant for dissociation, Reaction (56). Therefore, addition of  $\text{Br}_2$  to a solution with a relatively high concentration of  $\text{Br}^-$  would immediately result in the formation of tribromide ion, leaving little  $\text{Br}_2$  in solution.

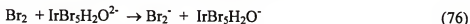
Pentabromide ion also forms in an aqueous mixture of  $\text{Br}^-$  and  $\text{Br}_2$ , Reaction (75) [65].



Although the equilibrium constant for this reaction is fairly high, 37.7 [63], the reaction is unimportant if the  $\text{Br}_2/\text{Br}^-$  ratio is kept small. The production of  $\text{Br}_5^-$  was neglected in the systems studied here.

### Solutions of $\text{Br}_2$ , $\text{Br}^-$ , and $\text{IrBr}_6^{3-}$

The reduction potential of the couple  $\text{IrBr}_5\text{H}_2\text{O}^-/\text{IrBr}_5\text{H}_2\text{O}^{2-}$  is considerably more positive (favorable) than the reduction potential of the couple  $\text{IrBr}_6^{2-}/\text{IrBr}_6^{3-}$  [66, 67]. Accordingly, oxidation of  $\text{IrBr}_6^{3-}$  to  $\text{IrBr}_6^{2-}$  is more favorable than oxidation of  $\text{IrBr}_5\text{H}_2\text{O}^{2-}$  to  $\text{IrBr}_5\text{H}_2\text{O}^-$ . Nevertheless, the published redox potentials predict that  $\text{Br}_2$  will react with  $\text{IrBr}_5\text{H}_2\text{O}^{2-}$  to give  $\text{IrBr}_5\text{H}_2\text{O}^-$ , Reactions (76) and (77). The corresponding two-electron process is represented by Reaction (78).



Although it is predicted that the two-electron redox reaction of  $\text{Br}_2$  with  $\text{IrBr}_5\text{H}_2\text{O}^{2-}$  is favorable, it is not clear through calculations based on reduction potentials whether the one-electron reaction of  $\text{Br}_2$  with  $\text{IrBr}_5\text{H}_2\text{O}^{2-}$ , followed by a second one-electron transfer reaction to form  $\text{Br}^-$  and  $\text{IrBr}_5\text{H}_2\text{O}^-$ , Reactions (76) and (77) is favorable. The main difficulty is that the redox potential for the formation of  $\text{Br}_2^-$  ion is not well established; several incompatible values can be found in the literature. However, during stopped-flow

studies in this laboratory, the reaction was found to be fast, as discussed further below.

In any event, oxidation by  $\text{Br}_2$  in the case of  $\text{IrBr}_5\text{H}_2\text{O}^{2-}$  should occur at a slower rate than oxidation of  $\text{IrBr}_6^{3-}$  because of the disparity between the respective oxidation potentials.

The oxidation reactions of  $\text{IrBr}_6^{3-}$  and  $\text{IrBr}_5\text{H}_2\text{O}^{2-}$  by both  $\text{Br}_2$  and  $\text{Br}_3^-$  in aqueous solution have been successfully carried out. The experiments will be discussed thoroughly later. However, for the present discussion it should be noted that the processes were found to occur favorably based on the experimentation discussed later. Theoretical aspects of these oxidation reactions will now be discussed.

The two-electron reduction potentials in aqueous solution of tribromide ion and bromine, Reactions (79) and (80), are 1.0874 V and 1.0503 V, respectively [68].



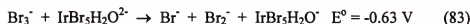
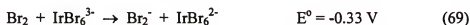
The reduction potentials for  $\text{IrBr}_6^{2-}/\text{IrBr}_6^{3-}$  and  $\text{IrBr}_5\text{H}_2\text{O}^-/\text{IrBr}_5\text{H}_2\text{O}^{2-}$  are 0.84 V and 0.970 V, respectively [67]. Using the two-electron reduction potential for bromine and the reduction potentials of  $\text{IrBr}_6^{2-}$  and  $\text{IrBr}_5\text{H}_2\text{O}^-$ , the standard two-electron cell potentials for  $\text{Br}_2$  reaction with  $\text{IrBr}_6^{2-}$  and with  $\text{IrBr}_5\text{H}_2\text{O}^-$  were calculated to be 0.25 V and 0.117 V, respectively. Using the two-electron reduction potential for tribromide ion and the reduction potentials of  $\text{IrBr}_6^{2-}$  and  $\text{IrBr}_5\text{H}_2\text{O}^-$ , the standard two-electron cell potentials for  $\text{Br}_3^-$  reaction with  $\text{IrBr}_6^{2-}$  and with  $\text{IrBr}_5\text{H}_2\text{O}^-$  were calculated to be 0.21 V and 0.080 V, respectively. All of the potentials listed above are favorable. However, the two-electron reduction of either  $\text{IrBr}_6^{2-}$  or  $\text{IrBr}_5\text{H}_2\text{O}^-$  by either  $\text{Br}_2$  or  $\text{Br}_3^-$  necessarily involves three molecules of reactant in either case. The corresponding kinetic expressions would therefore be ter-molecular, which is rarely encountered in practice. Accordingly, an

examination of the relevant one-electron reactions and their respective reduction potentials is warranted.

The chemical equations for the one-electron reduction potentials of  $\text{Br}_2$  and  $\text{Br}_3^-$  can be given as:



The standard cell potentials were calculated using literature values for the half-cell potentials. The half-cell potential for  $\text{IrBr}_5\text{H}_2\text{O}^-/\text{IrBr}_5\text{H}_2\text{O}^{2-}$  is 0.970 V [67]. The one-electron half-cell potential for  $\text{Br}_3^-/(\text{Br}^-, \text{Br}_2^-)$  is 0.34 V. This half-cell potential was calculated from the two-electron half-cell potential for  $\text{Br}_3^-/\text{Br}^-$  of 1.0503 V [68] and the one-electron reduction potential for  $\text{Br}_2/\text{Br}_2^-$  of 1.66 V, taken as a selected value from several sources, [69-77]. The one-electron cell potential for  $\text{Br}_2/\text{Br}_3^-$  of 0.510 V was taken as an average value from the literature [69-73]. The one-electron cell potentials were calculated to be:  $\text{Br}_2/\text{IrBr}_6^{3-}$ , -0.33 V;  $\text{Br}_2/\text{IrBr}_5\text{H}_2\text{O}^{2-}$ , -0.46 V;  $\text{Br}_3^-/\text{IrBr}_6^{3-}$ , -0.50 V;  $\text{Br}_3^-/\text{IrBr}_5\text{H}_2\text{O}^{2-}$ , -0.63 V. The corresponding cell reactions with their potentials obtained as described are:



Note that all four of the listed one-electron cell potentials are unfavorable under standard conditions as calculated. However, the actual cell potential should be considered for each one-electron reaction case using concentrations of the experiments

carried out, as opposed to one molar concentrations. For the one-electron reaction of  $\text{Br}_3^-$  with  $\text{IrBr}_6^{3-}$  or with  $\text{IrBr}_5\text{H}_2\text{O}^{2-}$ , the cell potential can be determined using Equation (1):

$$E = E^\circ - 0.0592V \log \frac{[\text{Ir}(IV)][\text{Br}^-][\text{Br}_2^-]}{[\text{Ir}(III)][\text{Br}_3^-]} \quad (1)$$

The cell potential for the one-electron reaction of  $\text{Br}_2$  with  $\text{IrBr}_6^{3-}$  or with  $\text{IrBr}_5\text{H}_2\text{O}^{2-}$  can be determined using Equation (2).

$$E = E^\circ - 0.0592V \log \frac{[\text{Ir}(IV)][\text{Br}_2^-]}{[\text{Ir}(III)][\text{Br}_2]} \quad (2)$$

Although the standard cell potentials for one-electron reactions of  $\text{Br}_2$  and  $\text{Br}_3^-$  with  $\text{IrBr}_6^{3-}$  and  $\text{IrBr}_5\text{H}_2\text{O}^{2-}$  are all unfavorable, it can be seen from Equations (1) and (2) above that the intermediate, dibromide ion, present in trace level concentrations, is in the numerator and that the concentration of  $\text{Br}_2^-$  is small throughout the reaction. Thus, the logarithm term in Equations (1) and (2) are not only positive, but are probably large enough throughout the reaction process for the reaction to be favorable.

From these considerations, it was expected that both bromine and tribromide ion would react with  $\text{IrBr}_6^{3-}$  or with  $\text{IrBr}_5\text{H}_2\text{O}^{2-}$ . The reduction potentials above suggest that the reaction of  $\text{Br}_3^-$  with  $\text{IrBr}_6^{3-}$  and with  $\text{IrBr}_5\text{H}_2\text{O}^{2-}$  would be slower than reaction of  $\text{Br}_2$  with  $\text{IrBr}_6^{3-}$  and with  $\text{IrBr}_5\text{H}_2\text{O}^{2-}$ . A simple polarity argument also suggests that reaction of a negatively charged reductant with a negatively charged oxidant would be slower than a similar case of a neutral reductant with a negatively charged oxidant. It is obvious that the first pair would have electrostatic repulsion whereas the second pair would not.

## Experimental

A series of experiments was carried out to establish the stability of  $\text{IrBr}_6^{3-}$  in aqueous solution with respect to  $\text{IrBr}_5\text{H}_2\text{O}^{2-}$ . The rate of conversion of  $\text{IrBr}_6^{3-}$  to  $\text{IrBr}_5\text{H}_2\text{O}^{2-}$  was of interest, as well as the reactivity of these two species with  $\text{Br}_2$  and  $\text{Br}_3^-$ . In these experiments, a solution of bromine was added to a solution of  $\text{IrBr}_6^{3-}$  and  $\text{Br}^-$ . The bromine was added to the solution at a lower concentration than bromide ion, and was the limiting reagent with respect to reaction with bromide ion. Also in these experiments, the concentration of added  $\text{IrBr}_6^{3-}$  was smaller than the  $\text{Br}_2$  concentration. The concentration relations were  $[\text{Br}^-] > [\text{Br}_2] > [\text{IrBr}_6^{3-}]$ . Thus, considering the large rate constant for the bromine-bromide ion reaction,  $1.5 \times 10^9 \text{ M}^{-1} \text{ s}^{-1}$  [45], and the large excess of  $\text{Br}^-$  relative to  $\text{IrBr}_6^{3-}$ , the added bromine reacted primarily with  $\text{Br}^-$  rather than with the iridium-bromide complexes. In consequence, only a small amount of the  $\text{IrBr}_6^{3-}$  was oxidized by  $\text{Br}_2$ .

The absorbances at the peak wavelengths of  $\text{IrBr}_5\text{H}_2\text{O}^-$  (675 nm and 587nm) and  $\text{IrBr}_6^{2-}$  (696 nm, 676 nm, and 584 nm) are too close to be distinguished experimentally. When  $\text{IrBr}_6^{2-}$  and  $\text{IrBr}_5\text{H}_2\text{O}^-$  are co-dissolved, there is little interference of spectral features of  $\text{IrBr}_5\text{H}_2\text{O}^-$  with the  $\text{IrBr}_6^{2-}$  peaks at 546 nm and at 512 nm. To determine which species was present in solutions undergoing oxidation by  $\text{Br}_2$  or  $\text{Br}_3^-$ , the absorbance at 584 nm was compared to the absorbance at 512 nm. Although  $\text{Br}_3^-$  absorbs some light at 512 nm, the extinction coefficient is small and any interference is not enough to hinder an analysis for  $\text{IrBr}_6^{2-}$  and  $\text{IrBr}_5\text{H}_2\text{O}^-$ . The spectrum of  $\text{Br}_3^-$  was given by L. Raphael in "Bromine Compounds," edited by D. Price, B. Iddon, and B. J. Wakefield [65]. A series of three experiments was conducted to examine the

reaction of  $\text{IrBr}_6^{3-}$  to form  $\text{IrBr}_5\text{H}_2\text{O}^{2-}$  in the presence of  $\text{Br}^-$  which was revealed by subsequent oxidation with  $\text{Br}_2$  at various times, as explained in detail below.

Direct ultraviolet-visible spectrophotometric measurements were not feasible for the determination of the stability of  $\text{IrBr}_6^{3-}$  in aqueous bromide solution. The spectrum of  $\text{IrBr}_6^{3-}$  is featureless, Figure (15). However,  $\text{IrBr}_6^{2-}$ , is clearly identifiable from an ultraviolet-visible spectrum, Figure (16). The ultraviolet-visible spectra in Figures (15) and (16) were scanned using a Hewlett Packard 8450A Diode Array Spectrophotometer.

The method used to perform the series of experiments involved, first, the preparation of a stock solution of  $\text{Br}_2$  with a desired concentration of ca. 2 mM. The concentration of  $\text{Br}_2$  was determined to be 1.79 mM, calculated based on the absorbance at 390 nm and the extinction coefficient of  $172 \text{ M}^{-1} \text{ cm}^{-1}$  [65]. Next, a 1mM stock solution of  $\text{Na}_3\text{IrBr}_6$  that was also 25 mM in NaBr was prepared. Aliquots of the hexabromoiridate (III) solution were converted to solutions of hexabromoiridate(IV) by adding the  $\text{Br}_2$  solution. The expected result was the conversion of  $\text{IrBr}_6^{3-}$  to  $\text{IrBr}_6^{2-}$  by  $\text{Br}_2$  according to the reactions discussed above. It was known that  $\text{IrBr}_6^{3-}$  was unstable and reacts to form  $\text{IrBr}_5\text{H}_2\text{O}^{2-}$ , as described earlier. The residual  $\text{IrBr}_6^{3-}$  in the  $\text{Br}^-$  solution was oxidized using the bromine solution at specific time intervals after preparation of the  $\text{IrBr}_6^{3-}$  solution. Ultraviolet-visible spectra were scanned and examined at various times after preparation, as described below. The spectra were then qualitatively compared to the spectrum of freshly prepared  $\text{IrBr}_6^{2-}$ .



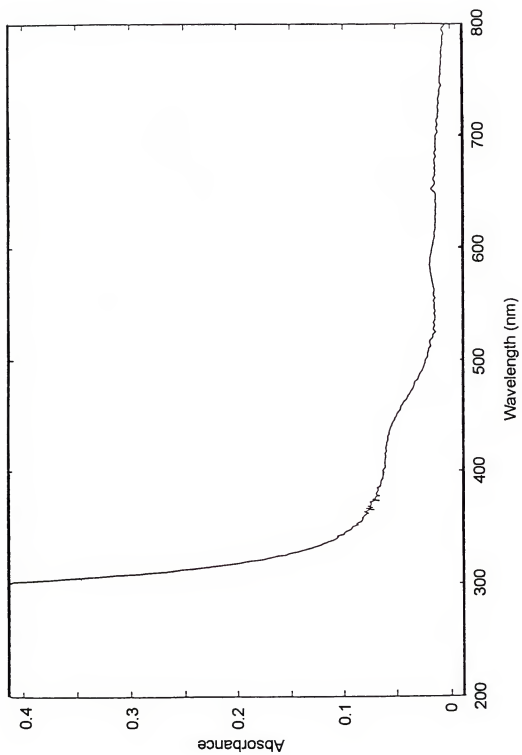


Figure (15). UV-visible spectrum of  $\text{IrBr}_6^{3-}$ .

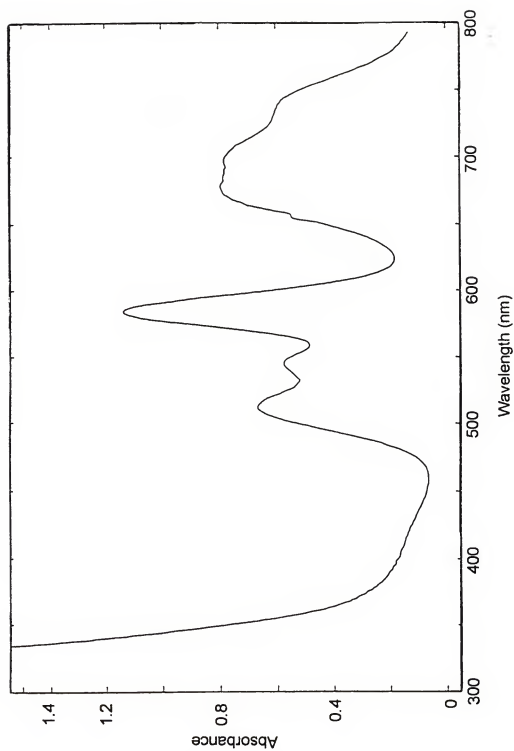


Figure (16). UV-visible spectrum of  $\text{IrBr}_6^{2-}$ .

### Procedure One: Prompt Addition of $\text{Br}_2$

In the first procedure, a 5 mL aliquot of the  $\text{IrBr}_6^{3-}/\text{Br}^-$  solution was added to a 10 mL aliquot of the  $\text{Br}_2$  solution. The volume of solution was brought up to 25 mL with water. An ultraviolet-visible spectrum was taken of the mixed solution at specific time intervals after mixing. The spectra and the peak absorbances over time were compared to determine the dynamics in the mixed solution as the  $\text{IrBr}_6^{3-}$  converted to  $\text{IrBr}_5\text{H}_2\text{O}^{2-}$ . In this procedure, the two forms of the iridium (III) complexes first reacted with  $\text{Br}_2$  and then with  $\text{Br}_3^-$ .

### Procedure Two: Delayed Addition of $\text{Br}_2$

In the second procedure, 5 mL aliquots of the  $\text{IrBr}_6^{3-}/\text{Br}^-$  solution were added to 10 mL aliquots of the  $\text{Br}_2$  solution at several time intervals after preparing the stock  $\text{IrBr}_6^{3-}/\text{Br}^-$  solution. Each of the samples was brought up to a total volume of 25 mL with water immediately after mixing. Ultraviolet-visible spectra of each of the mixed solutions were taken immediately (as close to the mixing time as possible, ca. 30 seconds). The peak absorbances and the spectra were compared. From the spectra, the relative amounts of  $\text{IrBr}_6^{2-}$  and  $\text{IrBr}_5\text{H}_2\text{O}^-$  in solution after reaction could be determined. Based on knowledge of the relative amounts of  $\text{IrBr}_6^{2-}$  and  $\text{IrBr}_5\text{H}_2\text{O}^-$ , information about the relative amounts of  $\text{IrBr}_6^{3-}$  and  $\text{IrBr}_5\text{H}_2\text{O}^{2-}$ , after partial aquation but before oxidation, could be surmised.

### Procedure Three: Double-Delay Experiments

In the third procedure, ultraviolet-visible spectra were taken of the mixed solutions from procedure two over several time periods after mixing. The peak absorbances and the spectra were compared. This procedure was a combination of procedures one and two in that a delay period was involved both prior to and subsequent to the mixing of the  $\text{IrBr}_6^{3-}/\text{Br}^-$  solution with the  $\text{Br}_2$  solution.

### Results and Calculations

Each of the three procedures of the stability studies was based on qualitative examination of the spectra of solutions composed of  $\text{IrBr}_6^{3-}/\text{IrBr}_5\text{H}_2\text{O}^{2-}$  in aqueous  $\text{Br}^-$  solution, oxidized by added  $\text{Br}_2$ . During the discussion regarding these studies, it is important to keep from confusing the meaning of several terms. The  $\text{IrBr}_6^{3-}$  solution "preparation time" refers to the time when the  $\text{Na}_3\text{IrBr}_6$  was dissolved in aqueous  $\text{NaBr}$ . The term "mixing" refers to the mixing of the  $\text{IrBr}_6^{3-}/\text{Br}^-$  solution with the aqueous bromine solution; the time at which this occurs is the "time of mixing." "Standing-time" refers to the length of time the  $\text{IrBr}_6^{3-}/\text{Br}^-$  solution was allowed to stand before the bromine solution was added. The last term that is of concern is the length of time between the time of mixing and the time the spectra were taken. This is referred to as the "post-oxidation standing-time," and is a central theme in procedures one and three.

### Procedure One: Prompt Addition of $\text{Br}_2$

In the first procedure of the stability studies, 10 mL of a 1.79 mM  $\text{Br}_2$  solution was added to 5 mL of a solution that was 25 mM in  $\text{NaBr}$  and 1 mM in  $\text{Na}_3\text{IrBr}_6$ . The

total volume was immediately brought up to 25 mL. In these experiments, the majority of the  $\text{Br}_2$  reacted with  $\text{Br}^-$  forming  $\text{Br}_3^-$ , although some  $\text{IrBr}_6^{2-}$  also formed at this time. Any aquopentabromoiridate (III) present in the solid or formed during the preparation procedure could also be oxidized by the  $\text{Br}_2$ . The bromine concentration was about four times the concentration needed to convert all of the iridium containing complexes from the 3 plus state to the 4 plus state, although most of it initially reacts with  $\text{Br}^-$ .

The shortest reasonable  $\text{IrBr}_6^{3-}/\text{Br}^-$  solution preparation-to-mixing time was about 2.75 minutes. This time period represents the amount of time between preparation of the  $\text{IrBr}_6^{3-}/\text{Br}^-$  solution (which took only a few seconds, starting with a previously weighed sample of  $\text{Na}_3\text{IrBr}_6$ ) and the time this solution was mixed with the  $\text{Br}_2$  solution prepared earlier. An Ultraviolet-visible spectrum taken immediately after mixing in the experiment described shows the characteristic peaks of  $\text{IrBr}_6^{2-}$ , Figure (17), (page 74).

This experiment proves that a freshly prepared solution of  $\text{IrBr}_6^{3-}/\text{Br}^-$ , when oxidized with  $\text{Br}_2/\text{Br}_3^-$ , resulted in a spectrum essentially identical to a spectrum of dissolved  $\text{Na}_2\text{IrBr}_6$  in water, Figure (16). Melvin and Haim tabulated the absorbance peaks and the corresponding extinction coefficients for  $\text{IrBr}_6^{2-}$  [59]. The peaks were listed as 696 nm, 676 nm, 584 nm, 547 nm, and 512 nm. Melvin and Haim also gave two peaks for  $\text{IrBr}_5\text{H}_2\text{O}^-$ , one at 675 nm and one 587 nm [59]. The extinction coefficients of  $\text{IrBr}_6^{2-}$  and  $\text{IrBr}_5\text{H}_2\text{O}^-$  and the peak absorbances of the freshly prepared  $\text{Na}_2\text{IrBr}_6$  solution mentioned early and the solution made by mixing the  $\text{IrBr}_6^{3-}/\text{Br}^-$  solution with the  $\text{Br}_2$  solution, with the 2.75-minute standing-time (listed as "initial spectrum") are tabulated in Table (3). The absorbances for the  $\text{Na}_2\text{IrBr}_6$  were divided by 4 to give absorbances more comparable to the absorbances of the 2.75-minute oxidized  $\text{IrBr}_6^{3-}/\text{Br}^-$  solution.

Table (3). Relevant extinction coefficients and absorbances of  $\text{IrBr}_6^{2-}$  and  $\text{IrBr}_5\text{H}_2\text{O}^-$ .

<u>Sample</u>	<u>Absorbance and Extinction Coefficients</u>						
	<u>696nm</u>	<u>676nm</u>	<u>674nm<sup>a</sup></u>	<u>588nm<sup>a</sup></u>	<u>584nm</u>	<u>546nm</u>	<u>512nm</u>
$\text{Na}_2\text{IrBr}_6$ spectrum	0.78	0.79	0.79 <sup>b</sup>	1.14 <sup>b</sup>	1.14	0.56	0.67
Scaled $\text{IrBr}_6^{2-}$ spectrum <sup>c</sup>	0.195	0.198	0.198	0.285	0.285	0.140	0.168
Initial spectrum	0.191	0.194	0.194	0.238	0.242	0.162	0.187
Extinction coef. $\text{IrBr}_6^{2-}$ <sup>d</sup>	2660	2710	( $\phi$ 2710) <sup>e</sup>	( $\phi$ 3870) <sup>e</sup>	3870	1820	2260
Ext. coef. $\text{IrBr}_5\text{H}_2\text{O}^-$ <sup>d</sup>			2000	3320			

<sup>a</sup> peak wavelengths of  $\text{IrBr}_5\text{H}_2\text{O}^-$ .

<sup>b</sup> estimated.

<sup>c</sup> values from the  $\text{Na}_2\text{IrBr}_6$  spectrum scaled by dividing the absorbances by 4 to reflect a lower concentration.

<sup>d</sup> extinction coefficients from Melvin and Haim [59].

<sup>e</sup> off-peak extinction coefficients for  $\text{IrBr}_6^{2-}$ .

The extinction coefficients in Table (3) are from Melvin and Haim [59], and are in units of  $\text{in M}^{-1} \text{cm}^{-1}$ . The instrument used to measure all spectra for this chapter gives only even values for wavelengths above 400 nm. Therefore, 546 nm has been used to represent the peak which, according to Melvin and Haim, is at 547 nm, 588 nm will be used for the 587 nm peak, and 674 nm will be used for the 675 nm peak.

Several more spectra of this mixture of  $\text{IrBr}_6^{3-}/\text{Br}^-$  and  $\text{Br}_2$  solutions were taken at later times, allowing for longer periods of time for the oxidation of hexabromoiridate (III)

by bromine or tribromide ion. These spectra show a greater absorbance at all of the peak wavelengths. The absorbances are listed in Table (4) (page 73).

The spectra taken are shown in Figures (17), (18), (19) and (20). As mentioned in the introduction to this chapter, experiments show that  $\text{IrBr}_6^{2-}$  converts to  $\text{IrBr}_5\text{H}_2\text{O}^-$  very slowly in water with a reaction rate of only 3 or 4 percent per day. In contrast,  $\text{IrBr}_6^{3-}$  readily converts to  $\text{IrBr}_5\text{H}_2\text{O}^{2-}$ ; therefore, any  $\text{IrBr}_5\text{H}_2\text{O}^-$  in solution was due to conversion of  $\text{IrBr}_6^{3-}$  to  $\text{IrBr}_5\text{H}_2\text{O}^{2-}$  followed by oxidation to  $\text{IrBr}_5\text{H}_2\text{O}^+$ , and not from oxidation of  $\text{IrBr}_6^{3-}$  to  $\text{IrBr}_6^{2-}$  followed by conversion to  $\text{IrBr}_5\text{H}_2\text{O}^-$ . It is clear from the increasing absorbance at all wavelengths in the spectra taken later than the Initial spectrum that, after the initial stage of the reaction process that occurs within the first 2.75 minutes of  $\text{Na}_3\text{IrBr}_6$  dissolution, there is a second stage in which more  $\text{IrBr}_6^{3-}$  and  $\text{IrBr}_5\text{H}_2\text{O}^{2-}$  is oxidized. Comparison of the peak absorbances listed in Table (4) (page 73) and the sequential spectra in Figures (17), (18), (19) and (20) show that, while there is an increase in the concentration of  $\text{IrBr}_6^{2-}$  as time progress, the increase in the concentration of  $\text{IrBr}_5\text{H}_2\text{O}^+$  is more profound.

The results can be easily understood as a two-stage process. During the initial stage, which begins at the moment the  $\text{Br}_2$  solution is added to  $\text{IrBr}_6^{3-}/\text{Br}^-$  solution and ends within 2.75 minutes (but probably much sooner), there is a fast competition between  $\text{IrBr}_6^{3-}$  and  $\text{Br}^-$  for the added  $\text{Br}_2$ . At short times after mixing, the primary reaction pathway can be represented by the following reactions.



Table (4). Absorbance due to  $\text{IrBr}_6^{2-}$  and  $\text{IrBr}_5\text{H}_2\text{O}^-$  at relevant wavelengths at time intervals after bromination of  $\text{IrBr}_6^{3-}/\text{Br}^-$  solution.

<u>Solution (identified by the post-oxidation standing-time")</u>	<u>Absorbance</u>						
	<u>696nm</u>	<u>676nm</u>	<u>674nm<sup>a</sup></u>	<u>588nm<sup>a</sup></u>	<u>584nm</u>	<u>546nm</u>	<u>512nm</u>
$\text{Na}_2\text{IrBr}_6$ spectrum	0.78	0.79	0.79 <sup>b</sup>	1.14 <sup>b</sup>	1.14	0.56	0.67
Initial spectrum <sup>c</sup>	0.191	0.194	0.194	0.238	0.242	0.162	0.187
12 minutes	0.197	0.204	0.204	0.260	0.265	0.172	0.192
99 minutes	0.238	0.247	0.246	0.318	0.322	0.206	0.216
192 minutes	0.266	0.274	0.274	0.352	0.357	0.228	0.236
Scaled $\text{IrBr}_6^{2-}$ spectrum <sup>d</sup>	0.244	0.238	0.238	0.357	0.357	0.175	0.209
Extinction coef. $\text{IrBr}_6^{2-}$ <sup>e</sup>	2660	2710	( $\approx 2710$ ) <sup>f</sup>	( $\approx 3870$ ) <sup>f</sup>	3870	1820	2260
Ext. coef. $\text{IrBr}_5\text{H}_2\text{O}^-$ <sup>e</sup>			2000	3320			

<sup>a</sup> peak wavelengths of  $\text{IrBr}_5\text{H}_2\text{O}^-$ .

<sup>b</sup> estimated.

<sup>c</sup>The standing-time of this sample was approximately 2.75 minutes. The spectrum is the same spectrum used in the previous table. The name will remain the same to avoid confusion.

<sup>d</sup> Values from the  $\text{Na}_2\text{IrBr}_6$  spectrum scaled by dividing the absorbances by 3.2 to reflect a lower concentration.

<sup>e</sup> extinction coefficients from Melvin and Haim [59].

<sup>f</sup> off-peak extinction coefficients for  $\text{IrBr}_6^{2-}$



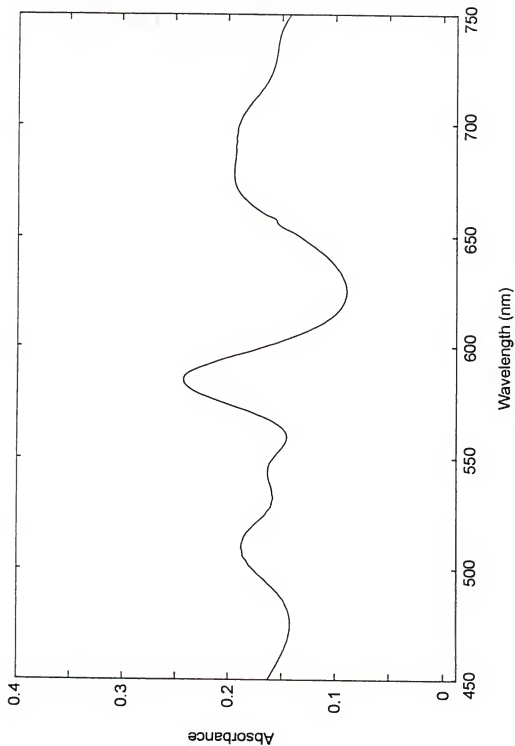


Figure (17). Spectrum of a solution immediately following the addition of excess aqueous  $\text{Br}_2$  solution to aqueous  $\text{IrBr}_6^{3-}/\text{Br}^-$ . The solutions were mixed 2.75 minutes after dissolving  $\text{Na}_3\text{IrBr}_6$  in the  $\text{NaBr}$  solution.

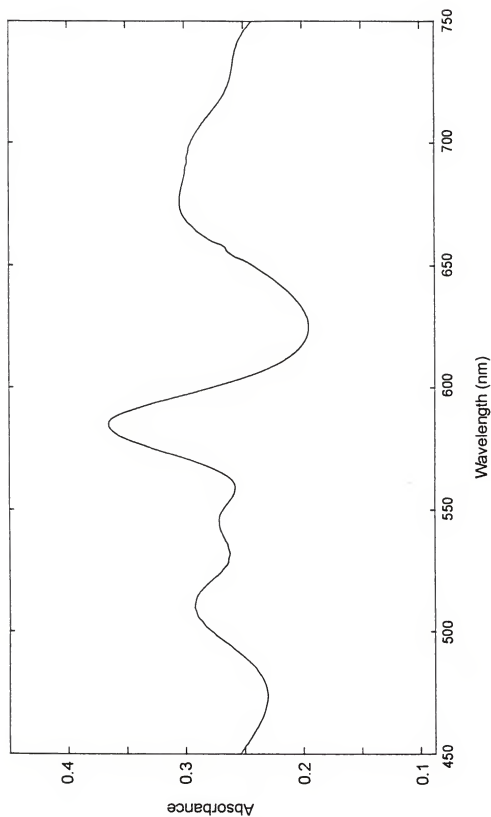


Figure (18). Spectrum of a solution 12 minutes after adding excess  $\text{Br}_2$  solution to aqueous  $\text{IrBr}_6^{3-}/\text{Br}^-$ . The solutions were mixed 2.75 minutes after dissolving  $\text{Na}_3\text{IrBr}_6$  in a NaBr solution.

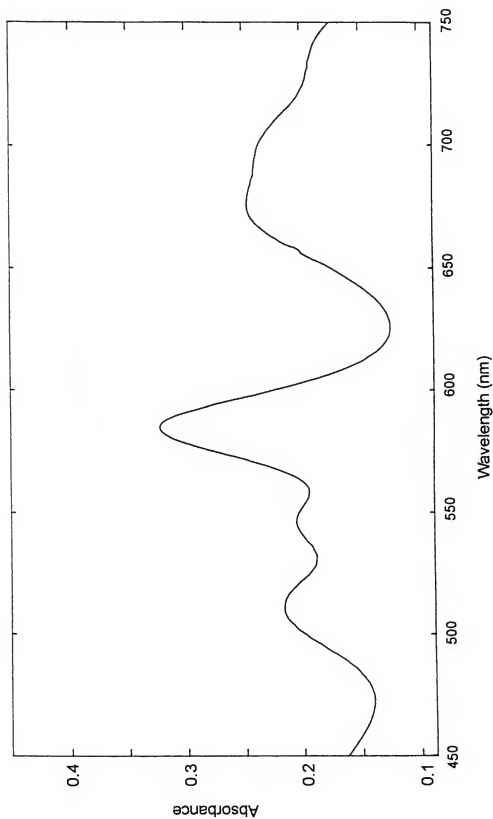


Figure (19). Spectrum of a solution 99 minutes after adding excess  $\text{Br}_2$  solution to aqueous  $\text{IrBr}_6^{3-}/\text{Br}^-$ . The solutions were mixed 2.75 minutes after dissolving  $\text{Na}_3\text{IrBr}_6$  in a  $\text{NaBr}$  solution.

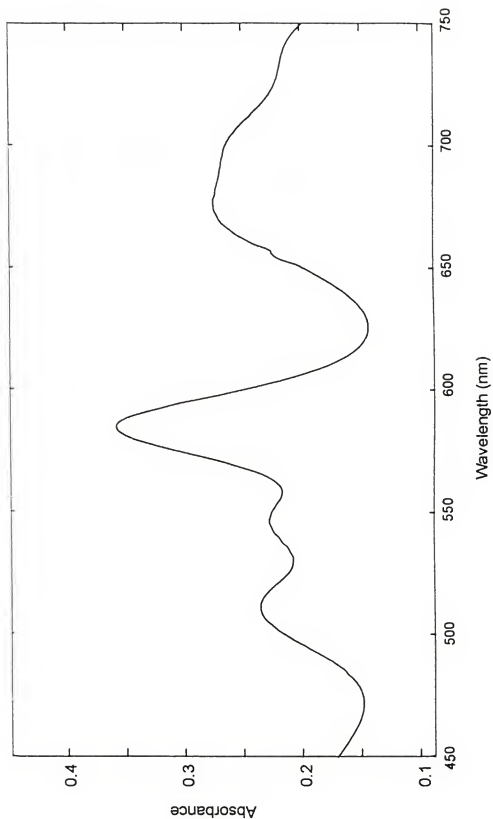
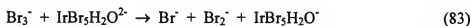
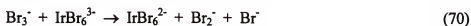


Figure (20). Spectrum of a solution 192 minutes after adding excess aqueous  $\text{Br}_2$  solution to aqueous  $\text{IrBr}_6^{3-}/\text{Br}^-$ . The solutions were mixed 2.75 minutes after dissolving  $\text{Na}_3\text{IrBr}_6$  in a NaBr solution.

The important reactions during stage one are Reactions (55) and (69). The reactions of  $\text{IrBr}_5\text{H}_2\text{O}^{2-}$  are unimportant at this stage because the concentration of  $\text{IrBr}_5\text{H}_2\text{O}^{2-}$  is very small. Any  $\text{Br}_3^-$  formed reacts with the iridium complexes but on a much longer time scale, as seen during stage two. By the end of stage one, essentially all of the  $\text{Br}_2$  was used up either by oxidizing the iridium complexes or by reacting with  $\text{Br}^-$  to form  $\text{Br}_3^-$  ion.

During stage two, the  $\text{Br}_3^-$  ion formed during stage one reacts with the remaining iridium complexes. However, the  $\text{IrBr}_6^{3-}$  present not only reacts with the  $\text{Br}_3^-$ , but also slowly converts to  $\text{IrBr}_5\text{H}_2\text{O}^{2-}$ , which can also react with  $\text{Br}_3^-$ . The spectra taken at longer post-oxidation standing-times, especially the spectrum of the solution with a post-oxidation standing-time of 199 minutes, show a greater increase in absorbance at 584 nm, where both  $\text{IrBr}_6^{2-}$  and  $\text{IrBr}_5\text{H}_2\text{O}^-$  absorb, than at 512 nm and 546 nm, where  $\text{IrBr}_6^{2-}$  absorbs strongly and  $\text{IrBr}_5\text{H}_2\text{O}^-$  absorbs only weakly. The importance of the oxidation reaction of  $\text{IrBr}_5\text{H}_2\text{O}^{2-}$  by  $\text{Br}_3^-$  increased with time, as can be seen from the spectral data. The reaction scheme for stage two is shown below.



Although the reaction of  $2\text{Br}_2^-$  to form  $\text{Br}^-$  and  $\text{Br}_3^-$  is chemically feasible, it makes a negligible contribution to the system because other reactions which consume  $\text{Br}_2^-$  occur more rapidly, namely, Reactions (68) and (77). Several reactions which are

the reverse of some the reactions listed are chemically feasible and certainly occur in the system. Consideration of such processes is necessary for a quantitative interpretation of the system, but is not needed for a qualitative understanding.

### Procedure Two: Delayed Addition of $\text{Br}_2$

The second procedure was performed by allowing the 1 mM  $\text{Na}_3\text{IrBr}_6$ /25 mM NaBr solution to stand for periods up to ca. 3 hours to observe changes in the solution. After a specific standing-time, 5 mL of the  $\text{IrBr}_6^{3-}/\text{Br}^-$  stock solution was pipetted into a 25 mL volumetric flask along with 10 mL of the 1.79 mM  $\text{Br}_2$  solution. As with the first procedure, the volume was brought up to 25 mL with water from a Millipore system. Ultraviolet-visible spectra were taken of the solutions immediately after mixing. This procedure was done to establish the contents of the solution at several different standing-times following dissolution of  $\text{Na}_3\text{IrBr}_6$  in water.

Each of the spectra considered in this procedure was taken immediately after mixing the  $\text{Br}_2$  solution and the  $\text{IrBr}_6^{3-}/\text{Br}^-$  stock solution, which had been allowed to stand for specific periods of time. The mixtures were prepared 2.75 minutes, 21.75 minutes, 77 minutes and 211 minutes after dissolving the  $\text{Na}_3\text{IrBr}_6$ . The spectra were clearly different, and showed a gradual shift from spectra that were similar to a spectrum of  $\text{IrBr}_6^{2-}$ , to spectra that were presumably more representative of  $\text{IrBr}_5\text{H}_2\text{O}^+$ , Figures (21), (22), (23) and (24).

The spectrum of the solution resulting from the mixing of the  $\text{IrBr}_6^{3-}/\text{Br}^-$  solution with the  $\text{Br}_2$  solution 2.75 minutes after preparation of the  $\text{IrBr}_6^{3-}/\text{Br}^-$  solution was very similar to a known spectrum of  $\text{IrBr}_6^{2-}$ , Figures (21) and (16). In fact, the spectra were

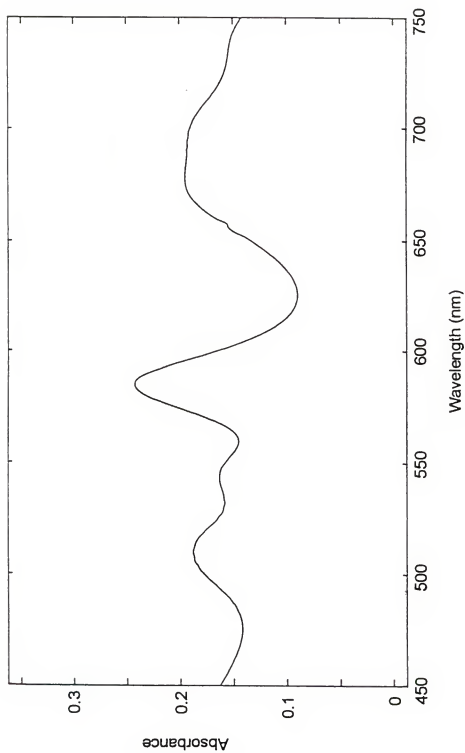


Figure (21). Spectrum of a solution immediately adding excess aqueous  $\text{Br}_2$  solution to aqueous  $\text{IrBr}_6^{3-}/\text{Br}^-$ . The solutions were mixed 2.75 minutes after dissolving  $\text{Na}_3\text{IrBr}_6$  in a NaBr solution.

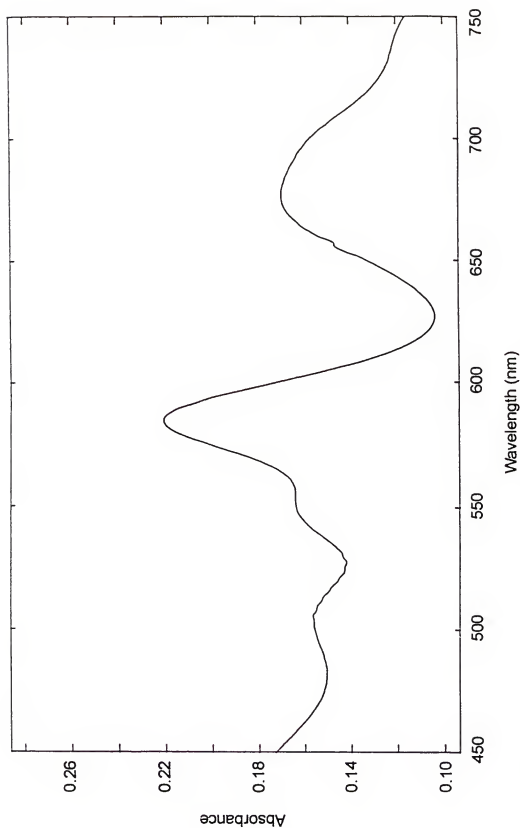


Figure (22). Spectrum of a solution taken immediately after adding excess aqueous  $\text{Br}_2$  solution to aqueous  $\text{IrBr}_6^{3-}/\text{Br}^-$ . The solutions were mixed 21.75 minutes after dissolving  $\text{Na}_3\text{IrBr}_6$  in a NaBr solution.



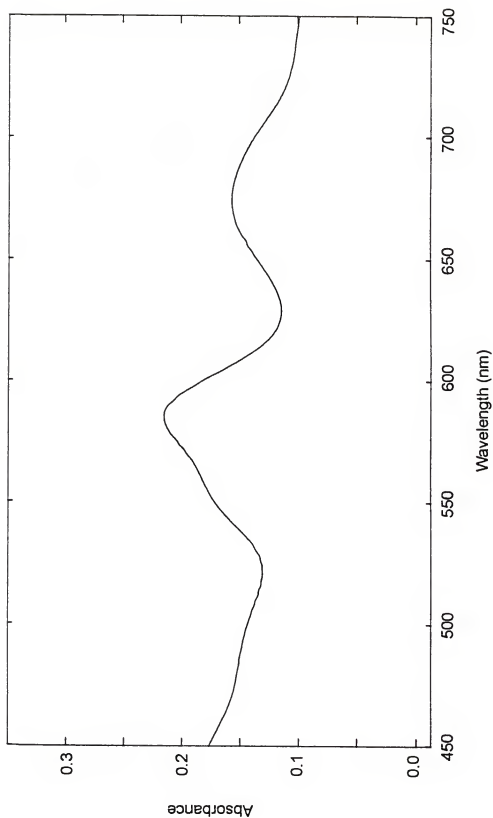


Figure (23). Spectrum of a solution taken immediately after adding excess aqueous  $\text{Br}_2$  solution to aqueous  $\text{IrBr}_6^{3-}/\text{Br}^-$ . The solutions were mixed 77 minutes after dissolving  $\text{Na}_3\text{IrBr}_6$  in a  $\text{NaBr}$  solution.

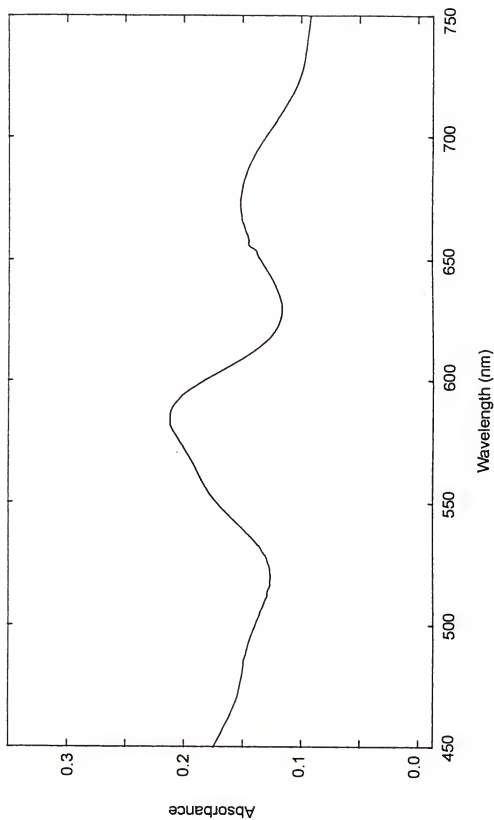


Figure (24). Spectrum of a solution taken immediately after adding excess  $\text{Br}_2$  solution to aqueous  $\text{IrBr}_6^{3-}/\text{Br}^-$ . The solutions were mixed 211 minutes after dissolving  $\text{Na}_3\text{IrBr}$  in a  $\text{NaBr}$  solution.

almost identical. There appeared to be little if any  $\text{IrBr}_5\text{H}_2\text{O}^-$  present. Accordingly, it was inferred that very little  $\text{IrBr}_6^{3-}$  had converted to  $\text{IrBr}_5\text{H}_2\text{O}^{2-}$  by the time of mixing, which was 2.75 minutes after the preparation of the  $\text{IrBr}_6^{3-}/\text{Br}^-$  solution.

The spectrum of the solution treated with  $\text{Br}_2$  21.75 minutes after preparation of the  $\text{IrBr}_6^{3-}/\text{Br}^-$  solution showed spectral evidence of the presence of  $\text{IrBr}_6^{2-}$ , but also showed some characteristics of  $\text{IrBr}_5\text{H}_2\text{O}^-$ . It appeared to have about equal quantities of each of the two iridium (IV) bromide complexes, in agreement with the known first order half-life of  $\text{IrBr}_6^{3-}$  for the aquation Reaction (73). The half-life is 19 minutes, calculated from the rate constant of  $6.2 \times 10^{-4} \text{ s}^{-1}$  for the aquation reaction, an average of the values published by Melvin and Haim [59].

The spectra taken of solutions mixed at long times after the preparation of the  $\text{IrBr}_6^{3-}/\text{Br}^-$  solution, 77 minutes and 211 minutes, were almost identical, Figures (19) and (20). They were also very different from the spectrum taken after the 21.75-minute standing-time, Figure (22), and differed even more from the spectrum taken after the 2.75-minute standing-time, Figure (21); the latter was similar to a known spectrum of  $\text{IrBr}_6^{2-}$ , Figure (16). The spectrum taken after 21.75 minutes standing-time appeared qualitatively intermediate between the two long standing-time spectra (77 minute and 211 minute standing-time samples) and the 2.75 minute standing-time sample (which was essentially the same as a spectrum of pure  $\text{IrBr}_6^{2-}$ ). This observation is consistent with a literature half-life of approximately 19 minutes, mentioned earlier.

The arguments presented above are all based on changes in peak intensities of spectra taken of solutions that were brominated at time periods of 2.75 minutes to 211

minutes after preparation of the  $\text{IrBr}_6^{3-}/\text{Br}^-$  solution. The relevant peak intensities of the spectra are listed in Table (5) (page 87).

Since  $\text{IrBr}_6^{2-}$  absorbs at both 512 nm and 584 nm whereas  $\text{IrBr}_5\text{H}_2\text{O}^-$  does not absorb at 512 nm and does absorb at 584 nm, the ratio of these peak absorbances can be used to determine the relative amounts of  $\text{IrBr}_6^{2-}$  and  $\text{IrBr}_5\text{H}_2\text{O}^-$  after oxidation of the  $\text{IrBr}_6^{3-}/\text{Br}^-$  solution by aqueous  $\text{Br}_2$  solution. Hence, with greater amounts of  $\text{IrBr}_5\text{H}_2\text{O}^-$  in solution, the 512 nm/584 nm peak absorbance ratio should be smaller.

The 512 nm/584 nm absorbance ratios decreased with time; Figure (25) shows this behavior. The decrease in time of the 512 nm/584 nm absorbance ratio agreed with the hypothesis that there was more  $\text{IrBr}_6^{3-}$  in the aqueous solution initially, and that the solution gradually converted to  $\text{IrBr}_5\text{H}_2\text{O}^{2-}$  over time.

### Procedure Three: Double-Delay Experiments

Procedure one described prompt bromination of the  $\text{IrBr}_6^{3-}/\text{Br}^-$  solution followed by periodic measurement of the spectra, showing a fast initial reaction with  $\text{Br}_2$  (studied in detail below) followed by a relatively slow reaction of  $\text{Br}_3^-$  with a solution which was predominately  $\text{IrBr}_6^{3-}$ . Less than 5% of the iridium complex converted to  $\text{IrBr}_5\text{H}_2\text{O}^{2-}$  during this experiment. Procedure two involved a time delay prior to bromination, followed by prompt measurement of the spectrum. This procedure revealed that  $\text{IrBr}_6^{3-}$  converts to  $\text{IrBr}_5\text{H}_2\text{O}^{2-}$  as a function of time, with a half-life of ca. 20 minutes.

The third procedure used in the stability studies was a combination of the first two methods. The solutions of  $\text{IrBr}_6^{3-}/\text{Br}^-$  were allowed to stand for either 77 minutes or

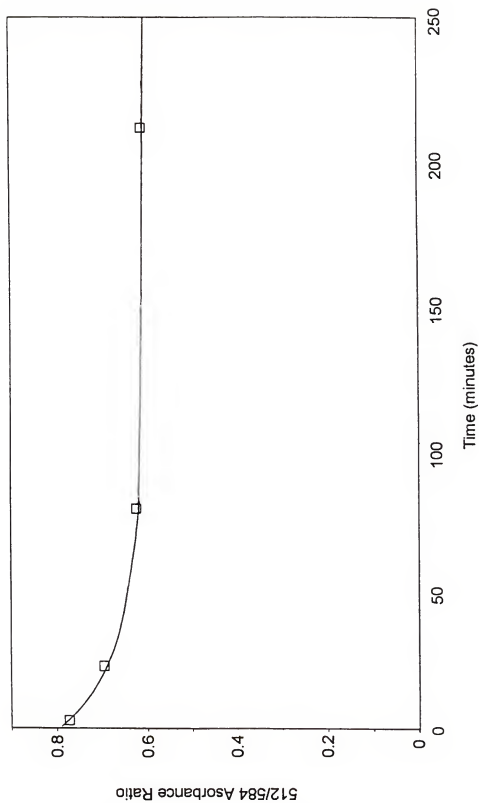


Figure (25). Plot displaying the change in the absorbance ratio 512 nm:584 nm versus the amount of time the solution of  $\text{IrBr}_6^{3-}$  was allowed to stand. The absorbance is due to  $\text{IrBr}_6^{2-}$  and  $\text{IrBr}_5\text{H}_2\text{O}^+$  after oxidation of  $\text{IrBr}_6^{3-}$  and  $\text{IrBr}_5\text{H}_2\text{O}^{2+}$  by  $\text{Br}_2$  in the presence of  $\text{Br}^-$ .

Table (5): Intensities of major peaks in the visible spectrum of  $\text{IrBr}_6^{2-}/\text{IrBr}_5\text{H}_2\text{O}^-$  after bromination of the iridium species.

<u><math>\text{IrBr}_6^{3-}</math> Solution</u>	<u>Absorbance</u>						
<u>Standing-time</u>	<u>696nm</u>	<u>676nm</u>	<u>674nm<sup>a</sup></u>	<u>588nm<sup>a</sup></u>	<u>584nm</u>	<u>546nm</u>	<u>512nm</u>
$\text{Na}_2\text{IrBr}_6$ spectrum	0.78	0.79	0.79 <sup>b</sup>	1.14 <sup>b</sup>	1.14	0.56	0.67
Scaled $\text{IrBr}_6^{2-}$ spectrum <sup>c</sup>	0.195	0.198	0.198	0.285	0.285	0.140	0.168
2.75 minutes	0.191	0.194	0.194	0.238	0.242	0.162	0.187
21.75 minutes	0.161	0.169	0.169	0.218	0.220	0.162	0.153
77 minutes	0.142	0.156	0.157	0.214	0.215	0.165	0.134
211 minutes	0.135	0.151	0.152	0.211	0.212	0.164	0.129
Extinction coef. $\text{IrBr}_6^{2-}$ <sup>d</sup>	2660	2710	( $\approx 2710$ ) <sup>e</sup>	( $\approx 3870$ ) <sup>e</sup>	3870	1820	2260
Ext. coef. $\text{IrBr}_5\text{H}_2\text{O}^-$ <sup>d</sup>			2000	3320			

<sup>a</sup> peak wavelengths of  $\text{IrBr}_5\text{H}_2\text{O}^-$

<sup>b</sup> estimated

<sup>c</sup> Values from the  $\text{Na}_2\text{IrBr}_6$  spectrum scaled by dividing the absorbances by 4 to reflect a lower concentration.

<sup>d</sup> extinction coefficients from Melvin and Haim [59]

<sup>e</sup> off-peak extinction coefficients for  $\text{IrBr}_6^{2-}$

211 minutes, then oxidized with aqueous  $\text{Br}_2$  solution. Finally, spectra were taken of these solutions 12.5 minutes and 39.25 minutes after bromination.

Spectra of the solutions of  $\text{IrBr}_6^{3-}$  with standing-times of 77 minutes and 211 minutes changed very little after the initial reaction with  $\text{Br}_2$  was complete. In both cases, the intensity of the spectra changed by a small amount while the qualitative appearance remained nearly the same, Figures (26), (27), (28), and (29). Apparently, 77 minutes was nearly sufficient time to convert the  $\text{IrBr}_6^{3-}$  to  $\text{IrBr}_5\text{H}_2\text{O}^{2-}$ . Furthermore, as before, it was found that a large portion of the  $\text{IrBr}_5\text{H}_2\text{O}^{2-}$  was promptly oxidized by  $\text{Br}_2$  to  $\text{IrBr}_5\text{H}_2\text{O}^+$ , but about 11% additional oxidation was noted 12.5 minutes after the  $\text{Br}_2$  addition, and a further 9% oxidation after an additional 26.5 minutes. As before it assumed that the slow oxidation reaction was due to  $\text{Br}_3^-$ .

Based on the above studies regarding the stability of  $\text{IrBr}_6^{3-}$  in aqueous 25 mM NaBr solution, we concluded that  $\text{IrBr}_6^{3-}$  converted to  $\text{IrBr}_5\text{H}_2\text{O}^{2-}$  with a half-life of ca. 20 minutes, in agreement with the literature [59]. Furthermore, it was found qualitatively that  $\text{Br}_2$  reacts rapidly with either  $\text{IrBr}_6^{3-}$  or  $\text{IrBr}_5\text{H}_2\text{O}^{2-}$ . Finally, reactions of both  $\text{IrBr}_6^{3-}$  and  $\text{IrBr}_5\text{H}_2\text{O}^{2-}$  with  $\text{Br}_3^-$  were observed, but with half-lives of ca. 10 minutes or more.

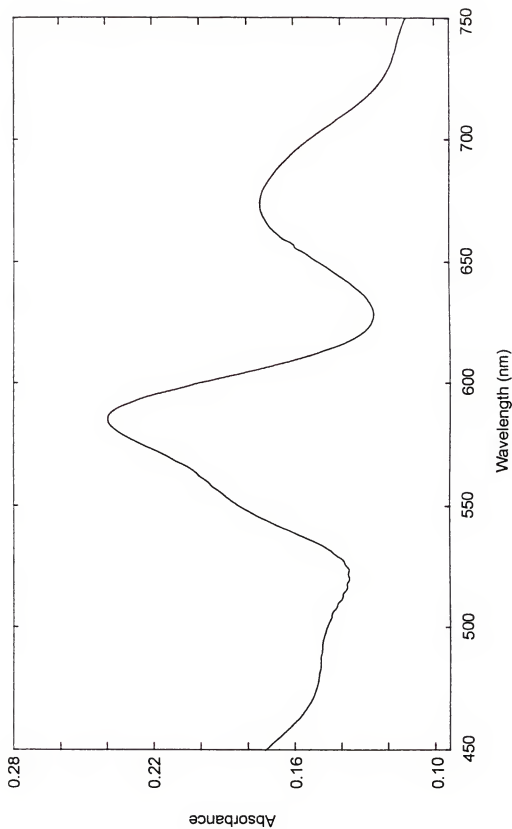


Figure (26). Spectrum of a solution taken 12.5 minutes after adding excess aqueous  $\text{Br}_2$  solution to aqueous  $\text{IrBr}_6^{3-}/\text{Br}^-$ . The solutions were mixed 77 minutes after dissolving  $\text{Na}_3\text{IrBr}_6$  in a  $\text{NaBr}$  solution.



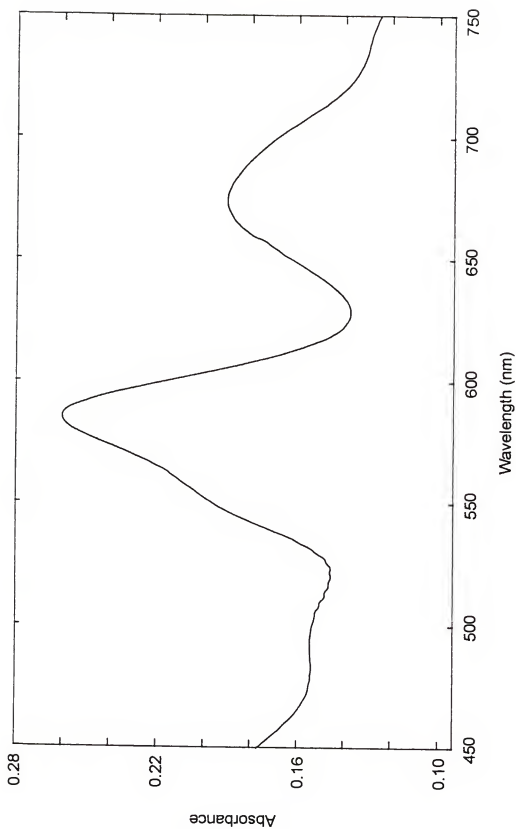


Figure (27). Spectrum of a solution taken 39.25 minutes after adding excess aqueous  $\text{Br}_2$  solution to aqueous  $\text{IrBr}_6^{3-}/\text{Br}^-$ . The solutions were mixed 77 minutes after dissolving  $\text{Na}_3\text{IrBr}_6$  in a  $\text{NaBr}$  solution.

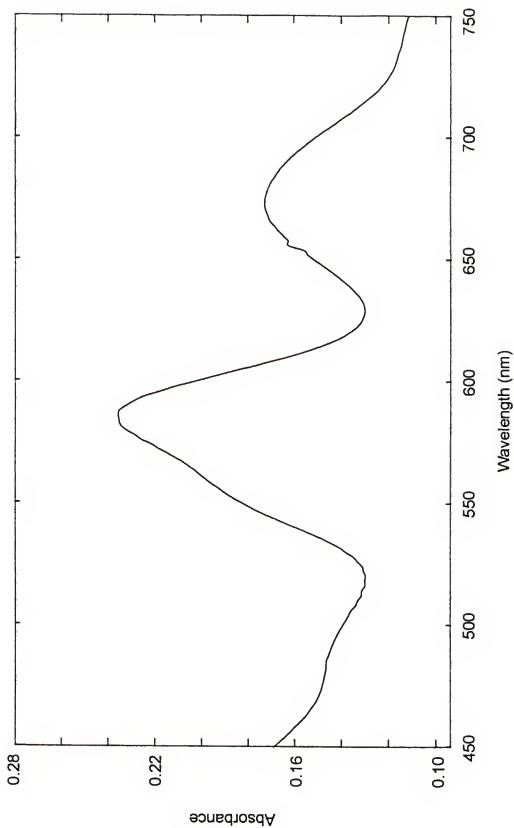


Figure (28). Spectrum of a solution taken 12.5 minutes after adding excess aqueous  $\text{Br}_2$  solution to aqueous  $\text{IrBr}_6^{3-}/\text{Br}^-$ . The solutions were mixed 211 minutes after dissolving  $\text{Na}_2\text{IrBr}_6$  in a  $\text{NaBr}$  solution.

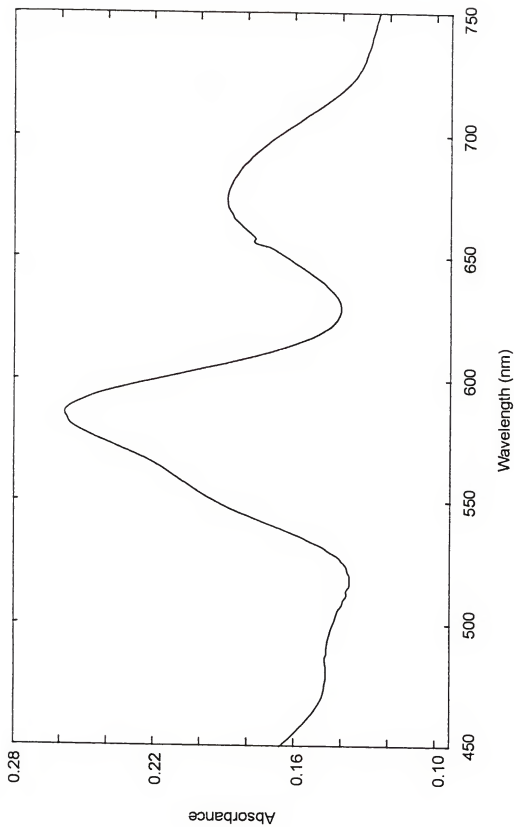


Figure (29). Spectrum of a solution taken 39.25 minutes after adding excess aqueous  $\text{Br}_2$  solution to aqueous  $\text{IrBr}_6^{3-}/\text{Br}^-$ . The solutions were mixed 211 minutes after dissolving  $\text{Na}_3\text{IrBr}_6$  in a  $\text{NaBr}$  solution.

## CHAPTER FIVE

### REACTION OF HEXABROMOIRIDATE WITH OH RADICAL: ALTERNATIVE METHOD FOR COMPETITION KINETICS

The purpose of the experiments in this section was to determine the rate constant for the reaction of hexabromoiridate with OH radical, Reaction (12).



The Febetron 706 electron accelerator was used for these measurements.

However, Reaction (12) occurred too rapidly to be measured directly using the accelerator and its peripheral instrumentation as presently set up. We used the carbonate competition method to measure the rate constant indirectly [78]. With this method, solutions with varying initial concentration ratios of  $\text{CO}_3^{2-}$  and  $\text{IrBr}_6^{3-}$  were subjected to the pulse from the Febetron. Both  $\text{CO}_3^{2-}$  and  $\text{IrBr}_6^{3-}$  react readily with OH radical. The application of pulse radiolysis to an aqueous solution containing both these ions, which had been treated with  $\text{N}_2\text{O}$  to create totally oxidizing conditions, leads to a competition between  $\text{IrBr}_6^{3-}$  and  $\text{CO}_3^{2-}$  for the OH radical, Reactions (12) and (84).



The concentration of  $\text{IrBr}_6^{2-}$  produced in Reaction (12) is dependent on several factors. These factors include the relative initial concentrations of  $\text{CO}_3^{2-}$  and  $\text{IrBr}_6^{3-}$  ions, the concentration of OH radical produced in solution by the pulse, and the ratio of the rate constants for Reactions (12) and (84),  $k_{\text{Ir}}$  and  $k_{\text{CO}_3}$ , respectively. The rate constant for Reaction (12) can be determined provided  $k_{\text{CO}_3}$  is known.

As shown below, the standard method of treating competition data required that the pulse size of the Febetron be constant throughout the collection of all data used in the competition graph. Unfortunately, the beam tube on the Febetron 706 in this facility is somewhat deteriorated; the pulse size varies over a range of about 10 %. Accordingly, a search was made for a method that was less critically dependent on a constant pulse size. A method alluded to in S. Benson's kinetics text [79], which we call the "elimination of time as independent variable," was used. Using this method, it was only necessary that the pulse size be constant while taking two successive shots at different wavelengths (for measurement of the two competition products), for any one of the specific reactant concentration ratios. This method made possible the elimination of  $[\cdot\text{OH}]_0$  from the mathematical treatment for the competing system.

## Experimental

Studies of transient species in solutions containing iridium bromide complexes were done using the University of Florida pulse radiolysis facility, based on a Febetron model 706 electron accelerator. As presently configured with a modified beam tube, the apparatus can deposit about 1 Joule of energy in a small liquid sample within a time of about 3 ns [48, 22].

The sources of the reagents were as follows:  $\text{Na}_3\text{IrBr}_6$ , Johnson Matthey/Materials Technology, U.K.;  $\text{Na}_2\text{CO}_3$ , Fisher Scientific Co.; KBr, J.T. Baker Chemical Co. All reagents were used as received. The solution required saturation with  $\text{N}_2\text{O}$  because reaction of  $\text{IrBr}_6^{3-}$  with OH radicals required totally oxidizing conditions. Totally oxidizing conditions were obtained by bubbling  $\text{N}_2\text{O}$  through the solution for 20 minutes.

The  $\text{N}_2\text{O}$  was supplied by Matheson, CP grade, 99.0%, and was also used as received. Water used in all pulse radiolysis experiments was prepared by fractional distillation of previously deionized water in the presence of KOH and  $\text{KMnO}_4$ . The water was equivalent in purity to "doubly-distilled" water.

Ultraviolet-Visible spectra of iridium (III) and iridium (IV) bromide complexes were scanned using a Hewlett Packard 8450A Diode Array Spectrophotometer. A Beckman DU Spectrophotometer was used to measure the concentration of the  $\text{IrBr}_6^{3-}$  solutions before each pulse radiolysis experiment. The extinction coefficient of  $\text{IrBr}_6^{3-}$  at 448 nm is  $1.65 \times 10^2 \text{ M}^{-1} \text{ cm}^{-1}$  [59]. The extinction coefficient for the analogous peak in the spectrum of  $\text{IrBr}_3\text{H}_2\text{O}^{2-}$  is shifted to a slightly lower wavelength.

A water-cooled 350 Watt Xenon arc lamp, described in detail in chapter 2, was used as the light source. For the competition studies, concentrations of  $\text{IrBr}_6^{2-}$  and  $\text{CO}_3^{2-}$  were extracted from the absorbances monitored at 512 nm and 626 nm, as described below.

## Results and Calculations

### Reaction of OH Radical with $\text{IrBr}_6^{3-}$ : the Standard Competition Method

In preliminary experiments, the standard carbonate competition method [78] was used to estimate the rate constant for the reaction of OH radical with  $\text{IrBr}_6^{3-}$ , Reaction (12). This was done as part of the studies that were incorporated in the Thesis work [23]. When a solution containing both reactants,  $\text{CO}_3^{2-}$  and  $\text{IrBr}_6^{3-}$ , is subjected to the pulse, the two reactants compete for the OH radicals formed from the interaction of the electron beam with water in the aqueous solution. If the solution is first treated with  $\text{N}_2\text{O}$  to create

totally oxidizing conditions, then most of the initial reactions involving  $\text{CO}_3^{2-}$  and  $\text{IrBr}_6^{3-}$  will be redox reactions with the OH radical, Reactions (12) and (84).



Although each of these processes has its own rate equation, the two equations share the common reactant OH radical. The rate laws in terms of product formation can be expressed as:

$$\frac{d[\text{IrBr}_6^{2-}]}{dt} = k_{\text{Ir}}[\cdot\text{OH}][\text{IrBr}_6^{3-}] \quad (3)$$

$$\frac{d[\text{CO}_3^{\cdot-}]}{dt} = k_{\text{CO}_3}[\cdot\text{OH}][\text{CO}_3^{2-}] \quad (4)$$

In equation (3),  $k_{\text{Ir}}$  is the rate constant for Reaction (3), and in equation (4),  $k_{\text{CO}_3}$  is the rate constant for Reaction (4). If the system is treating as a mass balance problem, the ratio of the yields of the products,  $\text{IrBr}_6^{2-}$  and  $\text{CO}_3^{2-}$ , can be equated to the ratio of their respective rates of formation, Equation (5).

$$\frac{[\text{IrBr}_6^{2-}]_{\text{pp}}}{[\text{CO}_3^{\cdot-}]_{\text{pp}}} = \frac{k_{\text{Ir}}[\text{IrBr}_6^{3-}]_0[\cdot\text{OH}]_0}{k_{\text{CO}_3}[\text{CO}_3^{2-}]_0[\cdot\text{OH}]_0} \quad (5)$$

In Equation (5),  $[\text{IrBr}_6^{2-}]_{\text{pp}}$  and  $[\text{CO}_3^{\cdot-}]_{\text{pp}}$  are the concentrations of  $\text{IrBr}_6^{2-}$  and the radical ion  $\text{CO}_3^{\cdot-}$ , the products of the competing reactions of  $\text{IrBr}_6^{3-}$  with  $\text{CO}_3^{2-}$  with OH radical, after the pulse (i.e., "post pulse" or "pp"). The initial OH radical concentration is  $[\cdot\text{OH}]_0$ , and  $[\text{IrBr}_6^{3-}]_0$  and  $[\text{CO}_3^{2-}]_0$  are the initial concentrations of iridium bromide complex and of carbonate ions, respectively. The initial concentration of OH radical can be canceled out of Equation (5) to give Equation (6).

$$\frac{[IrBr_6^{2-}]_{pp}}{[CO_3^-]_{pp}} = \frac{k_{Ir}[IrBr_6^{3-}]_o}{k_{CO_3}[CO_3^{2-}]_o} \quad (6)$$

Essentially all of the OH radical reacts with either  $IrBr_6^{3-}$  or  $CO_3^{2-}$ . Furthermore, since the sole products of Reactions (12) and (84) are  $IrBr_6^{2-}$  and  $CO_3^-$ , the initial concentration of the OH radical formed is equivalent to the sum of the  $IrBr_6^{2-}$  and  $CO_3^-$  product concentrations.

$$[OH]_o = [IrBr_6^{2-}]_{pp} + [CO_3^-]_{pp} \quad (7)$$

Equation (7) can be solved for the concentration of  $CO_3^-$  and substituted into Equation (6), to give Equation (8).

$$\frac{[OH]_o - [IrBr_6^{2-}]_{pp}}{[IrBr_6^{2-}]_{pp}} = \frac{k_{Ir}[IrBr_6^{3-}]_o}{k_{CO_3}[CO_3^{2-}]_o} \quad (8)$$

Equation (8) can then be manipulated to give the more useful Equation (9).

$$\frac{[OH]_o}{[IrBr_6^{2-}]_{pp}} - 1 = \frac{k_{Ir}[IrBr_6^{3-}]_o}{k_{CO_3}[CO_3^{2-}]_o} \quad (9)$$

If carbonate ion is not present, then all of the OH radicals created in the pulse react with hexabromoiridate, and the amount of  $IrBr_6^{2-}$  produced is equal to the initial OH radical concentration,  $[OH]_o$ , Equation (10).

$$[OH]_o = [IrBr_6^{2-}]_{max} \quad (10)$$

This was done experimentally. The concentration term was labeled  $[IrBr_6^{2-}]_{max}$ .

The half-cell reduction potential of the couple  $IrBr_6^{2-}/IrBr_6^{3-}$  is considerably less favorable than the half-cell reduction potential of the couple  $IrBr_5H_2O^-/IrBr_5H_2O^{2-}$  (less positive) as discussed above [66, 67]. Since the reduction potentials are related to the corresponding chemical driving force, it can be expected that the reaction of  $IrBr_5H_2O^{2-}$



with OH radical may be slower than the reaction of  $\text{IrBr}_6^{3-}$  with OH radical. Thus, in a solution containing both  $\text{IrBr}_6^{3-}$  and  $\text{IrBr}_5\text{H}_2\text{O}^{2-}$ , the majority of the OH radical produced in solution would be used up in reaction with  $\text{IrBr}_6^{3-}$ , and reaction of  $\text{IrBr}_5\text{H}_2\text{O}^{2-}$  could be neglected in the early part of the process.

Substituting  $[\text{IrBr}_6^{2-}]_{\text{max}}$  for  $[\cdot\text{OH}]_0$  based on Equation (10) in Equation (9) and adding 1 to both sides gives Equation (11).

$$\frac{[\text{IrBr}_6^{2-}]_{\text{max}}}{[\text{IrBr}_6^{2-}]_{\text{pp}}} = 1 + \frac{k_{\text{Ir}}}{k_{\text{CO}_3}} \times \frac{[\text{IrBr}_6^{3-}]_0}{[\text{CO}_3^{2-}]_0} \quad (11)$$

This is the mathematical expression normally applied in carbonate competition kinetics.

A graph of  $[\text{IrBr}_6^{2-}]_{\text{max}}$ , with no  $[\text{CO}_3^{2-}]$  present, divided by  $[\text{IrBr}_6^{2-}]_{\text{pp}}$  for each given experiment with no  $[\text{CO}_3^{2-}]$  present, versus the ratio of the initial concentrations of  $\text{IrBr}_6^{3-}$  and  $\text{CO}_3^{2-}$  for each given experiment gives a straight line with y-intercept equal to 1 and slope equal to  $k_{\text{Ir}}/k_{\text{CO}_3}$ .

In Equation (11),  $[\text{IrBr}_6^{2-}]_{\text{max}}$  is the concentration of  $\text{IrBr}_6^{2-}$  produced in an experiment when no  $\text{CO}_3^{2-}$ ;  $k_{\text{Ir}}$  is the rate constant for reaction of OH radical with  $\text{IrBr}_6^{3-}$ , and  $k_{\text{CO}_3}$  is the known rate constant for the competing reaction of  $\text{CO}_3^{2-}$  with OH radical. The concentrations  $[\text{IrBr}_6^{3-}]_0$  and  $[\text{CO}_3^{2-}]_0$  are the initial concentrations of  $\text{IrBr}_6^{3-}$  and  $\text{CO}_3^{2-}$  at the beginning of a particular experiment, while  $[\text{IrBr}_6^{2-}]_{\text{pp}}$  is the concentration of  $\text{IrBr}_6^{2-}$  produced in that same experiment.

With the method for standard competition kinetics, several experiments were conducted, while the initial reactant concentration ratio,  $[\text{CO}_3^{2-}]_0/[\text{IrBr}_6^{3-}]_0$ , was changed for each experiment. The post-pulse concentration of  $\text{IrBr}_6^{2-}$  was determined from the time-intensity graph for each experiment. Then the  $[\text{IrBr}_6^{2-}]_{\text{max}}/[\text{IrBr}_6^{2-}]_{\text{pp}}$  ratio was plotted versus  $[\text{IrBr}_6^{3-}]_0/[\text{CO}_3^{2-}]_0$  for each of the separate experiments. The value of  $k_{\text{Ir}}$

was calculated from the slope and  $k_{\text{CO}_3}$ . The value of  $k_{\text{CO}_3}$  is well established and has been reported to be  $4.2 \times 10^8 \text{ M}^{-1} \text{ s}^{-1}$  [80].

Note that in taking the entire data set for the competition graph, it was necessary for the  $[\cdot\text{OH}]_0$  to be the same throughout each experiment due to the substitution of Equation (7) into Equation (6), (the use of  $[\text{IrBr}_6^{2-}]_{\text{max}}$  in place of  $[\cdot\text{OH}]_0$ ). Since the OH radical concentration was dependent on the amount of energy deposited into the aqueous solution, it was required that the size of the pulse from the Febetron 706 be consistent throughout all of the experiments in a given series.

Although the spectral peak for the optical absorption by  $\text{CO}_3^{\cdot-}$  is centered at ca. 600-610 nm, there was still some absorption at 512 nm [81, 82], where the production of  $\text{IrBr}_6^{2-}$  was monitored in the earlier experiments. In a preliminary experiment using absorbances which were not corrected for this spectral interference, while using the standard Carbonate Competition method, the rate constant for reaction of OH radical with  $\text{IrBr}_6^{2-}$ , Reaction (12), was calculated to be  $1.2 \times 10^9 \text{ M}^{-1} \text{ s}^{-1}$ . This is slightly less than the value of  $1.4 \times 10^9 \text{ M}^{-1} \text{ s}^{-1}$  using the more careful procedure described below.

### **Reaction of OH Radical with $\text{IrBr}_6^{3-}$ : the Alternate Competition Method**

The standard competition method makes strong demands on the Febetron for pulse stability and pulse-size reproducibility due to the necessity of a constant initial OH radical concentration throughout all experiments in a given series. A second method for measuring  $k_{\text{Ir}}$  which would be less critically dependent on machine stability was sought. That is, it was desired that the method would be less demanding on the reproducibility of the pulse size from the Febetron. The method which was devised was similar to the

standard competition method in that a secondary reactant, again  $\text{CO}_3^{2-}$ , was added as a competing reagent. However, the mathematical treatment was different.

With the alternate method, the initial concentration of OH radical was factored out of the mathematical equation. This meant that the initial OH radical concentration was not only not required for the calculation of the rate constant ratio, but it was not required to be the same throughout all experiments. This will become evident below.

Although it was not necessary for the initial concentration of the OH radical to be the same throughout all of the experiments, it was still necessary that the Febetron was stable enough to give at least two successive shots that were of approximately the same total dose. This was necessary when taking two successive pulses of separate aliquots of a stock solution while monitoring the reaction at different wavelengths during each successive pulse. If a fast diode array detector were available, the stability of the Febetron would be completely unimportant. Even though it was required that two successive pulses be of approximately the same dose, the demand on the stability of the pulse size of the Febetron was greatly reduced.

It was necessary for the mathematical treatment that the chemical Reactions (12) and (84) were both second order and that they occurred simultaneously when  $\text{CO}_3^{2-}$  and  $\text{IrBr}_6^{3-}$  were both present in solution. Reactions (12) and (84) both involve one common reactant, OH radical.



Again, it was assumed that Reactions (12) and (84) were the only significant processes by which OH radical was consumed. As noted earlier, this was a valid assumption.

It follows that the ratio of the changes in concentration of  $\text{IrBr}_6^{3-}$  and  $\text{CO}_3^{2-}$  is proportionate to the ratio of the right-hand sides of the rate expressions. The rate equations for Reactions (12) and (84) in terms of consumption of reactants  $\text{IrBr}_6^{3-}$  and  $\text{CO}_3^{2-}$  are:

$$\frac{-d[\text{IrBr}_6^{3-}]}{dt} = k_{Ir}[\text{IrBr}_6^{3-}][\cdot\text{OH}] \quad (12)$$

and

$$\frac{-d[\text{CO}_3^{2-}]}{dt} = k_{\text{CO}_3}[\text{CO}_3^{2-}][\cdot\text{OH}] \quad (13)$$

Benson [79] mentioned that a system of this type could be treated by dividing the rate equations for the two competing reactions, Equations (12) and (13) in our case. Dividing these equations gives Equation (14), in which time has been formally eliminated as the independent variable.

$$\frac{d[\text{IrBr}_6^{3-}]}{d[\text{CO}_3^{2-}]} = \frac{k_{Ir}[\text{IrBr}_6^{3-}][\cdot\text{OH}]}{k_{\text{CO}_3}[\text{CO}_3^{2-}][\cdot\text{OH}]} \quad (14)$$

Expression (14) corresponds to dividing the rate law for Reaction (12) by the rate law for Reaction (84).

In order for this type of mathematical treatment to be valid, the chemical reactions must occur simultaneously in the same solution and all measurements of reactant or product concentrations must be taken concurrently. The OH radical concentration in Equation (14) was canceled, and the equation was rearranged and set up for integration.

$$\int_0^t \frac{d[\text{IrBr}_6^{3-}]}{[\text{IrBr}_6^{3-}]} = \frac{k_{Ir}}{k_{\text{CO}_3}} \int_0^t \frac{d[\text{CO}_3^{2-}]}{[\text{CO}_3^{2-}]} \quad (15)$$

Integration and rearrangement of Equation (15) gives Equation (16).

$$\ell n \left\{ \frac{[\text{IrBr}_6^{3-}]_t}{[\text{IrBr}_6^{3-}]_o} \right\} = \frac{k_{Ir}}{k_{CO_3}} \ell n \left\{ \frac{[\text{CO}_3^{2-}]_t}{[\text{CO}_3^{2-}]_o} \right\} \quad (16)$$

In Equation (16),  $[\text{IrBr}_6^{3-}]_t$  and  $[\text{CO}_3^{2-}]_t$  are the concentrations of  $\text{IrBr}_6^{3-}$  and  $\text{CO}_3^{2-}$  at any time after the pulse during a given experiment. For the purpose of these experiments, the values used in the alternate method were the "post-pulse" concentrations of the reactants,  $[\text{IrBr}_6^{3-}]_{pp}$  and  $[\text{CO}_3^{2-}]_{pp}$ . Also,  $[\text{IrBr}_6^{3-}]_o$  and  $[\text{CO}_3^{2-}]_o$  are the initial concentrations of  $\text{IrBr}_6^{3-}$  and  $\text{CO}_3^{2-}$  prior to the pulse. Note that, although the element of time was factored out of Equations (12) and (13) when they were divided, the conditions require that the concentrations of  $\text{IrBr}_6^{3-}$  and  $\text{CO}_3^{2-}$  be measured simultaneously. The left and right hand sides of Equation (16) are equal at any one specific time during the reaction from any one specific initial starting point. The equation can also be written:

$$\ell n \left\{ \frac{[\text{IrBr}_6^{3-}]_{t2}}{[\text{IrBr}_6^{3-}]_{t1}} \right\} = \frac{k_{Ir}}{k_{CO_3}} \ell n \left\{ \frac{[\text{CO}_3^{2-}]_{t2}}{[\text{CO}_3^{2-}]_{t1}} \right\} \quad (17)$$

In Equation (17),  $[\text{IrBr}_6^{3-}]_{t1}$  and  $[\text{CO}_3^{2-}]_{t1}$  are the concentrations of  $\text{IrBr}_6^{3-}$  and  $\text{CO}_3^{2-}$  at any one earlier time while  $[\text{IrBr}_6^{3-}]_{t2}$  and  $[\text{CO}_3^{2-}]_{t2}$  are the concentrations of  $\text{IrBr}_6^{3-}$  and  $\text{CO}_3^{2-}$  at any specific later time. However, for the experiments discussed in this work, initial and long-time concentrations of  $\text{IrBr}_6^{3-}$  and  $\text{CO}_3^{2-}$  have been used. If a diode array detector were available, Equation (17) could be used at any well separated pair of times following the pulse.

When using the alternate method and Equation (16) with our Febetron facility, the analysis wavelength was adjusted successively between 512 nm and 626 nm during separate runs in order to obtain absorbances at two wavelengths so that concentrations of both  $\text{IrBr}_6^{3-}$  and  $\text{CO}_3^{2-}$  could be calculated. The species  $\text{IrBr}_6^{2-}$  was the predominant

absorber at 512 nm, while  $\text{CO}_3^{2-}$  was the main absorber at 626 nm. However, both species absorb to some extent at both wavelengths, and it was necessary to resolve the absorbance due to each species at each wavelength using simultaneous equations as explained in detail below. The species  $\text{CO}_3^{2-}$  is unstable and decays via reaction with itself. This accounts for the falloff of the absorbance at 626 nm with time, as observed.

The reaction immediately after the pulse occurred too fast to measure with our apparatus. After the pulse and after the noise associated with the pulse, there was a considerable jump in the absorbance at both the measured wavelengths. There was also a considerable amount of falloff of the absorbance at 626 nm with time and only a slight falloff of the absorbance at 512 nm.

The absorbances of  $\text{IrBr}_6^{2-}$  and  $\text{CO}_3^{2-}$  at each wavelength were additive. Thus, the total absorbance at 512 nm,  $\text{Abs}_{512}$ , depends on the extinction coefficients of  $\text{IrBr}_6^{2-}$  and  $\text{CO}_3^{2-}$  at 512 nm,  $\epsilon_{\text{Ir}512}$  and  $\epsilon_{\text{CO}512}$ , and the associated molar concentration terms,  $[\text{IrBr}_6^{2-}]$  and  $[\text{CO}_3^{2-}]$ , Equation (18).

$$\text{Abs}_{512} = \epsilon_{\text{Ir}512}[\text{IrBr}_6^{2-}] + \epsilon_{\text{CO}512}[\text{CO}_3^{2-}] \quad (18)$$

Similarly, the absorbance at 626 nm,  $\text{Abs}_{626}$ , depended on the extinction coefficients at 626 nm,  $\epsilon_{\text{Ir}626}$  and  $\epsilon_{\text{CO}626}$ , and again the corresponding molar concentrations, Equation (19).

$$\text{Abs}_{626} = \epsilon_{\text{Ir}626}[\text{IrBr}_6^{2-}] + \epsilon_{\text{CO}626}[\text{CO}_3^{2-}] \quad (19)$$

Eliminating the  $[\text{CO}_3^{2-}]$  concentration between the two equations and rearranging gives Equation (20), which was used to calculate the concentration of  $\text{IrBr}_6^{2-}$  for each measured time increment.

$$[\text{IrBr}_6^{2-}]_t = \left( \frac{\text{Abs}_{512}}{e_{\text{CO}_3^{2-}}} - \frac{\text{Abs}_{626}}{e_{\text{CO}_626}} \right) \div \left( \frac{e_{\text{Ir}512}}{e_{\text{CO}_3^{2-}}} - \frac{e_{\text{Ir}626}}{e_{\text{CO}_626}} \right) \quad (20)$$

The analogous equation used for the calculation of the concentration of  $\text{CO}_3^{2-}$  at each time increment was:

$$[\text{CO}_3^{2-}]_t = \left( \frac{\text{Abs}_{626}}{e_{\text{CO}_626}} - \frac{\text{Abs}_{512}}{e_{\text{CO}_512}} \right) + \left( \frac{e_{\text{CO}_626}}{e_{\text{Ir}626}} - \frac{e_{\text{CO}_512}}{e_{\text{Ir}512}} \right) \quad (21)$$

The extinction coefficients for  $\text{CO}_3^{2-}$  used in Equations (20) and (21) were extracted from a spectrum of  $\text{CO}_3^{2-}$  taken from a spectrum measured by J. L. Weeks and J. Rabani [80].

The extinction coefficient values for  $\text{CO}_3^{2-}$ ,  $e_{\text{CO}_512}$  and  $e_{\text{CO}_626}$ , were determined to be  $895 \text{ M}^{-1} \text{ cm}^{-1}$  and  $1740 \text{ M}^{-1} \text{ cm}^{-1}$ , respectively. The extinction coefficients for  $\text{IrBr}_6^{2-}$  were measured in this laboratory from a reference spectrum taken of a solution of  $\text{Na}_2\text{IrBr}_6$ . The initial concentration of  $\text{IrBr}_6^{2-}$  in the reference solution was calculated using the literature value for the extinction coefficient at 584 nm, which was  $3870 \text{ M}^{-1} \text{ cm}^{-1}$  [59]. The extinction coefficients for  $\text{IrBr}_6^{2-}$  at 512 nm and 626 nm were measured to be  $2260 \text{ M}^{-1} \text{ cm}^{-1}$  and  $608 \text{ M}^{-1} \text{ cm}^{-1}$ , respectively.

When conducting the experiments, the absorbance was measured at 75 time increments during a short period before each pulse. The absorbance was also followed after the pulse with the A/D system set at 5 megahertz, giving time increments of 200 nanoseconds for a total time period of ca. 100 microseconds after the pulse. This was all done at one wavelength for a single pulse of the Febetron. The monochromator was then changed to the second wavelength, and a new aliquot of the same stock solution was transferred to the sample cell. The Febetron was pulsed again while the solution was monitored at the second wavelength. The monochromator was then reset to the first wavelength, a new aliquot transferred to the sample cell, and the Febetron pulsed; starting

the entire process over again. This sequence was continued until there was an adequate number of data sets at each wavelength to obtain a good average, usually a total of about 6 data sets.

Using this method, it was possible to average several sets of data (each set representing ca. 75 pre-pulse and 437 post-pulse time/intensity data pairs for one accelerator shot) at 512 nm, and separately average several sets of data at 626 nm. The data sets were averaged using a "normalization" program, which was written in Basic for the purpose of normalizing data sets that were saved from the program which controlled the Waag II analog to digital converter. The normalization program allows the user to input the data file. The program calculates the absorbance at each time period using the measured voltage at that time period along with stored values of the full-light and no-light signals. The program is capable of displaying as a graph up to twelve data sets. It can also average the absorbance at each time period for the user-chosen data sets, graph the averaged data set, and save as an ASCII file the averaged data set.

During the pulse radiolysis experiments, there were always two averaged data sets for each stock solution. Each stock solution had a different concentration ratio of the reactants,  $\text{IrBr}_6^{3-}$  and  $\text{CO}_3^{2-}$ . One averaged data set represented absorption by the products measured at 512 nm for 437 time periods, and the other averaged data set represented absorption by the products measured at 626 nm for 437 time periods. The averaged data sets for a typical experiment are shown in the upper graph in Figure (30).

Equations (20) and (21) were used to separate the absorbance at 512 nm and 626 nm of  $\text{IrBr}_6^{2-}$  and  $\text{CO}_3^-$  for each data point in the averaged data sets. The result was the calculation of the concentrations of  $\text{IrBr}_6^{2-}$  and  $\text{CO}_3^-$  at each time period after the pulse.



This is evident in the concentration graph in Figure (30), lower graph. The expected decay of  $\text{CO}_3^-$  and the stability of  $\text{IrBr}_6^{2-}$  are both easily discernable from the graph of the concentrations in Figure (30).

The work accomplished to this point is not yet sufficient to obtain a value of the rate constant for reaction of OH radical with  $\text{IrBr}_6^{3-}$ . What is available at this point is a pair of curves in Figure (30) (lower diagram) which shows an effectively constant value of  $\text{IrBr}_6^{2-}$  and the decay of  $\text{CO}_3^-$  corresponding to a single set of initial concentrations of the two OH radical scavengers,  $\text{IrBr}_6^{3-}$  and  $\text{CO}_3^{2-}$ . It was next necessary to extrapolate the  $\text{CO}_3^-$  curve to an initial time corresponding to the time of the pulse, giving  $[\text{CO}_3^-]_{pp}$ . Similarly, a back extrapolation of the almost constant  $[\text{IrBr}_6^{2-}]$  to the time of the pulse gave the value for  $[\text{IrBr}_6^{2-}]_{pp}$ .

The back extrapolations just described produced one  $[\text{IrBr}_6^{2-}]_{pp}$  and one  $[\text{CO}_3^-]_{pp}$  to be used in the equation for the Alternate Competition method, Equation (16). This one pair of concentration values was taken to be the product concentrations at infinite time relative to the fast  $\cdot\text{OH}$ /scavenger reaction (the "post-pulse" values), but effectively at "time zero" with respect to the subsequent loss of  $\text{CO}_3^-$ . This means that the concentrations used in the log-log plot for the determination of the rate constant,  $k_{Ir}$ , were taken immediately after the pulse, but before any of the products disappeared. The derivations of values of  $[\text{IrBr}_6^{2-}]_{pp}$  and  $[\text{CO}_3^-]_{pp}$  are described below.

Although  $\text{IrBr}_6^{2-}$  is stable after the pulse, the  $\text{CO}_3^-$  ion is not stable. It reacts with itself via second order kinetics with  $2k = 1.25 \times 10^7 \text{ M}^{-1} \text{ s}^{-1}$  (zero ionic strength) [80], [83]. The  $[\text{CO}_3^-]$  concentration after the pulse followed second order decay kinetics for at

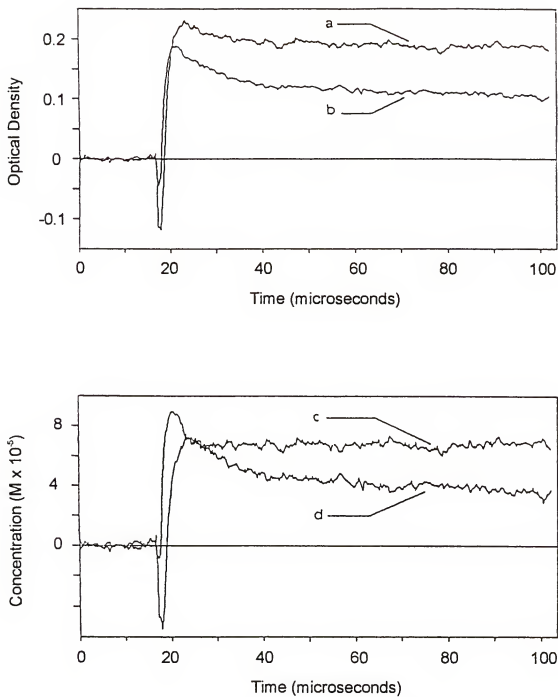


Figure (30). Plot of the optical densities at (a) 512 nm and (b) 626 nm and the concentrations of (c)  $\text{IrBr}_6^{2-}$  and (d)  $\text{CO}_3^-$  after spectral stripping using Equations (20) and (21).

least two half lives, with a rate constant of  $2k = 1.5 \times 10^7 \text{ M}^{-1} \text{ s}^{-1}$ . This was in reasonable agreement with the literature value of  $2k = 1.25 \times 10^7 \text{ M}^{-1} \text{ s}^{-1}$ .

The concentration of  $\text{CO}_3^-$  immediately following reaction of OH radical with  $\text{CO}_3^{2-}$ , the "post-pulse" concentration,  $[\text{CO}_3^-]_{\text{pp}}$ , was calculated using the second order rate law for reaction of  $\text{CO}_3^-$  with itself and extrapolation back to the time of the pulse. An example of the graph for this calculation is shown in Figure (31). (The figure shown is for a typical solution of  $\text{Na}_2\text{CO}_3$ ; graphs with added  $\text{IrBr}_6^{3-}$  are qualitatively similar.) Finally,  $[\text{CO}_3^{2-}]_{\text{pp}}$  was calculated by subtracting  $[\text{CO}_3^-]_{\text{pp}}$  from  $[\text{CO}_3^{2-}]_0$ .

The  $\text{IrBr}_6^{2-}$  product of the reaction of  $\text{IrBr}_6^{3-}$  with OH radical was stable, as seen in the concentration graph in Figure (30). The "post-pulse" concentration of  $\text{IrBr}_6^{2-}$ ,  $[\text{IrBr}_6^{2-}]_{\text{pp}}$ , was calculated using data regression followed by an essentially horizontal extrapolation to the time of the pulse. The value of  $[\text{IrBr}_6^{3-}]_{\text{pp}}$  was calculated by subtracting  $[\text{IrBr}_6^{2-}]_{\text{pp}}$  from the initial concentration of the hexabromoiridate,  $[\text{IrBr}_6^{3-}]_0$ . Graphs of raw data (averaged for several shots at each wavelength) are shown in curves a and b of Figure (30), and the corresponding concentrations of  $\text{IrBr}_6^{2-}$  and  $\text{CO}_3^-$ , derived as explained above, are shown as curves c and d of Figure (30), respectively.

The data treatment described above and illustrated in Figure (30) was performed for several aqueous solutions of  $\text{Na}_2\text{CO}_3$  and  $\text{Na}_3\text{IrBr}_6$ . Each of the solutions was 10 millimolar in  $\text{Na}_2\text{CO}_3$  and of various concentrations of  $\text{Na}_3\text{IrBr}_6$ . A plot of the logarithm of the  $[\text{IrBr}_6^{3-}]_{\text{pp}}/[\text{IrBr}_6^{3-}]_0$  concentration ratio versus the logarithm of the  $[\text{CO}_3^{2-}]_{\text{pp}}/[\text{CO}_3^{2-}]_0$  concentration ratio, based on Equation (16), is shown in Figure (32). The origin was included in the plot as prescribed by Equation (16). (Note that the figure involves negative coordinate values for both the ordinate and the abscissa; the origin is at

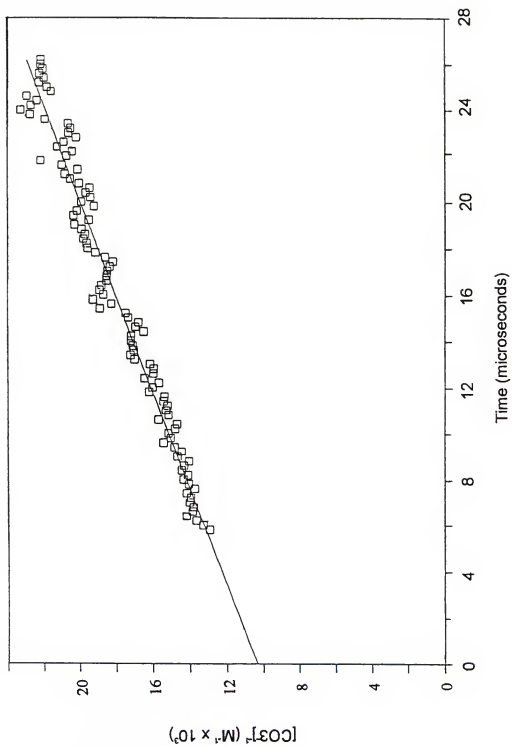


Figure (31). Second order plot of the reaction for the decay of  $\text{CO}_3^{2-}$ .

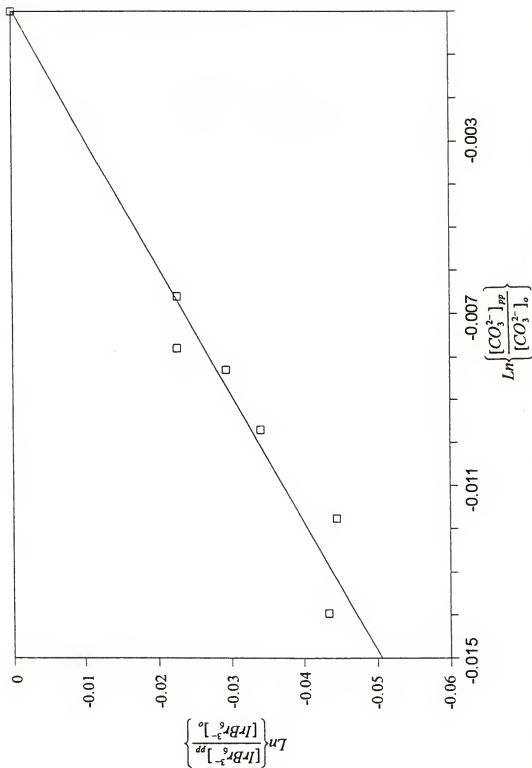


Figure (32). Plot based on the alternate method of the mathematical treatment of competition kinetics. The natural logarithm of the concentration ratio of  $\text{IrBr}_6^{3-}$  versus the natural logarithm of the concentration ratio of  $\text{CO}_3^{2-}$ .

the upper right corner of the graph.) A preliminary value of the rate constant was calculated based on the slope of this line and Equation (16) as  $1.4 \times 10^9 \text{ M}^{-1} \text{ s}^{-1}$ , using initial concentrations of  $\text{IrBr}_6^{3-}$  based on the mass of the sample and confirmed with the Beckman DU Spectrophotometer. At this stage, there was no correction for reaction of  $\text{IrBr}_6^{3-}$  to  $\text{IrBr}_5\text{H}_2\text{O}^{2-}$ , which was expected to occur during the 20-minute period of bubbling with  $\text{N}_2\text{O}$  after the solution was prepared but before pulsing it with the Febetron.

The rate constant was also calculated using an estimated concentration of  $\text{IrBr}_6^{3-}$ , with respect to its conversion to  $\text{IrBr}_5\text{H}_2\text{O}^{2-}$  in water. The half-life of  $\text{IrBr}_6^{3-}$  is about 19 minutes at  $25^\circ\text{C}$ , based on the published value for the aquation reaction rate constant [59].

All solutions were subject to saturation with  $\text{N}_2\text{O}$  by bubbling the gas through the solution for 20 minutes. This is approximately one half-life of the  $\text{IrBr}_6^{3-}$ . It was a fair approximation to estimate the initial concentrations of  $\text{IrBr}_6^{3-}$  for each experimental run to be equal to half the dissolved concentrations (before any conversion to  $\text{IrBr}_5\text{H}_2\text{O}^{2-}$  occurred).

The rate constant for Reaction (12) was calculated using the alternate competition method and initial concentration values for  $\text{IrBr}_6^{3-}$  that were estimated to be half the initial dissolved  $\text{IrBr}_6^{3-}$  concentrations. Reaction of  $\text{IrBr}_5\text{H}_2\text{O}^{2-}$  with OH radical was neglected based on the assumption that  $\text{IrBr}_5\text{H}_2\text{O}^{2-}$  is ca. 50 times more stable than  $\text{IrBr}_6^{3-}$  with respect to oxidation by  $\text{Br}_2$  as measured in this laboratory, which correlates with the respective reduction potentials. A plot of the natural logarithm of the  $[\text{IrBr}_6^{3-}]_{pp}/[\text{IrBr}_6^{3-}]_0$  concentration ratio versus the natural logarithm of the  $[\text{CO}_3^{2-}]_{pp}/[\text{CO}_3^{2-}]_0$  concentration

ratio is shown in Figure (33). The rate constant based on this plot was  $2.8 \times 10^9 \text{ M}^{-1} \text{ s}^{-1}$ . As expected, this value is two times the value calculated without consideration for the loss of  $\text{IrBr}_6^{3-}$  by conversion to  $\text{IrBr}_5\text{H}_2\text{O}^{2-}$ .

Graphs were also prepared using the data collected for the log-log method, but plotted according to the standard competition equation. Equation (9) was rearranged to give Equation (22).

$$\frac{[\cdot\text{OH}]_o}{[\text{IrBr}_6^{2-}]_{pp}} = 1 + \frac{k_{Ir}}{k_{\text{CO}_3}} \times \frac{[\text{IrBr}_6^{3-}]_o}{[\text{CO}_3^{2-}]_o} \quad (22)$$

The initial OH radical concentrations ( $[\cdot\text{OH}]_o$ ) were calculated for each experimental run and were taken to be equal to the sum of the "post-pulse" concentrations of  $\text{IrBr}_6^{2-}$  and  $\text{CO}_3^{\cdot -}$  formed. The graphs were prepared based on both no loss of  $\text{IrBr}_6^{3-}$  by aquation and loss of 50 percent of the initial dissolved  $\text{IrBr}_6^{3-}$ . The graph based on the assumption of no  $\text{IrBr}_6^{3-}$  loss is shown in Figure (34), and the graph with the estimated initial  $\text{IrBr}_6^{3-}$  concentration equal to half the initial dissolved  $\text{IrBr}_6^{3-}$  concentration is shown in Figure (35). Consistent with Equation (22), the y-intercept is unity. Thus, the y-intercepts of these graphs were included.

The rate constant calculated from the slope of the graph and Equation (22) for the case with the assumption of no loss of  $\text{IrBr}_6^{3-}$  due to aquation was  $1.3 \times 10^9 \text{ M}^{-1} \text{ s}^{-1}$ , in fair agreement with the value of  $1.4 \times 10^9 \text{ M}^{-1} \text{ s}^{-1}$ , calculated using the log-log method. The rate constant calculated using standard competition kinetics and assuming 50 percent loss of  $\text{IrBr}_6^{3-}$  was  $2.6 \times 10^9 \text{ M}^{-1} \text{ s}^{-1}$ . This was twice the value calculated assuming no  $\text{IrBr}_6^{3-}$  loss, as expected.

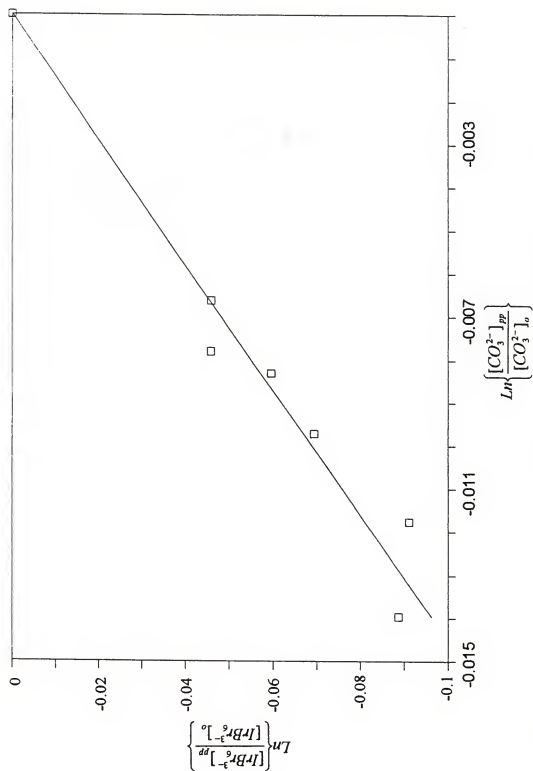


Figure (33). Plot based on the alternate method using the assumption that 50% of the  $\text{IrBr}_6^{3-}$  hydrolyzed. The natural logarithm of the concentration ratio of  $\text{IrBr}_6^{3-}$  versus the natural logarithm of the concentration ratio of  $\text{CO}_3^{2-}$ .



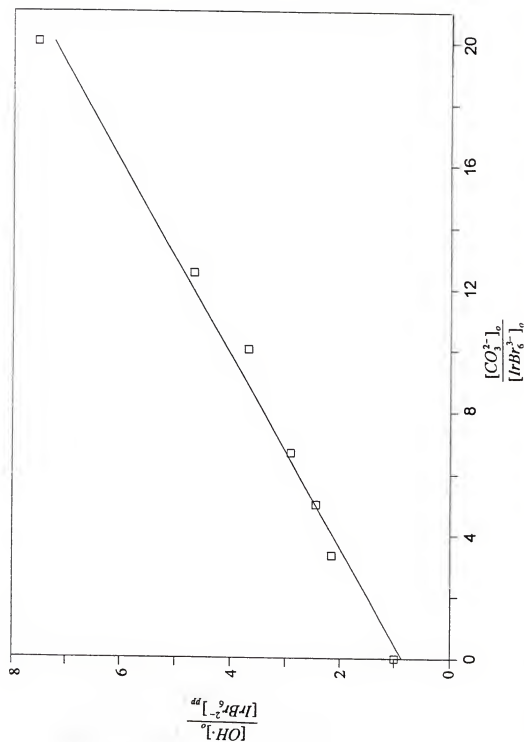


Figure (34). Plot based on the standard competition method. Aquation of  $\text{IrBr}_6^{3-}$  was not considered. The concentration ratios are plotted based on Equation (22).

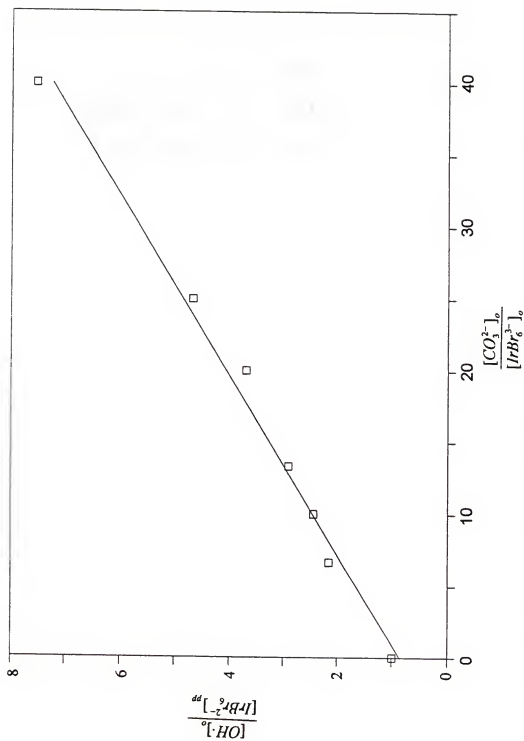


Figure (35). Plot based on the standard competition method, assuming 50% hydrolyzation of  $IrBr_6^{3-}$ . The concentration ratios are plotted based on Equation (22).

The rate constants calculated using the standard competition method and the log-log method are tabulated in Table (6). Two values are given in each case, one based on no aquation of  $\text{IrBr}_6^{3-}$  and one based on 50 percent conversion to  $\text{IrBr}_5\text{H}_2\text{O}^{2-}$  as described earlier in the present section.

Table (6). Rate constants calculated using the alternate competition method and the standard competition method. The rate constants were calculated under the assumption of no  $\text{IrBr}_6^{3-}$  loss by conversion to  $\text{IrBr}_5\text{H}_2\text{O}^{2-}$  and 50 percent  $\text{IrBr}_6^{3-}$  loss by aquation.

Method Used	50% loss of $\text{IrBr}_6^{3-}$ due to	$k_{\text{Ir}}$ ( $\text{M}^{-1} \text{s}^{-1}$ )
	aquation considered	
Alternate (Equation (16))	No	$1.4 \times 10^9$
Alternate (Equation (16))	Yes	$2.8 \times 10^9$
Standard (Equation (22))	No	$1.3 \times 10^9$
Standard (Equation (22))	Yes	$2.6 \times 10^9$

## CHAPTER SIX

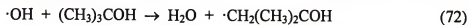
### REDUCTION OF HEXABROMOIRIDATE (IV) BY AQUEOUS ELECTRON

Hexabromoiridate (IV) was reduced by the aqueous electron using pulse radiolysis experiments. The chemical equation for the reaction is:



Reactions of  $e_{\text{aq}}^-$  are usually very fast, with rate constants typically in the range of  $10^9$  to  $10^{10} \text{ M}^{-1} \text{ s}^{-1}$ . In the present work, we were able to follow the reaction directly by spectrophotometry. However,  $\text{IrBr}_6^{2-}$  absorbs strongly in the same region (500-650 nm) where  $e_{\text{aq}}^-$  absorbs. Accordingly, a Gear integrator was employed to resolve the time concentration data for the relevant chemical species so that the rate constant for Reaction (10) could be determined.

As previously discussed, a solution can be made totally reducing by making it 0.100 M in t-butanol, and deoxygenating it by bubbling an inert gas such as nitrogen or helium through the solution for ca. 20 minutes. The reagent tert-butanol reacts with OH radical to produce the much less reactive t-butanol cation, Reaction (72) [55].



At this stage, the reactive intermediates in solution are  $e_{\text{aq}}^-$ , the hydrogen atom, and the much less reactive tert-butanol radical.

Several attempts were made to measure the rate constant for the reaction using different gases as the deoxygenating gas, including nitrogen, argon, and high purity

helium. There was some type of impurity in the system. Ultrahigh purity helium was purchased and used; it was further purified by passing it through an adsorption filter, a liquid nitrogen trap, and an alumina column. The gas was also passed through a coil to allow it to reach ambient temperature before it bubbled through the sample solution. All of the copper tubing was thoroughly cleaned using a solution of 6 M HCl, followed by copious amounts of distilled water, acetone, and distilled water again. The complete setup for the gas-flow system is shown in Figure (36).

The impurity problem improved significantly with the use of the ultrahigh purity helium and the traps. It was postulated that if the  $\text{IrBr}_6^{2-}$  concentration were made high enough, reaction of  $e_{aq}^-$  with the impurity would be negligible. Under these circumstances, the majority of the disappearance of  $e_{aq}^-$  was due to its reaction with  $\text{IrBr}_6^{2-}$ .

## Experimental

Solutions of various concentrations of  $\text{IrBr}_6^{2-}$  were prepared from an aqueous stock solution of  $\text{K}_2\text{IrBr}_6$  that was also 0.10 molar in t-butanol. The water used in all of these experiments was deionized water further purified by distillation from an aqueous solution of NaOH and  $\text{KMnO}_4$ . A stock solution of 0.10 molar t-butanol was also prepared. Solutions of various concentrations of  $\text{K}_2\text{IrBr}_6$  were made by pipetting specific amounts of the stock  $\text{IrBr}_6^{2-}$ /t-butanol solution into a 100 mL volumetric flask and filling to the mark with the stock 0.10 molar t-butanol solution. The concentration of  $\text{IrBr}_6^{2-}$  in each solution was verified using a Beckman DU spectrophotometer. The wavelength and

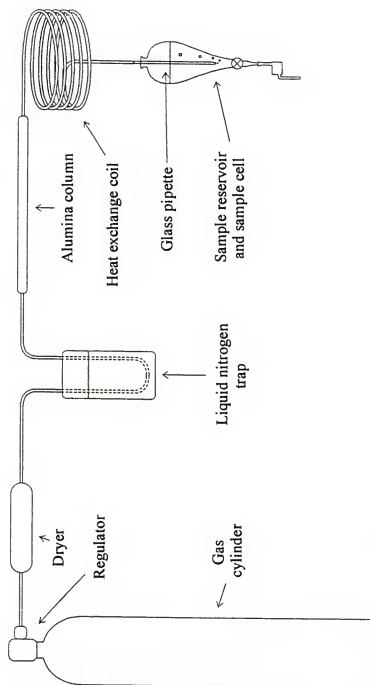


Figure (36). Schematic diagram of the gas tubing arrangement that used when purging aqueous solutions of  $\text{IrBr}_6^{2-}$  of dissolved oxygen prior to subjecting the solution to pulse radiolysis studies.

extinction coefficient used for verification of the concentration was 584 nm and  $3870 \text{ M}^{-1} \text{ cm}^{-1}$  [59], respectively.

Each of the solutions was added to the sample reservoir and then treated with ultrahigh-purity helium, passed through the traps represented in Figure (36), by bubbling the gas through the solution for 20 minutes. Aliquots of the solution were introduced into the sample cell and subjected to the pulse from the Febetron. The solution was monitored at 634 nm using the He-Ne laser. The extinction coefficient for  $\text{IrBr}_6^{2-}$  at 634 nm was measured in this laboratory using a reference solution of  $\text{K}_2\text{IrBr}_6$ . The concentration of the reference solution was calculated using the extinction coefficient of  $3870 \text{ M}^{-1} \text{ cm}^{-1}$  at 584 nm [59]. The extinction coefficient for  $\text{e}_{\text{aq}}^-$  at 634 nm was extracted from a plot of extinction coefficient versus wavelength given by Buxton [33]. The extinction coefficient used for  $\text{IrBr}_6^{2-}$  at 634 nm was  $906 \text{ M}^{-1} \text{ cm}^{-1}$  while the extinction coefficient used for  $\text{e}_{\text{aq}}^-$  at 634 nm was  $16100 \text{ M}^{-1} \text{ cm}^{-1}$ .

### Results and Calculations

The calculations of the concentration at each time interval for the experiments regarding the rate constant for reaction of  $\text{e}_{\text{aq}}^-$  with  $\text{IrBr}_6^{2-}$  (Reaction (10)) were fairly tedious, but straightforward. In the following discussion it is necessary to consider the relation between the intensity of the analyzing light and the voltage signal of the photomultiplier tube. The voltage across a fixed resistor caused by the current from the PM-tube was measured and digitized by the WAAG II A/D converter. In all cases the measurement of the concentration of chemical species from an absorbance involves a ratio of two light intensities and the associated units cancel out. For this reason it is valid

in the following discussion to treat light intensities and voltage measurements as if they were in the same units.

Since  $\text{IrBr}_6^{2-}$  absorbs at 634 nm and was initially present before the discharge of the Febetron, it was necessary in every experiment to back-calculate the full-light intensity of the analyzing light from the previously determined concentration of  $\text{IrBr}_6^{2-}$ . The  $\text{IrBr}_6^{2-}$  concentration was initially determined using the Beckman DU Spectrophotometer.

Now consider the spectrophotometric measurements made during the pulse radiolysis experiments. The measurements made are voltages across the resistor caused by the current from the PM-tube. A representation of the voltage signals discussed below is shown in Figure (37). The signal from the PM-tube through a blank solution is the full-light voltage,  $V_{fl}$ . The no-light voltage,  $V_{nl}$ , is the signal from the PM tube when the light path is blocked, and the sample voltage,  $V_s$ , is the voltage through the sample before and after the pulse. (Note that the latter voltage changes with time during the experiment). Although in practice the no-light voltage was not represented on the final graph, it is included in Figure (37) for clarity in understanding the calculations below. Also, it was not possible to measure the full-light voltage directly, but it could be inferred as described below. A hypothetical full-light signal is shown in Figure (37).

The no-light signal,  $V_{nl}$ , was measured with the light path blocked, then saved by the computer program. The voltage signal of the sample,  $V_s$ , is the signal from the PM-tube for 75 time increments before the pulse and 437 time increments after the pulse. The signal voltage of the sample starts at a higher point on the graph because the solution initially contains a certain amount of  $\text{IrBr}_6^{2-}$ , a light absorber at 634 nm. The signal



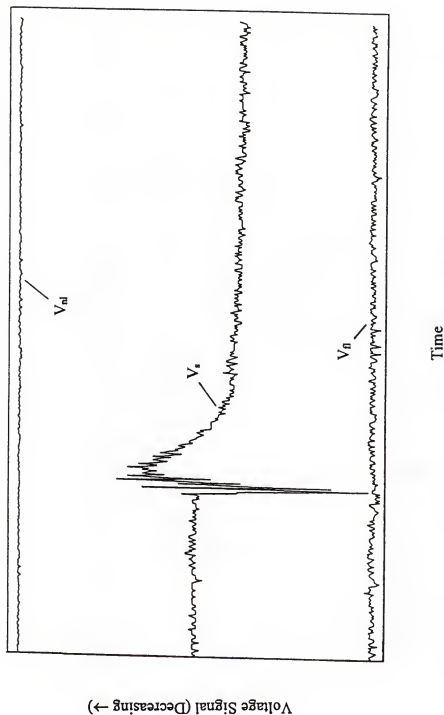


Figure (37). Expected results for a typical experiment in the determination of the rate constant for reaction of  $\text{IrBr}_6^{2-}$  with  $\text{e}_{\text{aq}}^-$ . The no-light voltage,  $V_{\text{nl}}$ , is the voltage across a resistor due to the current from the photomultiplier tube when the light path is blocked. The full-light voltage,  $V_n$ , is the voltage signal when there is a sample blank in the light path, and  $V_s$  is the voltage signal with the sample in place. All voltage values were taken for 512 time periods. In practice with this experiment, there was no way to measure  $V_n$  because the solution contained  $\text{IrBr}_6^{2-}$ , a light absorber at the analyzing wavelength. The full-light voltage is shown here for clarity. The shape of the sample voltage is explained in detail in the body of the text.

voltage decreases following the pulse noise, because  $e_{aq}^-$  strongly absorbs at 634 nm. The signal voltage from the PM-tube rapidly increases after the pulse, because both light absorbers react with each other via Reaction (10) to produce  $IrBr_6^{3-}$ , which does not absorb light appreciably at 634 nm. After the pulse induced reaction was complete, the signal voltage was greater than before the pulse because some but not all of the  $IrBr_6^{2-}$  was consumed in the reaction process. (It is important to note that, while the signal voltage increases, the absorbance of the solution decreases.)

The spectrophotometric measurements made in the Febetron experiments can be understood using Beer's Law, Equation (23).

$$Abs. = \epsilon \ell [IrBr_6^{2-}]_t \quad (23)$$

In Equation (23), Abs. is the absorbance,  $\epsilon$  is the extinction coefficient, and  $\ell$  is the path length. The path length is 1 cm and is common to all experiments, so it can be canceled out of the equation. The absorbance is equal to the base 10 logarithm of the light intensity ratio in the form  $I_o/I_t$ , Equation (24).

$$Abs. = \log \frac{I_o}{I_t} = \log \left\{ \frac{V_{fl} - V_{nl}}{V_s - V_{nl}} \right\} \quad (24)$$

In equation (24),  $I_o$  and  $I_t$  are, respectively, the full-light intensity and the time dependent light intensity of the sample. The absorbance can also be given in terms of measured A/D voltage values, as shown.

In the numerator of the right-hand expression of Equation (24), the full-light intensity is equal to the full-light voltage,  $V_{fl}$ , minus the no-light voltage,  $V_{nl}$ , Equation (25).

$$I_o = V_{fl} - V_{nl} \quad (25)$$

In the denominator of the right-hand expression of Equation (24), the time dependent sample intensity,  $I_t$ , is equal to the sample voltage,  $V_s$ , minus the no-light voltage,  $V_{nl}$ , Equation (26).

$$I_t = V_s - V_{nl} \quad (26)$$

Equation (27) was used to back-calculated the full-light intensity of the analyzing light source for each experiment. It was derived by setting Equations (23) and (24) equal to each other and solving for  $I_o$ .

$$I_o = I_t^* \times 10^{\epsilon [IrBr_6^{2-}]_o} \quad (27)$$

In equation (27),  $I_t^*$  is the average of the time dependent sample intensity before the pulse. The final concentration of  $IrBr_6^{2-}$  was calculated using the full-light intensity, the no-light voltage, and the average sample voltage after reaction with  $e_{aq}^-$  was complete, Equation (28).

$$[IrBr_6^{2-}]_f = \epsilon \log \left\{ \frac{I_o}{(V_s' - V_{nl})} \right\} \quad (28)$$

Where  $I_o$  is inferred as described, and  $V_s'$  is the average of the time dependent sample intensity after reaction of  $IrBr_6^{2-}$  with  $e_{aq}^-$  is complete.

The pulse size of the Febetron 706 is somewhat unreliable, as previously discussed, leaving solutions of different concentrations of  $e_{aq}^-$  after each shot. Because of this and because  $e_{aq}^-$  reacts with itself while at the same time both  $e_{aq}^-$  and  $IrBr_6^{2-}$  absorb light at the analyzing wavelength, it was difficult to determine the initial concentration of  $e_{aq}^-$  from the initial and final concentrations of  $IrBr_6^{2-}$ . Therefore, the rate constant for reaction of  $e_{aq}^-$  with  $IrBr_6^{2-}$  was determined using a successive approximation approach and the Gear integration program.

A reaction mechanism for the pulse radiolysis of water was compiled from previous studies. The mechanistic steps for the fast reactions that would occur when t-butanol and  $\text{IrBr}_6^{2-}$  were present in de-aerated aqueous solution were proposed and added to the radiolysis mechanism. (It would also have been acceptable to leave out the t-butanol reactions and to set the OH radical concentration equal to zero.)

The initial concentrations of  $e_{aq}^-$  to be used in the simulations were first estimated to be a little higher than the change in the concentration of  $\text{IrBr}_6^{2-}$  from beginning to end of the reaction process. Concentrations of the rest of the products of the pulse radiolysis of the aqueous solution were calculated using a Basic program. The program was designed to calculate the concentrations of  $\cdot\text{OH}$ ,  $\text{H}_3\text{O}^+$ ,  $\text{H}\cdot$ ,  $\text{H}_2\text{O}_2$ ,  $\text{HO}_2\cdot$ , and  $\text{O}_2\cdot^-$  based on the relative G-values for each species and a value for the  $e_{aq}^-$  concentration input by the operator. The program then listed and saved the calculated concentrations as an ASCII file that could be readily used in the mechanistic simulation file. The program is listed in Appendix (B).

The proposed mechanism listed in Table (7) and the concentrations of t-butanol,  $\text{IrBr}_6^{2-}$ , and the radiolysis products were entered into the Gear integrator program. Attempts were made to approximate the rate constant for the reaction of  $\text{IrBr}_6^{2-}$  with  $e_{aq}^-$ , Reaction (10). Simulations were performed and files prepared of the simulated concentrations of  $\text{IrBr}_6^{2-}$  and  $e_{aq}^-$  over time for a given experiment. The simulated concentrations of the  $\text{IrBr}_6^{2-}$  and  $e_{aq}^-$  were imported to Lotus 123. The absorbance due to  $e_{aq}^-$  and  $\text{IrBr}_6^{2-}$  were calculated from the simulated concentrations for each time period using the extinction coefficients of  $e_{aq}^-$  and  $\text{IrBr}_6^{2-}$  at 634 nm,  $16100 \text{ M}^{-1} \text{ cm}^{-1}$  and  $906 \text{ M}^{-1} \text{ cm}^{-1}$ , respectively. The sum of the two absorbances was calculated for each time

Table (7): Mechanism used in the simulation of the pulse radiolysis of aqueous t-butanol/IrBr<sub>6</sub><sup>2-</sup> solution.

Reaction	Rate Const.	Ref.
$e_{aq}^- + e_{aq}^- \rightarrow H_2 + 2OH^-$	$5.6 \times 10^9$ [25]	(13)
$e_{aq}^- + \cdot OH \rightarrow OH^-$	$3.0 \times 10^{10}$ [25]	(14)
$e_{aq}^- + H^+ \rightarrow H$	$2.3 \times 10^{10}$ [26]	(15)
$e_{aq}^- + H \rightarrow H_2 + OH^-$	$2.5 \times 10^{10}$ [25]	(16)
$e_{aq}^- + HO_2^- \rightarrow \cdot OH + 2OH^-$	$3.5 \times 10^9$ [27]	(17)
$e_{aq}^- + O^- \rightarrow 2OH^-$	$2.2 \times 10^{10}$ [25]	(18)
$e_{aq}^- + H_2O_2 \rightarrow OH^- + \cdot OH$	$1.1 \times 10^{10}$ [26]	(19)
$e_{aq}^- + O_2 \rightarrow O_2^-$	$1.9 \times 10^{10}$ [28]	(20)
$e_{aq}^- + O_2^- \rightarrow O_2^{2-}$	$1.3 \times 10^{10}$ [26]	(21)
$e_{aq}^- + H_2O \rightarrow H + OH^-$	$1.9 \times 10^1$ [26]	(22)
$H + OH^- \rightarrow e_{aq}^-$	$2.2 \times 10^7$ [26]	(23)
$H + H \rightarrow H_2$	$7.8 \times 10^9$ [29]	(24)
$\cdot OH + \cdot OH \rightarrow H_2O_2$	$5.5 \times 10^9$ [26]	(25)
$H + \cdot OH \rightarrow H_2O$	$7.0 \times 10^9$ [30]	(26)
$H^+ + OH^- \rightarrow H_2O$	$1.4 \times 10^{11}$ [31]	(27)
$H_2O \rightarrow H^+ + OH^-$	$2.6 \times 10^{-5}$ [31]	(28)
$\cdot OH + H_2 \rightarrow H + H_2O$	$4.2 \times 10^7$ [26]	(29)
$\cdot OH + H_2O_2 \rightarrow HO_2 + H_2O$	$2.7 \times 10^7$ [32]	(30)
$2HO_2 \rightarrow H_2O_2 + O_2$	$2.7 \times 10^6$ [26]	(31)

Table (7) continued.

Reaction	Rate Const.	Ref.	
$O_2^- + HO_2 \rightarrow HO_2^- + O_2$	$4.4 \times 10^7$	[33]	(32)
$H + H_2O_2 \rightarrow \cdot OH + H_2O$	$9 \times 10^7$	[34]	(33)
$HO_2 + H \rightarrow H_2O_2$	$1 \times 10^{10}$	[35]	(34)
$HO_2 + \cdot OH \rightarrow H_2O + O_2$	$6 \times 10^9$	[36]	(35)
$H + O_2 \rightarrow HO_2$	$2.1 \times 10^{10}$	[26]	(36)
$O_2^- + H^+ \rightarrow HO_2$	$4.7 \times 10^{10}$	[37]	(37)
$HO_2 \rightarrow H^+ + O_2^-$	$8 \times 10^5$	a	(38)
$H^+ + HO_2^- \rightarrow H_2O_2$	$3 \times 10^{10}$	b	(39)
$H_2O_2 \rightarrow H^+ + HO_2^-$	$3 \times 10^{-2}$	c	(40)
$H_2O_2 + OH^- \rightarrow HO_2^- + H_2O$	$5.0 \times 10^8$	[38]	(41)
$HO_2^- + H_2O \rightarrow H_2O_2 + OH^-$	$5.7 \times 10^4$	[38]	(42)
$\cdot OH + OH^- \rightarrow O^- + H_2O$	$1.2 \times 10^{10}$	[33]	(43)
$O^- + H_2O \rightarrow \cdot OH + OH^-$	$9.3 \times 10^7$	[33]	(44)
$\cdot OH + HO_2^- \rightarrow OH^- + HO_2$	$7.5 \times 10^9$	[32]	(45)
$H + H_2O \rightarrow H_2 + \cdot OH$	$1 \times 10$	[26]	(46)
$\cdot OH + O^- \rightarrow HO_2^-$	$2 \times 10^{10}$	[39]	(47)
$\cdot OH + O_2^- \rightarrow OH^- + O_2$	$1.0 \times 10^{10}$	[40]	(48)
$O^- + H_2 \rightarrow H + OH^-$	$8.0 \times 10^7$	[25]	(49)
$O^- + H_2O_2 \rightarrow O_2^- + H_2O$	$5 \times 10^8$	[26]	(50)
$O^- + HO_2^- \rightarrow O_2^- + OH^-$	$4 \times 10^8$	[26]	(51)

Table (7) continued.

Reaction	Rate Const.	Ref.	
$O^- + O_2 \rightarrow O_3^-$	$3.6 \times 10^9$	[33]	(52)
$O^- + O_2^- + H_2O \rightarrow 2OH^- + O_2$	$6.0 \times 10^8$	[41]	(53)
$\cdot OH + (CH_3)_3COH \rightarrow H_2O + \cdot CH_2(CH_3)_2COH$	$6.0 \times 10^8$	[55]	(72)
$IrBr_6^{2-} + e_{aq}^- \rightarrow IrBr_6^{3-}$	$1.6 \times 10^{10}$	d	(10)
$IrBr_6^{2-} + H \rightarrow IrBr_6^{3-} + H^+$	$9.2 \times 10^9$	b	(64)
$IrBr_6^{3-} + H \rightarrow IrBr_6^{4-} + H^+$	$6 \times 10^9$	b	(65)
$IrBr_6^{4-} + IrBr_6^{2-} \rightarrow 2IrBr_6^{3-}$	$9.2 \times 10^8$	d	(66)
$IrBr_6^{3-} + e_{aq}^- \rightarrow IrBr_6^{4-}$	$2.61 \times 10^9$	d	(11)
$IrBr_6^{3-} + \cdot OH \rightarrow IrBr_6^{2-} + OH^-$	$2 \times 10^9$	e	(12)

a Calculated to give  $pK = 4.8$  with respect to Reaction (37).

b Estimated.

c Calculated to give  $pK = 11.8$  with respect to Reaction (39).

d Measured, this laboratory, previous work.

e Best fit, this laboratory, previous work.

period. Graphical representation of the theoretical absorbance and the experimental absorbance over the time of the reaction were compared. The value of the rate constant for  $\text{IrBr}_6^{2-}$  reaction with  $\text{e}_{\text{aq}}^-$  and the initial  $\text{e}_{\text{aq}}^-$  concentration were then adjusted, new simulations made using the Gear integrator, and graphical representations of the simulated and experimental absorbances over time compared in Lotus 123. This operation was continued until the estimated values gave a "best" fit for the change in the simulated absorbance over time to the change in the experimental absorbance over time.

It was possible to determine the values of the  $\text{e}_{\text{aq}}^-$  and the rate constant for reaction of  $\text{e}_{\text{aq}}^-$  with  $\text{IrBr}_6^{2-}$  using the successive approximation method and the Gear integrator because both values affected the simulated curvature of the combined concentrations and, hence, absorbances, of  $\text{e}_{\text{aq}}^-$  and  $\text{IrBr}_6^{2-}$ , while the  $\text{e}_{\text{aq}}^-$  yield affects the final plateau value. A typical fit of the theoretical absorbances to the experimental absorbances over time is shown in Figure (38). Using this method, the  $\text{e}_{\text{aq}}^-$  concentration and rate constant for  $\text{e}_{\text{aq}}^-$  reaction with  $\text{IrBr}_6^{2-}$  were determined for each of the experimental pulses.

A single value for the  $\text{e}_{\text{aq}}^-$  plus  $\text{IrBr}_6^{2-}$  rate constant that would give a good fit for all of the separate experimental pulses was not obtainable using the method described. It was possible, though, to arrive at a range of rate constants with an average of  $1.4 \times 10^{10} \text{ M}^{-1} \text{ s}^{-1}$ . The values for the rate constant ranged from  $1.2 \times 10^{10} \text{ M}^{-1} \text{ s}^{-1}$  to  $2.4 \times 10^{10} \text{ M}^{-1} \text{ s}^{-1}$ . Furthermore, the selection of best-fit values had a pattern. Experiments with the higher initial concentrations of  $\text{IrBr}_6^{2-}$  required lower rate constants for best-fit. A graph of the selected rate constant versus the  $\text{IrBr}_6^{2-}$  concentration was prepared, as shown in Figure (39). It was observed that higher rate constants were required to obtain good fits for experiments with lower concentrations of  $\text{IrBr}_6^{2-}$ , whereas



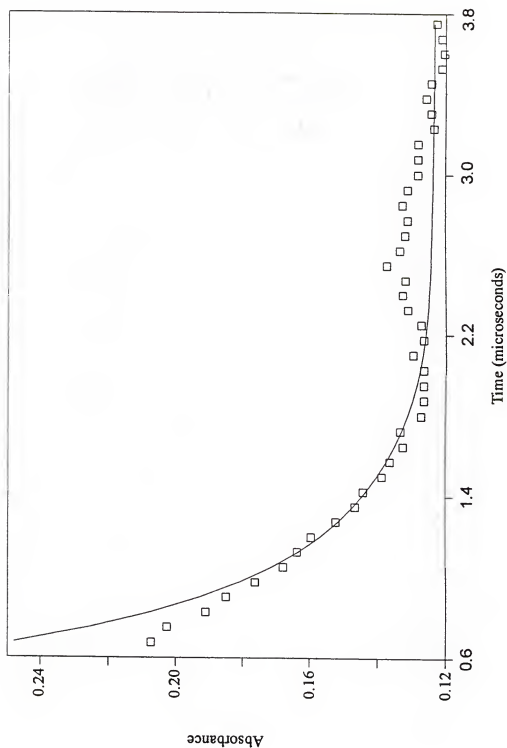


Figure (38). The fit of the absorbance at 634 nm calculated from the product concentrations of  $\text{IrBr}_6^{2-}$  and  $\text{e}_{\text{aq}}^-$  over time computed with the Gear integrator. The squares are the experimental values and the smooth curve represents the simulated values. The reaction of the impurity was not used in the mechanism when the simulated values were computed.

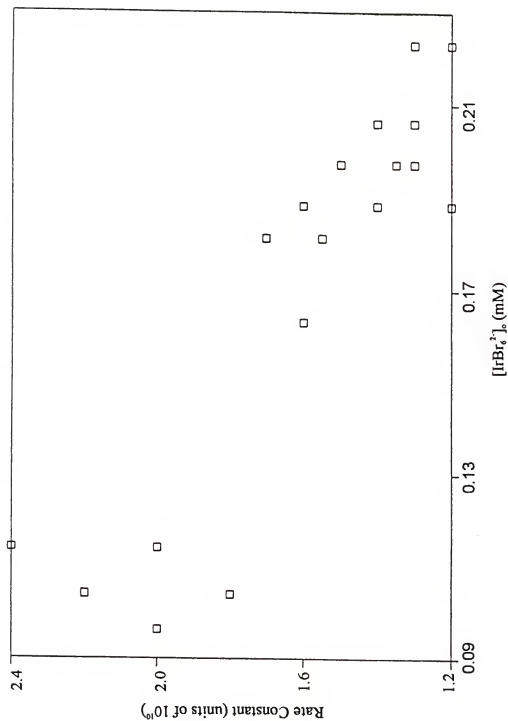


Figure (39). Plot showing the relation of the rate constant for reaction of  $\text{IrBr}_6^{2-}$  with  $e_{aq}^-$  and the concentration of  $\text{IrBr}_6^{2-}$  that were used in the Gear integrator. Note that the lower the concentration of  $\text{IrBr}_6^{2-}$ , the higher the rate constant necessary to get a good "fit" using the Gear integrator.

lower rate constants were suitable for higher  $\text{IrBr}_6^{2-}$  concentrations. This indicated that there was an impurity in the system which reacted with  $e_{aq}^-$ , causing a measurable contribution to the rate of consumption of  $e_{aq}^-$ .

It was very difficult to locate the source of the impurity. All of the glassware associated with the distillation of the water used to make the solutions was cleaned, the glassware used to make the solutions was cleaned, and the t-butanol was passed through a small alumina column. It was possible that the ultrahigh-purity helium used as a purging gas contributed a small amount of an impurity to the system.

A modification was proposed to the mechanism for the system. The modification consisted of adding a reaction of the impurity, Xx, with  $e_{aq}^-$ , Reaction (85).



The Gear integrator was again utilized to create files for the simulated concentrations of  $e_{aq}^-$  and  $\text{IrBr}_6^{2-}$  over the experimental time period of the reaction. There were four unknown values in the simulations; the concentrations of  $e_{aq}^-$  and the impurity, and the rate constants for reactions of the  $e_{aq}^-$  with  $\text{IrBr}_6^{2-}$  and with the impurity.

It was possible to predict rate constants for all of the experimental pulses that were better correlated when the effect of the impurity was included as described. All of the values of the rate constant for reaction of  $e_{aq}^-$  with  $\text{IrBr}_6^{2-}$  were between  $1.1 \times 10^{10} \text{ M}^{-1} \text{ s}^{-1}$  and  $2.0 \times 10^{10} \text{ M}^{-1} \text{ s}^{-1}$ . However, the majority of the rate constants were between  $1.1 \times 10^{10} \text{ M}^{-1} \text{ s}^{-1}$  and  $1.3 \times 10^{10} \text{ M}^{-1} \text{ s}^{-1}$ , and the average value was  $1.2 \times 10^{10} \text{ M}^{-1} \text{ s}^{-1}$ . An example of a satisfactory fit for the total absorbance based on concentrations predicted with the Gear integrator over the time of the reaction, compared to the experimental absorbance values is shown in Figure (40).

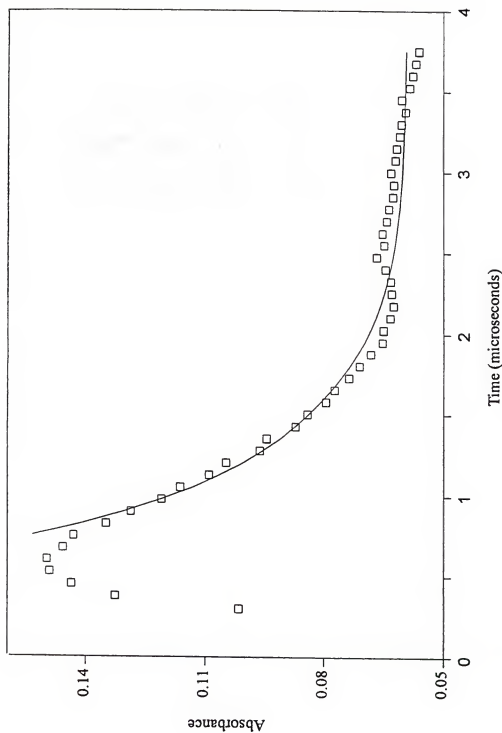


Figure (40). The fit of the absorbance at 634 nm calculated from the product concentrations of  $\text{IrBr}_6^{2-}$  and  $\text{e}_{\text{aq}}^-$  over time computed with the Gear integrator. The squares are the experimental values and the smooth curve represents the simulated values. The reaction of an impurity was used in the mechanism when the simulated values were computed.

## CHAPTER SEVEN

### STOPPED-FLOW INVESTIGATION OF REACTION OF HEXABROMOIRIDATE WITH BROMINE

#### Experimental

Water used in all of the experiments for the determination of the rate constant for reaction of  $\text{IrBr}_6^{3-}$  with  $\text{Br}_2$  was deionized water further processed with a Millipore Ion-exchange system. A stock aqueous solution that was 0.157 mM in  $\text{Br}_2$ , was prepared. The concentration of  $\text{Br}_2$  in the solution was determined using a Hewlett Packard 8450A Diode Array Spectrophotometer at 390 nm with an extinction coefficient of  $172 \text{ M}^{-1} \text{ cm}^{-1}$  [65].

Since  $\text{IrBr}_6^{3-}$  is unstable in water, special precautions were taken. Specific amounts of  $\text{Na}_3\text{IrBr}_6$  were weighed out in advance of each experiment. Each sample was the amount necessary to make either 100 or 250 mL of a solution of a specific concentration ranging from 0.02 mM to 0.05 mM. The weighed samples were placed in packets, which were then sealed and stored in the presence of a desiccant until needed. During the stopped-flow experiments, the concentration of  $\text{Br}_2$  after mixing was 0.0785 mM, and the concentrations of  $\text{IrBr}_6^{3-}$  in solution ranged from 0.01 mM to 0.025 mM. The stopped-flow experiments were conducted using the Durrum stopped-flow spectrophotometer, model D-110.

As discussed earlier, hexabromoiridate (III) is unstable in water and undergoes

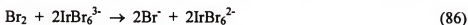
aquation to form  $\text{IrBr}_5\text{H}_2\text{O}^{2-}$ , Reaction (73) [59, 61], and the half-life for this aquation reaction is about 19 minutes at 25 °C.



In order to minimize the conversion to  $\text{IrBr}_5\text{H}_2\text{O}^{2-}$ , each stopped-flow experiment was done immediately after a pre-weighed packet of  $\text{Na}_3\text{IrBr}_6$  was dissolved. The reactions were begun and completed within three minutes of the  $\text{Na}_3\text{IrBr}_6$  solution preparation. Using this method, the amount of time for the aquation reaction was kept to a minimum, so that the reaction involved almost entirely  $\text{IrBr}_6^{3-}$ , with very little  $\text{IrBr}_5\text{H}_2\text{O}^{2-}$  present.

### Results and Calculations

$\text{IrBr}_6^{3-}$  reacts with  $\text{Br}_2$  according to the overall Reaction (86):



It was postulated that the process was initiated by the bimolecular reaction of  $\text{Br}_2$  with  $\text{IrBr}_6^{3-}$ , Reaction (69),



followed by a second bimolecular step in which  $\text{Br}_2^-$  is reduced by  $\text{IrBr}_6^{3-}$ .



The two mechanistic steps add to give net Reaction (86).

The second order rate equation for Reaction (86), based on the reaction being first order in  $\text{Br}_2$  and first order in  $\text{IrBr}_6^{3-}$ , is:

$$-\frac{1}{2} \times \frac{d[\text{IrBr}_6^{3-}]}{dt} = k[\text{IrBr}_6^{3-}][\text{Br}_2] \quad (29)$$

In Equation (29),  $k$  is the rate constant for the overall Reaction (86). Assuming that the

mechanism for the net Reaction (86) consists of the mechanistic steps (68) and (69), a simple steady-state analysis shows that the rate constant for Reaction (86) is identical to the second order rate constant for the mechanistic step, Reaction (69),

The mixtures produced in the reaction chamber during the stopped-flow experiments were monitored spectrophotometrically at 586 nm. The data files were averaged and converted to Lotus 123 format, and the concentrations of the  $\text{IrBr}_6^{2-}$  produced during the reaction were calculated for each time increment using the extinction coefficient of  $3.87 \times 10^3 \text{ M}^{-1} \text{ cm}^{-1}$  [59]. The concentration of  $\text{IrBr}_6^{3-}$  initially present was equal to the total concentration of  $\text{IrBr}_6^{2-}$  produced at long reaction time. The rate constant was calculated using the standard second order rate equation for reaction of two species with a two:one stoichiometric ratio of reactants [84]. Applied to Reaction (86), the rate law can be written as:

$$\frac{1}{2[\text{Br}_2]_o - [\text{IrBr}_6^{3-}]_o} \ln \left\{ \frac{[\text{IrBr}_6^{3-}]_o \left( [\text{Br}_2]_o - \frac{1}{2} [\text{IrBr}_6^{2-}]_t \right)}{[\text{Br}_2]_o \left( [\text{IrBr}_6^{3-}]_o - [\text{IrBr}_6^{2-}]_t \right)} \right\} = kt \quad (30)$$

A graph plotting the left-hand side of Equation (30) against time is shown in Figure (41) for one of the sets of data. The average rate constant calculated using the above method is  $3.11 \times 10^6 \text{ M}^{-1} \text{ s}^{-1}$ . The complete set of data is given in Table (9) (page 138).

In preliminary studies done in this laboratory, it was determined that if a solution of  $\text{Na}_3\text{IrBr}_6$  was allowed to stand for over 30 minutes prior to use, reaction with  $\text{Br}_2$  was slower by a factor of at least 10 to 15 times. This was due to the conversion of  $\text{IrBr}_6^{3-}$  to the less reactive  $\text{IrBr}_5\text{H}_2\text{O}^{2-}$ . Based on experiments discussed in the next chapter, the rate constant for the reaction of  $\text{IrBr}_5\text{H}_2\text{O}^{2-}$  with  $\text{Br}_2$ , Reaction (76), was found to be

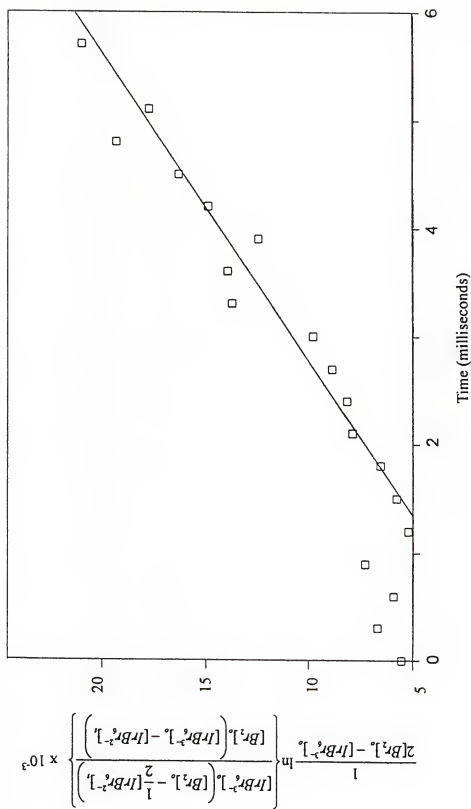


Figure (41). Second order plot used to determine the rate constant for the reaction of  $\text{IrBr}_6^{2-}$  with  $\text{Br}_2$ .



Table (9) Calculation of the second order rate constant for reaction of  $\text{IrBr}_6^{3-}$  with  $\text{Br}_2$ .

Experiment number	Concentration $\text{IrBr}_6^{3-}$ (mM)	$10^6 k$ ( $\text{M}^{-1} \text{s}^{-1}$ )
1	0.010	2.90
2	0.014	3.04
3	0.017	3.60
4	0.019	2.66
5	0.021	3.43
6	0.023	3.02

$4.1 \times 10^3 \text{ M}^{-1} \text{ s}^{-1}$ . The rate of reaction measured in the present section for reaction of  $\text{IrBr}_6^{3-}$  with  $\text{Br}_2$  was more than 200 times as fast as the rate of reaction of  $\text{Br}_2$  with  $\text{IrBr}_5\text{H}_2\text{O}^{2-}$ . This confirms that the effort described above to carry out the present studies sufficiently rapidly to prevent conversion of  $\text{IrBr}_6^{3-}$  to  $\text{IrBr}_5\text{H}_2\text{O}^{2-}$  was successful.

CHAPTER EIGHT  
STOPPED-FLOW STUDIES OF THE REACTION OF  
AQUOPENTABROMOIRIDATE (III) WITH BROMINE

**Experimental**

The water used to make all solutions was deionized water further treated with the Millipore system. It was purged of dissolved oxygen by bubbling nitrogen through the solution (4.8 Prepurified Grade nitrogen, from The BOC Group, Inc., Murray Hill, NJ, 07974) for approximately 15 hours in a nitrogen filled glove box. The nitrogen atmosphere in the glove box was maintained using Industrial Grade nitrogen from The BOC Group, Inc. All solutions were prepared and kept until needed in the glove box under the nitrogen atmosphere.

A stock solution of  $\text{IrBr}_5\text{H}_2\text{O}^{2-}$  was made using  $\text{Na}_3\text{IrBr}_6$  furnished by Johnson Matthey/Materials Technology U.K. The stock solution was subsequently diluted to make four solutions of varied concentrations. The diluted solutions were allowed to stand for at least 1 hour, 45 minutes before use. The half-life for the aquation reaction of  $\text{IrBr}_6^{3-}$  is about 19 minutes. The standing-time was at least 5 half-lives, and was an adequate amount of time for the conversion reaction of  $\text{IrBr}_6^{3-}$  to  $\text{IrBr}_5\text{H}_2\text{O}^{2-}$  to reach equilibrium. Even when  $\text{IrBr}_6^{3-}$  is added to a solution containing 25 mM  $\text{Br}^-$ , the equilibrium for conversion of  $\text{IrBr}_6^{3-}$  to  $\text{IrBr}_5\text{H}_2\text{O}^{2-}$  lies almost completely on the product side, as seen in the stability studies (Chapter 4). In the present case, with no added  $\text{Br}^-$

and an adequate amount of time allowed for the aquation reaction, the solution probably consisted almost entirely of  $\text{IrBr}_5\text{H}_2\text{O}^{2-}$ , along with a negligible concentration of  $\text{IrBr}_6^{3-}$ . (The literature implies that the further aquation of  $\text{IrBr}_5\text{H}_2\text{O}^{2-}$  is unimportant under our working conditions [57-59, 61,62].) Since the light absorption by the iridium bromide complexes in the plus 3 oxidation state is nearly negligible, the initial concentrations of  $\text{IrBr}_5\text{H}_2\text{O}^{2-}$  in each of these solutions was determined using spectrophotometric analysis of the  $\text{IrBr}_5\text{H}_2\text{O}^+$  product after oxidation by  $\text{Br}_2$ . Reaction (78) represents the net reaction for the oxidation of  $\text{IrBr}_5\text{H}_2\text{O}^{2-}$  by  $\text{Br}_2$ .



The  $\text{IrBr}_5\text{H}_2\text{O}^+$  concentration was determined using the absorbance at 586 nm and an extinction coefficient of  $3320 \text{ M}^{-1} \text{ cm}^{-1}$ . The extinction coefficient was taken as equivalent to the extinction coefficient at 587 nm listed by Melvin and Haim [59]; the diode array spectrometer was not capable of distinguishing between 587 and 586 nm.

The  $\text{Br}_2$  solution used in all experiments was prepared using "Purified" bromine from Great Lakes Chemical Corporation, P.O. Box 2200, Lafayette, Indiana. The initial concentration of  $\text{Br}_2$  was determined to be 0.66 mM using an ultraviolet-visible spectrophotometer. The extinction coefficient at 390 nm is  $172 \text{ M}^{-1} \text{ cm}^{-1}$  [65].

Stopped-flow experiments were conducted using a Durrum stopped-flow spectrophotometer, model D-110, described in Chapter 3. Successive stopped-flow experiments were performed by injecting into the reaction chamber equal quantities (approximately 0.25 mL) of the  $\text{Br}_2$  solution and one of the  $\text{IrBr}_5\text{H}_2\text{O}^{2-}$  solutions. The mixture in the reaction chamber was monitored spectrophotometrically at 586 nm. The data sets were averaged and converted to Lotus 123 files, and the concentrations of

$\text{IrBr}_5\text{H}_2\text{O}^-$  produced were calculated for each time increment using the extinction coefficient of  $3.32 \times 10^3 \text{ M}^{-1} \text{ cm}^{-1}$  [59].

### Results and Calculations

The Gear integrator computer simulation program was used to generate reaction curves for the build-up of the concentration of  $\text{IrBr}_5\text{H}_2\text{O}^-$  produced for each of the stopped-flow experiments. The simulation program required the input of a data set containing each individual mechanistic step of the proposed mechanism, and the corresponding rate constant for each step, as well as the initial concentrations of all reactant and product species and the time increment and final time desired. The rate constants for several of the mechanistic steps were found in the literature. Initial values of rate constants that were not available in the literature were estimated based on comparable reactions. After generating a reaction curve for the build-up of the measured product concentration over time, corresponding to the experimental reaction curve, the simulated curve was compared to the experimental curve. The previously estimated rate constants were re-evaluated, new estimates made and input to the Gear integrator, and a new simulation run was computed and again compared with the experimental reaction curve. This procedure was repeated until a best-fit was achieved; the estimated rate constants were noted.

Generation of simulated reaction curves and comparison to experimental values was done for each of the four diluted iridium solutions. All of the estimated rate constants were compared. New simulations based on new estimates were made. This iteration process was repeated until a single set of estimated rate constants was achieved

which was as consistent as possible with all of the separate experiments. The proposed mechanism used for the simulation is listed in Table (10).

Table (10). Mechanism used for the simulation of the production of  $\text{IrBr}_5\text{H}_2\text{O}^-$  for reaction of  $\text{IrBr}_5\text{H}_2\text{O}^{2-}$  with  $\text{Br}_2$ .

Reaction	Rate Const.	Ref.
$\text{Br}_2 + \text{Br}^- \rightarrow \text{Br}_3^-$	$1.5 \times 10^9$	[58] (55)
$\text{Br}_3^- \rightarrow \text{Br}_2 + \text{Br}^-$	$8 \times 10^7$	a (56)
$2\text{Br}_2^- \rightarrow \text{Br}_3^- + \text{Br}^-$	$1.7 \times 10^9$	[43] (57)
$\text{Br}_2^- + \text{IrBr}_5\text{H}_2\text{O}^{2-} \rightarrow 2\text{Br}^- + \text{IrBr}_5\text{H}_2\text{O}^-$	$6.8 \times 10^8$	b (77)
$\text{Br}_2 + \text{IrBr}_5\text{H}_2\text{O}^{2-} \rightarrow \text{Br}_2^- + \text{IrBr}_5\text{H}_2\text{O}^-$	$4.1 \times 10^3$	c (76)
$\text{Br}_2^- + \text{IrBr}_5\text{H}_2\text{O}^- \rightarrow \text{IrBr}_5\text{H}_2\text{O}^{2-} + \text{Br}_2$	$2.0 \times 10^7$	c (87)

- a. Calculated from the rate constant for Reaction (56) to give literature value of  $K_{\text{eq}} = 16.85$  [64]. This value was also confirmed as the rate constant that was mistakenly left out of the paper by Marie-Françoise Ruasse, et al. through personal correspondence [45].
- b. The value used for this rate constant was taken from the literature [60]. However, the value was published in the literature as the rate constant for reaction of  $\text{IrBr}_6^{3-}$  with  $\text{Br}_2^-$ . As explained later, we felt that the authors did not adequately account for the aquation reaction of  $\text{IrBr}_6^{3-}$  in their studies.
- c. Estimated, this work.

The initial concentration of  $\text{IrBr}_5\text{H}_2\text{O}^{2-}$  used in the Gear integrator for each sample was based on the total amount of  $\text{IrBr}_5\text{H}_2\text{O}^-$  produced. The rate constant for reaction of  $\text{Br}_2$  with  $\text{Br}^-$ , Reaction (55), in all simulations was based on a value reported by Ruasse and coworkers,  $1.5 \times 10^9 \text{ M}^{-1} \text{ s}^{-1}$  [45].



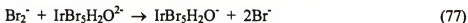
The rate constant used for the reverse of the above reaction, Reaction (56), in all simulations was  $8 \times 10^7 \text{ s}^{-1}$ . This value was corrected from the published value [45] as a result of correspondence with Dr. Ruasse as discussed in Chapter 4. This value is consistent with the measured value of the rate constant for Reaction (55) and the literature value of the equilibrium constant,  $K_{\text{eq}} = 16.85$  [64].



The rate constant for reaction of  $\text{Br}_2^-$  ion with itself to produce  $\text{Br}_3^-$  and  $\text{Br}^-$  ions, Reaction (57), was  $1.7 \times 10^9 \text{ M}^{-1} \text{ s}^{-1}$  [43].



In our simulation we employed the rate constant for Reaction (77) of  $6.8 \times 10^8 \text{ M}^{-1} \text{ s}^{-1}$  [60]. However, we feel the validity of this value is questionable.



M. DeFelippis, et al., carried out a brief investigation of the reaction of  $\text{Br}_2^-$  with solutions of hexabromoiridate (III) in connection with a study of the pulse radiolysis of tyrosine and tryptophan. They used 0.1 M  $\text{Br}^-$  solution with the hope that it would ensure the stability of  $\text{IrBr}_6^{3-}$ ; they report that they measured the rate constant within 20 minutes after the preparation of the iridium solution. However, it was shown in the present work that addition of 0.025 M  $\text{Br}^-$  had little or no effect on the stability of  $\text{IrBr}_6^{3-}$ . It appears

unlikely to us that a concentration of 0.1 M  $\text{Br}^-$  was sufficient to achieve stability of  $\text{IrBr}_6^{3-}$ . Although DeFelippis, et al. attempted to measure the reaction within 20 minutes after preparing the solution, it should be recalled that that time period is about one half-life with respect to conversion  $\text{IrBr}_6^{3-}$  to  $\text{IrBr}_5\text{H}_2\text{O}^{2-}$  [60]. Accordingly, it appears that the solution studied by DeFelippis, et al. may have contained from 25 to 50 percent  $\text{IrBr}_5\text{H}_2\text{O}^{2-}$ . Thus, the rate constant they measured for this reaction probably corresponded to a mixture of  $\text{IrBr}_6^{3-}$  and  $\text{IrBr}_5\text{H}_2\text{O}^{2-}$ . In the present study, their rate constant was tentatively assigned to reaction of  $\text{Br}_2^-$  with  $\text{IrBr}_5\text{H}_2\text{O}^{2-}$ . Provisional computations with the Gear integrator proved that an increase or decrease in the rate constant by a factor of two gave simulations that were in obvious disagreement with experimental results.

The rate constants for Reactions (76) and (87) were adjusted as described above. The simulated production curve for the concentration of  $\text{IrBr}_5\text{H}_2\text{O}^-$ , superimposed on the experimental data for the production of  $\text{IrBr}_5\text{H}_2\text{O}^-$  is shown in Figure (42). The rate constants used for Reactions (76) and (87) in the simulations for each of the experiments are listed in Table (11) (page 146). The initial concentrations listed in Table (11) are the initial concentrations after the mixing of equal quantities of reactant solutions during the stopped-flow experiments.

It can be seen that there is good agreement of the rate constants for reaction of  $\text{IrBr}_5\text{H}_2\text{O}^{2-}$  with  $\text{Br}_2$ , and reasonable agreement of the rate constants for the reverse reaction. The average rate constant for reaction of  $\text{IrBr}_5\text{H}_2\text{O}^{2-}$  with  $\text{Br}_2$  determined using the Gear integrator was  $4.1 \times 10^3 \text{ M}^{-1} \text{ s}^{-1}$ , while the average rate constant for the reverse

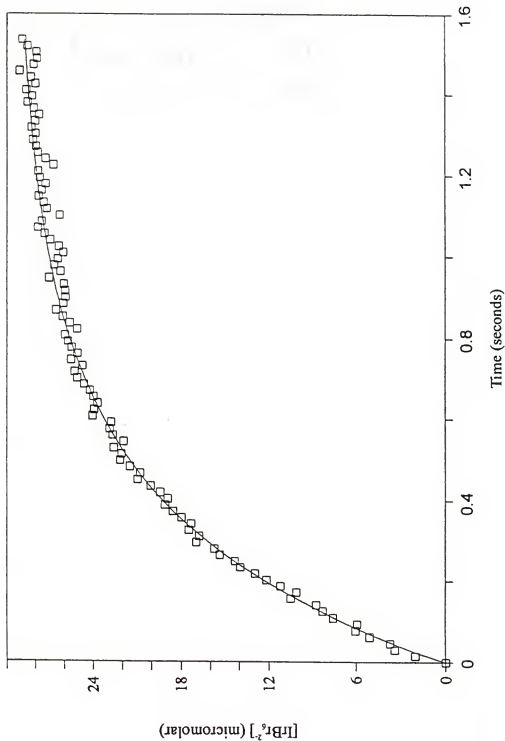


Figure (42). Plot of the concentration of  $\text{IrBr}_5\text{H}_2\text{O}^-$  produced over time computed using the Gear integrator (smooth curve) superimposed over the experimental production of  $\text{IrBr}_3\text{H}_2\text{O}^-$  over time by reaction of  $\text{IrBr}_5\text{H}_2\text{O}^{2-}$  with  $\text{Br}_2$ .

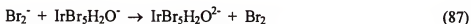


Table (11) Rate constants used in the Gear integrator during simulations of the production of  $\text{IrBr}_5\text{H}_2\text{O}^-$  for reaction of  $\text{IrBr}_5\text{H}_2\text{O}^{2-}$  with  $\text{Br}_2$  in several solutions of various reactant concentrations.

Experiment Number	$[\text{IrBr}_5\text{H}_2\text{O}^{2-}]_0$ (mM)	$[\text{Br}_2]_0$ (mM)	$10^{-3}k_{76}$ ( $\text{M}^{-1} \text{s}^{-1}$ )	$10^{-7}k_{87}$ ( $\text{M}^{-1} \text{s}^{-1}$ )
1	0.030	0.33	4.1	3.0
2	0.037	0.33	4.1	1.0
3	0.046	0.33	4.1	2.0
4	0.051	0.33	4.2	2.0

reaction, Reaction (87), was  $2.0 \times 10^7 \text{ M}^{-1} \text{s}^{-1}$ . Production curves computed with the Gear integrator are compared to data for each experiment as shown in Figure (43).

Since the measurements reported in this section include both forward and reverse rate constants for the one-electron reduction of  $\text{IrBr}_5\text{H}_2\text{O}^-$  by  $\text{Br}_2^-$ , Reaction (87), it is of interest to related the results to equilibrium electrochemical measurements.



The corresponding equilibrium expression for Reaction (87) is

$$K_{eq} = \frac{[\text{IrBr}_5\text{H}_2\text{O}^{2-}][\text{Br}_2]}{[\text{IrBr}_5\text{H}_2\text{O}^-][\text{Br}_2^-]} = \frac{k_1}{k_{-1}} \quad (31)$$

where  $k_1$  and  $k_{-1}$  have both been measured in the present work; we find that

$$k_1/k_{-1} = 2.05 \cdot 10^4.$$

If the process is described from the viewpoint of electrochemistry, we can write



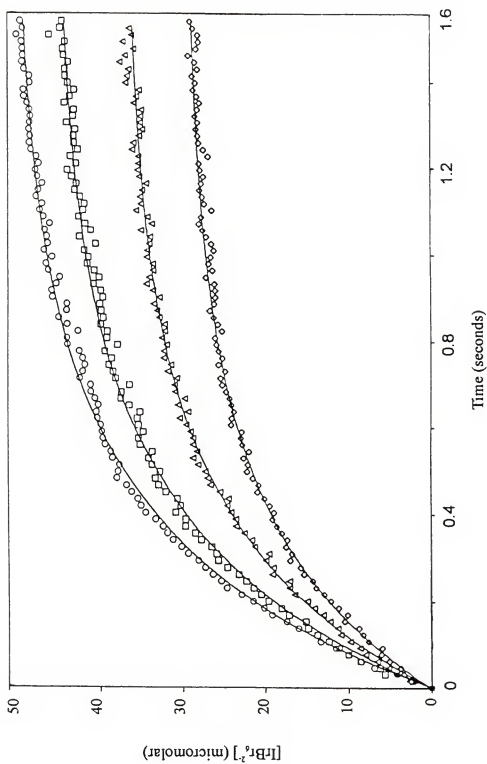
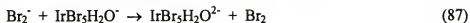


Figure (43). Simulated product curve (smooth line) fit to the formation of  $\text{IrBr}_6^{3-}$  over time by reaction of  $\text{IrBr}_3\text{H}_2\text{O}^{2-}$  with  $\text{Br}_2$  for each experiment.

The overall cell reaction is:



The cell potential can be written as

$$E_{\text{net}}^o = (0.218\text{V}) = \frac{RT}{nF} \ln K_{eq} \quad (32)$$

where  $n = 1$ . If  $K_{eq}$  is set equal to the experimental value reported here, namely  $2.05 \times 10^{-4}$ , then  $E_{\text{net}}^o = 0.218\text{ V}$  as shown, and correspondingly, the one-electron reduction potential of  $\text{Br}_2$  is found to be  $0.752\text{ V}$ . This is a high compared to previously reported range of values of  $0.300\text{ V}$ ,  $0.410\text{ V}$ ,  $0.430\text{ V}$ ,  $0.510\text{ V}$ ,  $0.520\text{ V}$ , and  $0.680\text{ V}$  [69-74], but not unreasonable considering the values of the range..

## CHAPTER NINE

### CONCLUSION

The study of the stability of aqueous solutions of  $\text{IrBr}_6^{3-}$  confirmed that this species readily converts to  $\text{IrBr}_5\text{H}_2\text{O}^{2-}$  upon standing, and that  $\text{IrBr}_6^{3-}$  is also unstable when dissolved in aqueous 25 mM NaBr solution. The quality of the spectra taken periodically over time after conversion of both  $\text{IrBr}_6^{3-}$  and  $\text{IrBr}_5\text{H}_2\text{O}^{2-}$  to the plus four oxidation state deteriorates from the three sharp peaks of  $\text{IrBr}_6^{3-}$  to the low resolution, smoother double peak of  $\text{IrBr}_5\text{H}_2\text{O}^{2-}$ . It was found that  $\text{IrBr}_6^{3-}$  converted to  $\text{IrBr}_5\text{H}_2\text{O}^{2-}$  with a half-life consistent with the literature value of 19 minutes.

The alternate method for the determination of the rate constant for reaction of  $\text{IrBr}_6^{3-}$  with OH radical worked very well. The OH radical concentration was factored out of the mathematical relation for the two competing species. The rate constant for the reaction was calculated based on either of two possible assumptions. The first assumption was that there was no conversion of  $\text{IrBr}_6^{3-}$  to  $\text{IrBr}_5\text{H}_2\text{O}^{2-}$ . The second assumption was that the maximum amount of conversion would be half the original concentration based on the amount of time that had elapsed and the half-life. The rate constant calculated based on the first assumption was  $1.4 \times 10^9 \text{ M}^{-1} \text{ s}^{-1}$ , and the rate constant calculated according to the assumption of 50 percent loss was  $2.8 \times 10^9 \text{ M}^{-1} \text{ s}^{-1}$ .

Essentially the same rate constants were computed using the standard competition method based on Equation (9), using the same two assumptions regarding the conversion

of  $\text{IrBr}_6^{3-}$  to  $\text{IrBr}_5\text{H}_2\text{O}^{2-}$ . The rate constant calculated with the assumption that no  $\text{IrBr}_6^{3-}$  converted to  $\text{IrBr}_5\text{H}_2\text{O}^{2-}$  was  $1.3 \times 10^9 \text{ M}^{-1} \text{ s}^{-1}$ , while the rate constant assuming 50% conversion to  $\text{IrBr}_5\text{H}_2\text{O}^{2-}$  was  $2.6 \times 10^9 \text{ M}^{-1} \text{ s}^{-1}$ .

There are advantages and disadvantages to using the two different competition procedures. For the standard method, the initial concentration of OH radical must be constant throughout all experiments. This requires that the intensity of the pulse from the accelerator be constant. Although initial concentrations of both of the reactants must be known, the concentration of only one of the reactant/product pairs needs to be followed during the reaction. Of course, it is always an advantage to follow the concentrations of both product species to verify that the system behaves as expected.

Using the alternate competition method, the concentrations of either both reactants or both products must be monitored during the reaction. It was important that the initial concentration of OH radical was constant between successive pulses while monitoring the reaction at the two different wavelengths with any given initial reactant concentration ratio,  $[\text{IrBr}_6^{3-}]_0/[\text{CO}_3^{2-}]_0$ . However, it was not required for the initial concentration of the OH radical to be constant for subsequent measurements when using other reactant initial concentration ratios. This reduced the rigidity of the requirement that the pulse size be constant throughout all experiments.

The stability of the pulse size would become unimportant if a multi-channel detector were available. Both species could be monitored at the same time and the concentration ratios could then be compared, with no requirement for a constant OH radical concentration.

Another advantage to the alternate method was that data for all pairs of initial reactant concentration ratios fall on single straight line, even if a different pulse size and therefore a different initial value of  $[\cdot\text{OH}]_0$ , is used for each pair. Indeed, data taken with different accelerators or in different laboratories should also fall on the same straight line.

Attempts to measure the rate constant of the reaction of  $\text{IrBr}_6^{2-}$  with  $e_{\text{aq}}^-$  lead to a range of values from  $1.2 \times 10^{10} \text{ M}^{-1} \text{ s}^{-1}$  to  $2.4 \times 10^{10} \text{ M}^{-1} \text{ s}^{-1}$ , with an average value of  $1.4 \times 10^{10} \text{ M}^{-1} \text{ s}^{-1}$ . However, there was an obvious trend in the results, with higher values of initial concentrations of  $\text{IrBr}_6^{2-}$  corresponding to lower values of the rate constant.

This led to a postulate that there was an impurity in the solution capable of reacting with  $e_{\text{aq}}^-$ . Inclusion of this assumption in modeling of the experiments with a Gear integrator produced a range of rate constants for the reaction of  $e_{\text{aq}}^-$  with  $\text{IrBr}_6^{2-}$  ranging from  $1.1 \times 10^{10} \text{ M}^{-1} \text{ s}^{-1}$  to  $2.0 \times 10^{10} \text{ M}^{-1} \text{ s}^{-1}$ , with an average value of  $1.2 \times 10^{10} \text{ M}^{-1} \text{ s}^{-1}$ .

The stopped-flow apparatus was used to determine the rate constant for the reaction of  $\text{IrBr}_6^{3-}$  with  $\text{Br}_2$ . The reaction followed second order kinetics, and there was good correlation of the rate constants determined for each experiment, with an average of  $3.11 \times 10^6 \text{ M}^{-1} \text{ s}^{-1}$ .

The stopped-flow apparatus was also used to determine the rate constant for the reaction of  $\text{IrBr}_5\text{H}_2\text{O}^{2-}$  with  $\text{Br}_2$ . However, interpretation of the system using the Gear integrator required consideration of the reverse process, reaction of  $\text{IrBr}_5\text{H}_2\text{O}^-$  with  $\text{Br}_2^\cdot$ . Treatment of the data using the Gear integrator gave excellent results, assuming the rate constant for reaction of  $\text{IrBr}_5\text{H}_2\text{O}^{2-}$  with  $\text{Br}_2$  was  $4.1 \times 10^3 \text{ M}^{-1} \text{ s}^{-1}$ , while the rate constant for the reverse reaction, Reaction (87), was  $2.0 \times 10^7 \text{ M}^{-1} \text{ s}^{-1}$ .

The equilibrium constant implied by the above mentioned reversible reaction pair was applied to the computation of the one-electron reduction potential for  $\text{Br}_2$ . The equilibrium constant for reaction of  $\text{IrBr}_5\text{H}_2\text{O}^{2-}$  with  $\text{Br}_2$  to form  $\text{IrBr}_5\text{H}_2\text{O}^-$  and  $\text{Br}_2^-$  ion was calculated to be  $2.05 \times 10^{-4}$ . Using this equilibrium constant and the literature value for the reduction potential of  $\text{IrBr}_5\text{H}_2\text{O}^-$ , the one-electron reduction potential for  $\text{Br}_2$  was calculated to be 0.752 V. This value was higher but still comparable to the extended range given in the literature.

Overall, the system of  $\text{IrBr}_6^{3-}$  in aqueous solution is fairly complex. Although it undergoes oxidation reactions similar to the analogous  $\text{IrCl}_6^{3-}$  ion, it is much less stable in aqueous solution. A realistic system using the iridium bromide complex for solar energy production would probably be practical only if the chemistry of the system is feasible in a solution of high  $\text{Br}^-$  concentration (ca. 1 molar  $\text{Br}^-$  or more), needed to stabilize the iridium bromide complex.

APPENDIX A  
COMPUTER PROGRAM TO OPERATE THE STOPPED-FLOW APPARATUS  
COMPUTERIZED DATA-ACQUISITION SYSTEM

```

10 ' *****
20 ' * Program NEWADCS.BAS, MARCH, 1993 *
30 ' * Written by C M Hoag *
40 ' * This program will run the waag a-d converter *
50 ' * Parts of DEBEST9.BAS (DATA GRABBER) were used with the permission*
60 ' * of Robert Hanrahan *
70 ' * ** DATA GRABBER ** *
80 ' * *
90 ' * ***** File DEBEST9.BAS, OCT. 12, 1989 ***** *
100 ' * *
110 ' * FOR USE WITH MICROSOFT QUICK BASIC COMPILER VERSION 4.0
    WITH 8087*
120 ' * COPYRIGHT 1988, 1989 BY JOHN BROGDON AND ROBERT HANRAHAN
130 ' * RADIATION CHEMISTRY LAB, 406 NSC, U OF FLA GAINESVILLE 32611*
140 ' * TEL 904-392-1442 OR 376-7754 *
150 ' *****
160 '
170 SEGMENT% = &HD000
180 PORT0% = &H178
190 PORT1% = &H179
200 PORT2% = &H17A
210 PORT3% = &H17B
220 DEF FNLOBT (%) = X% AND &HFF 'define low byte
230 DEF FNHIBT (%) = ((% AND &HFF00) \ 256) AND &HFF 'define high byte
240 TOFFSET% = 197
250 TDELAY% = 75
255 PER = 0
260 PERIOD$ = "250NS"
270 COUNT% = 511
280 MULTFACT% = 1
285 TFILENAME$ = "NO FILES HAVE BEEN SAVED YET"
290 QMINX = 0: QMAXX = 0: QMINY = 0: QMAXY = 0: QN = 0:
300 L = 1: EE = 3000: FLORD = 0: FLCAL = 0:
310 V0 = 0: VFULL = 0: VM = 0: LEFF = 0
320 DIM AGI$(100), BGI$(100), DSPM$(10), TRGSRC$(10), OD(512)

```



```

330 DIM QY(521), QX(521), VERLN(147), QLY(512), BTARY(3400), CON(513)
340 SCREEN 2: CLS : GET (1, 80)-(639, 99), BTARY
350 FOR KKQ = 1 TO 520: QY(KKQ) = 0: NEXT
360 KEY OFF
370 DEF FNQSC (S, QXS, QNS, QXO, QNO) = INT(O - (O - QNO) / (S -
      QNS) * (S - QS) + .5)
380 ROUTINES$ = "START"
390 PRINT : GOTO 410
400 '***** MENU *****
410 CLS
420 PRINT : PRINT "RETURNING TO MENU": PRINT
430 PRINT "CALIBRATION      CALIBRATE THE WAAG BOARD FOR
      EXPERIMENT"
440 PRINT "DATA      ACQUIRE DATA"
450 PRINT "PLOTTER      PLOT RAW DATA ON SCREEN"
460 PRINT "LEAST SQUARES  LINEAR REGRESION FOR CURRENT DATA"
470 PRINT "LOAD      LOAD DATA FROM DISK"
480 PRINT "SAVE      SAVE DATA ON DISK"
490 PRINT "ORDER      CHOOSE ORDER OF REACTION"
500 PRINT "COMPARE      COMPARE DATA SETS ON GRAPH"
510 PRINT "MAN      MANUAL CHANGE V0,VM,L,OR E"
520 PRINT "DIR      DISK DIRECTORY"
530 PRINT "END      END SESSION "
540 PRINT : INPUT "COMMAND": B$
550 B$ = LEFT$(B$, 3)
560 IF B$ = "END" THEN GOTO 8680
570 RESTORE
580 FOR I = 1 TO 11
590 IF I = 11 THEN PRINT "BAD COMMAND": PRINT : GOTO 540
600 READ A$
610 IF B$ = A$ THEN GOTO 630
620 NEXT I
630 ON I GOSUB 5830, 7460, 670, 2940, 8340, 8030, 3870, 4080, 5220, 5580
640 PRINT : GOTO 410
650 DATA "CAL", "DAT", "PLO", "LEA", "LOA", "SAV", "ORD", "COM", "MAN", "DIR"
660 GOTO 8680
670 '***** PLOTTER *****
680 N = 1: QMINX = QX(1): QMAXX = QX(512)
690 RHGRFLAG = 0
700 IF ROUTINES$ = "START" THEN GOTO 730
710 IF ROUTINES$ = "CAL" THEN GOTO 730
720 GOTO 740
730 PRINT "NO DATA SOURCE. RETURNING TO MENU": RETURN
740 INPUT "WHAT RESOLUTION WOULD YOU LIKE (1 TO 20)": QRES
750 IF QRES < 1 OR QRES > 20 THEN QRES = 1
760 QN = 512: QFLG = 0: GOSUB 1590

```

```

770 GOSUB 810
780 RETURN
790 ***** LEFT & RIGHT BOARDERS *****
800 RHGRFLAG = 0
810 PUT (0, QLNB + 11), BTARY, PSET: LOCATE INT((LNB / 200) * 25 + 1) + 2, 1
820 IF RHGRFLAG = 1 THEN FOR ASEC = 1 TO 12000: AMIN = LOG(ASEC):
    NEXT
830 INPUT "DO YOU WANT TO CHANGE THE LEFT OR RIGHT BORDERS"; B$:
    B$ = LEFT$(B$, 1)
840 IF B$ = "N" THEN RETURN
850 IF B$ <> "Y" THEN GOTO 830
860 GET (LNL, QLNT)-(LNL, QLNB), VERLN
870 PUT (0, QLNB + 11), BTARY, PSET: LOCATE INT((LNB / 200) * 25 + 1) + 2, 1
880 INPUT "DO YOU WISH TO MOVE THE LEFT BORDER"; B$
890 B$ = LEFT$(B$, 1)
900 LNPOS = QLNL
910 IF B$ = "N" THEN GOTO 1070
920 IF B$ <> "Y" THEN GOTO 870
930 LNPOS = QLNL + 25
940 C$ = "R"
950 PUT (LNPOS, QLNT), VERLN
960 PUT (0, QLNB + 11), BTARY, PSET: LOCATE INT((LNB / 200) * 25 + 1) + 2, 1
970 PRINT "L-LEFT,R-RIGHT,S-STOP OR NUMBER OF SPACES"; : B$ =
    INPUT$(1)
980 D = VAL(B$) ^ 2
990 IF D = 0 AND (B$ = "L" OR B$ = "R" OR B$ = "S") THEN C$ = B$
1000 IF C$ = "S" THEN GOTO 1070
1010 PUT (LNPOS, QLNT), VERLN
1020 IF C$ = "R" THEN LNPOS = LNPOS + D
1030 IF C$ = "L" THEN LNPOS = LNPOS - D
1040 IF LNPOS < QLNL THEN LNPOS = QLNL: C$ = "R"
1050 IF LNPOS > QLNR THEN LNPOS = QLNR: C$ = "L"
1060 PUT (LNPOS, QLNT), VERLN: GOTO 960
1070 N = ((MAXPX - QMINPX) * QSCLX * (LNPOS - QLNL)) / (LNR - QLNL)
1080 N = INT((N - QX(1)) / QY(513))
1090 PUT (0, QLNB + 11), BTARY, PSET: LOCATE INT((LNB/200) * 25 + 1) + 2, 1
1100 INPUT "DO YOU WISH TO MOVE THE RIGHT BORDER"; B$
1110 B$ = LEFT$(B$, 1)
1120 LNPOS = QLNR
1130 IF B$ = "N" THEN GOTO 1290
1140 IF B$ <> "Y" THEN GOTO 1090
1150 LNPOS = QLNR - 100
1160 C$ = "L"
1170 PUT (LNPOS, QLNT), VERLN
1180 PUT (0, QLNB + 11), BTARY, PSET: LOCATE INT((LNB/200) * 25 + 1) + 2, 1
1190 PRINT "L-LEFT,R-RIGHT,S-STOP OR NUMBER OF SPACES "; : B$ =

```

```

INPUT$(1)
1200 D = VAL(B$) ^ 2
1210 IF D = 0 AND (B$ = "L" OR B$ = "R" OR B$ = "S") THEN C$ = B$
1220 IF C$ = "S" THEN GOTO 1290
1230 PUT (LNPOS, QLNT), VERLN
1240 IF C$ = "L" THEN LNPOS = LNPOS - D
1250 IF C$ = "R" THEN LNPOS = LNPOS + D
1260 IF LNPOS < QLNL THEN LNPOS = QLNL: C$ = "R"
1270 IF LNPOS > QLNR THEN LNPOS = QLNR: C$ = "L"
1280 PUT (LNPOS, QLNT), VERLN: GOTO 1180
1290 J = ((MAXPX - QMINPX) * QSCLX * (LNPOS - QLNL)) / (LNR - QLNL)
1300 J = INT((J - QX(1)) / QY(513))
1310 IF J < N THEN CC = J: J = N: N = CC
1320 IF J > 512 THEN J = 512
1330 IF N < 1 THEN N = 1
1340 INPUT "CREATE A NEW FILE FOR COMP SIMU?"; RNBANS$
1350 C$ = (LEFT$(RNBANS$, 1))
1360 IF C$ = "N" OR C$ = "" THEN GOTO 1530
1370 INPUT "CREAT 'OD' FILE (ES) ELSE CON FILE CREATED?"; CLCANSS
1380 C$ = (LEFT$(RLCANSS$, 1))
1390 IF C$ = "Y" THEN GOTO 5680
1400 INPUT "WHICH DRIVE"; DRV$: IF DRV$ = " " THEN DRV$ = "C"
1410 DRV$ = LEFT$(DRV$, 1)
1420 IF DRV$ = "A" OR DRV$ = "B" GOTO 1450
1430 IF DRV$ = "C" OR DRV$ = "D" GOTO 1450
1440 GOTO 1400
1450 DRV$ = DRV$ + ":"
1460 INPUT "FILE NAME"; FILENAME$
1470 B$ = DRV$ + LEFT$(FILENAME$, 8)
1480 OPEN "O", #2, B$
1490 FOR I = N TO J STEP 5
1500 PRINT #2, QX(I), ",", CON(I), ","
1510 NEXT I
1520 CLOSE #2
1530 PUT (0, QLNB + 11), BTARY, PSET: LOCATE INT((LNB/200) * 25 + 1) + 2, 1
1540 INPUT "ORDER OF REACTION (0,1,2 or 3)"; ORDER
1550 IF ORDER < 0 OR ORDER > 3 GOTO 1470
1560 PUT (0, QLNB + 11), BTARY, PSET: LOCATE INT((LNB/200) * 25 + 1) + 2, 1
1570 GOSUB 2970
1580 RETURN
1590 '***** HERE COMES PLOTTER *****
1600 QQYY = 95: QQXX = 317
1610 REM qflg=0 - grid and plot , = 1 - grid only, = 2 - plot only
1620 IF QFLG > 1 THEN 2360
1630 Q$ = "##.#"
1640 REM approximate number of vertical and horizontal intervals

```

```

1650 QNINX = 5: QNINY = 4.8
1660 REM left and right borders
1670 QLNL = 40: QLNR = 639
1680 REM bottom and top borders
1690 QLNB = 164: QLNT = 9: QLOCX1 = 1
1700 SCREEN 2: CLS : KEY OFF
1710 QLOCY1 = INT(LNT / 8 + .5)
1720 QLOCY2 = QLOCY1 + 1
1730 QLOCY3 = INT(LNB / 8 + .625)
1740 QLOCY4 = QLOCY3 + 1
1750 QLOCY5 = QLOCY4 + 1
1760 QLOCX2 = INT(LNL / 8 - 4)
1770 QLOCX3 = QLOCX2 + 1
1780 QLOCX4 = QLOCX3 + INT((LNR - QLNL) / 8 + .625) - 1
1790 REM find "nice" x-scale intervals
1800 QMIN = QMINX: QMAX = QMAXX: QNIN = QNINX
1810 GOSUB 2490
1820 QSCLX = QSCL: QMINPX = QMINP: QMAXPX = QMAXP
1830 QNINPX = QNINP: QWDTX = QWDT
1840 REM find "nice" y-scale intervals
1850 QMIN = QMINY: QMAX = QMAXY: QNIN = QNINY
1860 GOSUB 2490
1870 QSCLY = QSCL: QMINPY = QMINP: QMAXPY = QMAXP
1880 QNINPY = QNINP: QWDTY = QWDT
1890 REM draw title
1900 IF PLOTTABLE$ = "NEWDATASOURCE" THEN DSRC$ = "New Data"
1910 IF PLOTTABLE$ = "FILESOURCE" THEN DSRC$ = FILENAME$
1920 RH33 = QSCLX: RH33 = RH33 * (1.0001)
1930 REM PRINT "MULTIPLY Y-AXIS BY"; QSCLY; "Units
1940 PRINT "MULT. X-AXIS BY ";
1950 PRINT USING "###^"; RH33; : PRINT " Sec. Y-AXIS BY ";
1960 PRINT USING "###^"; QSCLY; : PRINT " Units. SOURCE: "; DSRC$
1970 IF FLORD = 0 GOTO 2070
1980 LOCATE 2, 35
1990 IF ORDER = 1 THEN B$ = "ln(R)=ln(Ro)-K*t"
2000 IF ORDER = 2 THEN B$ = "(1/C)=(1/Co)+K*t"
2010 IF ORDER = 3 THEN B$ = "(1/C)^2=(1/Co)^2+2*K*t"
2020 IF ORDER = 4 THEN B$ = "C=Co-K*t"
2030 PRINT B$
2040 IF B > 0 THEN LOCATE 3, 8
2050 IF B < 0 THEN LOCATE 3, INT(LNR * 80 / 640 - .5) - 15
2060 FLORD = 0
2070 QLOCWY = (LOCY3 - QLOCY2 + 1) / QNINPY
2080 QLNWY = (LNB - QLNT) / QNINPY
2090 REM draw vertical grid and labels
2100 FOR QI = 0 TO QNINPY

```

```

2110 IF QI = 0 THEN 2140
2120 LOCATE INT(LOCY3 - QI * QLOCWY + 1), QLOCX2
2130 PRINT USING Q$; QMINPY + QI * QWDTY;
2140 QNLY1 = QNLB - QI * QLNWY
2150 NEXT QI
2160 GOSUB 2830
2170 LINE (LNL, QLNB)-(LNR, QLNB)
2180 QLOCWX = (LOCX4 - QLOCX3 + 1) / QNINPX
2190 QLNWX = (LNR - QNLN) / QNINPX
2200 REM draw horizontal grid and labels
2210 FOR QI = 0 TO QNINPX
2220 QLOC = QLOCY4
2230 LOCATE QLOC, INT(LOCX3 + QI * QLOCWX + .5)
2240 PRINT USING Q$; QMINPX + QI * QWDTX;
2250 QNLX1 = QNLN + QI * QLNWX
2260 NEXT QI
2270 LINE (LNL, QLNB)-(LNL, QLNT)
2280 GOSUB 2720
2290 IF QFLG = 1 THEN RETURN
2300 REM draw qx-qy array
2310 FOR QI = N TO QN STEP QRES
2320 GOSUB 2450
2330 LINE (2, QY2)-(2, QY2), , B
2340 NEXT QI
2350 RETURN
2360 IF QSCL > 0 THEN 2380
2370 PRINT "NO GRID DRAWN, CHECK QFLG PARAMETER": RETURN
2380 FOR QI = N TO QN STEP QRES
2390 GOSUB 2450
2400 REM check for points outside the grid
2410 IF QX2 < QNLN OR QX2 > QLNR OR QY2 > QLNB OR QY2 < QLNT
    THEN QFL2 = 1 ELSE QFL2 = 0
2420 IF QFL2 = 0 THEN LINE (2, QY2)-(2, QY2), , B
2430 NEXT QI
2440 RETURN
2450 REM routine for linear transformation from subject to object space
2460 QX2 = FNQSC(I) / QSCLX, QMAXPX, QMINPX, QLNR, QNLN)
2470 QY2 = FNQSC(I) / QSCLY, QMAXPY, QMINPY, QLNT, QLNB)
2480 RETURN
2490 REM routine to find "nice" scale intervals
2500 IF QMIN >= QMAX THEN BEEP: PRINT "Array can not be plotted": STOP
2510 QEPS = .025: QA = ABS(MIN)
2520 IF ABS(MIN) < ABS(MAX) THEN QA = ABS(MAX)
2530 QSCL = 10 ^ INT(LOG(ABS(A)) / LOG(10))
2540 QMINA = QMIN / QSCL: QMAXA = QMAX / QSCL
2550 IF QMIN = 0 THEN QMIN = -1

```

```

2560 QD = (MAXA - QMINA) / QNIN: QJ = QD * QEPS
2570 QE = INT(LOG(ABS(D)) / LOG(10))
2580 QF = QD / 10 ^ QE: QV = 10
2590 IF QF < SQR(50) THEN QV = 5
2600 IF QF < SQR(10) THEN QV = 2
2610 IF QF < SQR(2) THEN QV = 1
2620 QWDT = QV * 10 ^ QE
2630 QG = INT(MINA / QWDT)
2640 IF ABS(G + 1 - QMINA / QWDT) < QJ THEN QG = QG + 1
2650 QMINP = QWDT * QG
2660 QH = INT(MAXA / QWDT) + 1
2670 IF ABS(MAXA / QWDT + 1 - QH) < QJ THEN QH = QH - 1
2680 QMAXP = QWDT * QH
2690 QNINP = QH - QG
2700 IF ABS(MAXP) >= 10 OR ABS(MINP) >= 10 THEN QSCL = QSCL * 10:
      GOTO 2540
2710 RETURN
2720 REM routine to draw x tic marks
2730 QLNXB1 = QLNR
2740 QDTPX = INT((LNR - QLNL) / QNINPX)
2750 QLNXB1 = QLNXB1 + QDTPX
2760 FOR QQ = 1 TO QNINPX
2770 QLNXB1 = QLNXB1 - QDTPX
2780 IF QLNXB1 < QLNL THEN RETURN
2790 QLNB3 = QLNB - 3
2800 LINE (LNXB1, QLNB)-(LNXB1, QLNB3)
2810 NEXT QQ
2820 RETURN
2830 REM routine to draw y tic marks
2840 QYLN1 = QLNB
2850 QDTYP = INT((LNB - QLNT) / QNINPY)
2860 FOR QQ = 1 TO QNINPY
2870 QYLN1 = QYLN1 - QDTYP
2880 QLNL4 = QLNL + 4
2890 LINE (LNL, QYLN1)-(LNL4, QYLN1)
2900 IF QQ = QNINPY AND QDTYP = 1 THEN QQ = QQ - 34
2910 NEXT QQ
2920 RETURN
2930 '***** LINEAR REGRESSION *****
2940 INPUT "LEFT MOST BORDER (1-512)"; N
2950 INPUT "RIGHT MOST BORDER (1-512)"; J
2960 QLNB = 164
2970 DEFDBL P, S
2980 M = J - N + 1
2990 SX = 0: SY = 0: PX = 0: PY = 0: PC = 0
3000 IF ORDER < 1 OR ORDER > 4 THEN ORDER = 4

```

```

3010 FOR I = N TO J
3020 IF ORDER = 4 THEN QLY(I) = CON(I)
3030 IF ORDER = 1 THEN QLY(I) = -2.303 * LOG(ABS(RO(I)))
3040 IF ORDER = 2 THEN QLY(I) = 1 / CON(I)
3050 IF ORDER = 3 THEN QLY(I) = (1 / CON(I)) ^ 2
3060 RHGRFLAG = 1
3070 SX = SX + QX(I); SY = SY + QLY(I)
3080 PX = PX + QX(I) * QX(I); PY = PY + QLY(I) * QLY(I)
3090 PC = PC + QX(I) * QLY(I)
3100 NEXT I
3110 D# = M * PX - SX * SX
3120 A = (SY * PX - PC * SX) / D#
3130 B = (M * PC - SX * SY) / D#
3140 VX# = (PX - SX * SX / M) / (M - 1)
3150 VY# = (PY - SY * SY / M) / (M - 1)
3160 RR# = B * B * VX# / VY#
3170 r = SQR(RR#)
3180 E = SQR((1 - RR#) / (M - 2)) / r
3190 RE = (M - 1) * VY# * (1 - RR#)
3200 GB = ABS(E * B)
3210 GA = GB * SQR(PX / M)
3220 GP = SQR(RE / (M - 1))
3230 K = ABS(B); IF ORDER = 3 THEN K = K / 2
3240 PRINT "INTCPT="; : PRINT USING "###.###^"; A;
3250 PRINT " (STD DEV="; : PRINT USING "###.###^"; GA;
3260 PRINT ") SLOPE="; : PRINT USING "###.###^"; B;
3270 PRINT " (STD DEV="; : PRINT USING "###.###^"; GB; : PRINT ") "
3280 PRINT "R="; r; " E="; E; " STD DEV PTS="; GP;
3290 IF r > .8 GOTO 3340
3300 PUT (0, QLNB - 64), BTARY, PSET
3310 LOCATE INT(((LNB - 64)/200) * 25 + 1) + 1, 1
3320 PRINT TAB(30); : PRINT "THIS IS NOT A WELL FIT CURVE"
3330 REM FOR LLKK = 1 TO 2000:MYBADOOG=LOG(LLKK):NEXT
3340 IF INKEY$ = "" THEN 3340
3350 PUT (0, QLNB + 11), BTARY, PSET: LOCATE INT((LNB/200) * 25 + 1) + 2, 1
3360 INPUT "WOULD YOU LIKE A PLOT OF THE RESULTS"; B$
3370 B$ = LEFT$(B$, 1)
3380 IF B$ = "N" THEN RETURN
3390 PUT (0, QLNB + 11), BTARY, PSET: LOCATE INT((LNB/200) * 25 + 1) + 2, 1
3400 IF B$ <> "Y" THEN GOTO 3350
3410 FLORD = 1
3420 INPUT "WHAT RESOLUTION WOULD YOU LIKE TO GRAPH (1 TO
10)"; QRES
3430 IF QRES < 1 OR QRES > 20 THEN QRES = 1
3440 FOR I = N TO J
3450 CC = QY(I)

```

```

3460 QY(I) = QLY(I)
3470 QLY(I) = CC
3480 NEXT I
3490 QFLG = 0: QMINX = QX(N): QMAXX = QX(J): QMINY = QY(N)
3500 QMAXY = QY(J): QN = J
3510 QYN = B * QX(N) + A
3520 QYJ = B * QX(J) + A
3530 IF B < 0 GOTO 3560
3540 IF QYN < QY(N) THEN QMINY = QYN ELSE QMINY = QY(N)
3550 IF QYJ > QY(J) THEN QMAXY = QYJ ELSE QMAXY = QY(J)
3560 IF B > 0 GOTO 3590
3570 IF QYN > QY(N) THEN QMAXY = QYN ELSE QMAXY = QY(N)
3580 IF QYJ < QY(J) THEN QMINY = QYJ ELSE QMINY = QY(J)
3590 GOSUB 1590
3600 QYN = FNQSC(N / QSCLY, QMAXPY, QMINPY, QLNT, QLNB)
3610 QXN = FNQSC(N) / QSCLX, QMAXPX, QMINPX, QLNR, QLNL)
3620 QY2 = FNQSC(J / QSCLY, QMAXPY, QMINPY, QLNT, QLNB)
3630 QX2 = FNQSC(J) / QSCLX, QMAXPX, QMINPX, QLNR, QLNL)
3640 LINE (N, QYN)-(2, QY2)
3650 FOR I = N TO J
3660 CC = QY(I)
3670 QY(I) = QLY(I)
3680 QLY(I) = CC
3690 NEXT I
3700 QMINX = QX(1): QMAXX = QX(512): QMINY = QY(515)
3710 QMAXY = QY(514): QN = 512
3720 FLLOOP = 1 + FLLOOP
3730 IF FLLOOP > 1 THEN GOTO 3840 ELSE GOSUB 810
3740 PUT (0, QLNB + 1), BTARY, PSET
3750 LOCATE INT((LNB / 200) * 25 + 1) + 2, 1
3760 PRINT "INTCPT="; : PRINT USING "###.###^"; A;
3770 PRINT " (STD DEV="; : PRINT USING "###.###^"; GA;
3780 PRINT ") SLOPE="; : PRINT USING "###.###^"; B;
3790 PRINT " (STD DEV="; : PRINT USING "###.###^"; GB; : PRINT ") "
3800 PRINT "R="; r; " E="; EE; " STD DEV PTS="; GP;
3810 REM FOR LLKK = 1 TO 2000:MYBADDOG=LOG(LLKK):NEXT
3820 IF INKEY$ = "" THEN GOTO 3820
3830 FLLOOP = 0
3840 REM GOSUB 1570
3850 RETURN
3860 '***** N'th ORDER *****
3870 PRINT : PRINT "CHOOSE THE ORDER OF THE REACTION": PRINT
3880 PRINT "1) FIRST ORDER      ln(R)=ln(Ro)-K*t"
3890 PRINT "2) SECOND ORDER      (1/C)=(1/Co)+K*t"
3900 PRINT "3) THIRD ORDER      (1/C)^2=(1/Co)^2+2*K*t"
3910 PRINT "4) ABSORBANCE ONLY      C=Co-K*t": PRINT

```



```

3920 INPUT "WHICH NUMBER"; ORDER
3930 IF ORDER < 1 OR ORDER > 4 GOTO 3870
3940 RETURN
3950 '***** ERROR *****
3960 IF(57=ERR)AND(180 > ERL) THEN RESUME 160
3970 IF 57 = ERR THEN PRINT "DP600 OR DISK I/O ERROR": RESUME 230
3980 IF 53 = ERR GOTO 4040
3990 IF 4970 = ERL THEN GOTO 4040
4000 IF 4980 = ERL THEN GOTO 4040
4010 REM PRINT "STOP": PRINT ERR, ERL
4020 REM IF ERR=6 THEN BAD=ERL:GOTO ERL
4030 RESUME NEXT
4040 PRINT "FILE "; B$; " NOT FOUND"
4050 FILENAME$ = ""
4060 CLOSE #2
4070 RESUME 8340
4080 '***** COMPARE *****
4090 INPUT "HOW MANY PLOTS DO YOU WISH TO MAKE (1 TO 3)"; NOPLO
4100 IF NOPLO < 1 OR NOPLO > 3 GOTO 4090
4110 PRINT : PRINT "LOAD FIRST DATA SET FROM DISK": PRINT
4120 GOSUB 8340      'LOAD
4130 GOSUB 670      'PLOTTER
4140 N1 = N: J1 = J
4150 DIM QY1(515)
4160 FOR I = N TO J
4170 QY1(I) = QLY(I)
4180 NEXT I
4190 IF B < 0 GOTO 4210
4200 QY1(515) = QY1(N): QY1(514) = QY1(J): GOTO 4220
4210 QY1(515) = QY1(J): QY1(514) = QY1(N)
4220 IF NOPLO = 1 GOTO 4520
4230 PRINT : PRINT "LOAD SECOND DATA SET FROM DISK": PRINT
4240 GOSUB 8340      'LOAD
4250 GOSUB 670      'PLOTTER
4260 N2 = N: J2 = J
4270 DIM QY2(J)
4280 FOR I = N TO J
4290 QY2(I) = QLY(I)
4300 NEXT I
4310 IF B < 0 GOTO 4350
4320 IF QY2(N) < QY1(515) THEN QY1(515) = QY2(N)
4330 IF QY2(J) > QY1(514) THEN QY1(514) = QY2(J)
4340 GOTO 4370
4350 IF QY2(N) > QY1(514) THEN QY1(514) = QY2(N)
4360 IF QY2(J) < QY1(515) THEN QY1(515) = QY2(J)
4370 IF NOPLO = 2 GOTO 4520

```

```

4380 PRINT : PRINT "LOAD THIRD DATA SET FROM DISK": PRINT
4390 GOSUB 8340      'LOAD
4400 GOSUB 670      'PLOTTER
4410 N3 = N: J3 = J
4420 DIM QY3(J)
4430 FOR I = N TO J
4440 QY3(I) = QLY(I)
4450 NEXT I
4460 IF B < 0 GOTO 4500
4470 IF QY3(N) < QY1(515) THEN QY1(515) = QY3(N)
4480 IF QY3(J) > QY1(514) THEN QY1(514) = QY3(J)
4490 GOTO 4520
4500 IF QY3(N) > QY1(514) THEN QY1(514) = QY3(N)
4510 IF QY3(J) < QY1(515) THEN QY1(515) = QY3(J)
4520 N = N1: J = J1
4530 IF N2 < N1 AND NOPLO > 1 THEN N = N2
4540 IF J2 > J1 AND NOPLO > 1 THEN J = J2
4550 IF N3 < N AND NOPLO > 2 THEN N = N3
4560 IF J3 > J AND NOPLO > 2 THEN J = J3
4570 QFLD = 0: FLORD = 0: QMINX = QX(N): QMAXX = QX(J)
4580 QMINY = QY1(515): QMAXY = QY1(514): QN = J1: N = N1
4590 PRINT : INPUT "WHAT RESOLUTION WOULD YOU LIKE (1 TO 10)"; QRES
4600 FOR I = N1 TO J1
4610 QY(I) = QY1(I)
4620 NEXT I
4630 ERASE QY1
4640 FLORD = 0
4650 GOSUB 1600
4660 LOCATE 1, 59
4670 PRINT "      "
4680 IF NOPLO = 1 GOTO 4820
4690 QFLG = 2: QN = J2: N = N2
4700 FOR I = N2 TO J2
4710 QY(I) = QY2(I)
4720 NEXT I
4730 ERASE QY2
4740 GOSUB 1600
4750 IF NOPLO = 2 GOTO 4820
4760 QN = J3: N = N3
4770 FOR I = N3 TO J3
4780 QY(I) = QY3(I)
4790 NEXT I
4800 GOSUB 1600
4810 ERASE QY3
4820 PUT (0, QLNB + 11), BTARY, PSET: LOCATE INT((LNB/200) * 25 + 1) + 2, 1
4830 PRINT "YOU WILL NEED A NEW DATA SOURCE AFTER RETURNING TO

```

## MENU"

```

4840 IF INKEY$ = "" THEN GOTO 4840
4850 PUT (0, QLNB + 11), BTARY, PSET: LOCATE INT((LNB/200) * 25 + 1) + 2, 1
4860 PRINT "PRESS ANY KEY ONCE TO GET A SCREEN DUMP"
4870 PRINT "TWICE TO RETURN TO MENU";
4880 IF INKEY$ = "" THEN GOTO 4880
4890 PUT (0, QLNB + 11), BTARY, PSET: LOCATE INT((LNB/200) * 25 + 1) + 2, 1
4900 IF INKEY$ = "" THEN GOTO 4900
4910 FLDATA = 0
4920 RETURN
4930 REM SUBROUTINE GET INFO
4940 '
4950 CLS
4960 REM OPEN "com1:9600,n,8,1,cs,ds,cd" AS #1
4970 BOUT$ = BS
4980 PRINT #1, BOUT$
4990 FOR I = 1 TO 1500: QWERT1 = QWERT1 + 1
5000 NEXT I
5010 J = 1
5020 V = LOC(1): IF V < 1 THEN PRINT "NO MESSAGE": GOTO 5210
5030 FOR ZQQZ = 1 TO 500: FF = ZQQZ * ZQQZ: NEXT
5040 AGI$(J) = INPUT$(V, #1)
5050 ON ERROR GOTO 3950
5060 V = LOC(1): IF V < 1 THEN GOTO 5090
5070 J = J + 1
5080 GOTO 5020
5090 FOR HH = 1 TO J
5100 BGI$(HH) = ""
5110 REM PRINT AGI$(HH), VAL(AGI$(HH))
5120 FOR UU = 1 TO LEN(AGI$(HH))
5130 QAA$ = MID$(AGI$(HH), 1)
5140 ZORP$ = BGI$(HH)
5150 IF ASC(QAA$) = 45 THEN GOTO 5170
5160 IF ASC(QAA$) < 48 OR ASC(QAA$) > 91 THEN GOTO 5200
5170 BGI$(HH) = BGI$(BB) + QAA$
5180 NEXT UU
5190 NEXT HH
5200 MYINFO = VAL(ZORP$)
5210 RETURN
5220 REM *****CHANGE V0,VMAX *****
5230 INPUT "DO YOU WANT TO CHECK ACTUAL VOLTAGE VALUES OF
        DATASET"; ANANS$
5240 IF LEFT$(ANANS$, 1) = "N" THEN GOTO 5320
5250 INPUT "FIRST , LAST DATA TO USE "; POINT1, POINT2
5260 TEMPSUM = 0
5270 FOR KZ = POINT1 TO POINT2

```

```

5280 TEMPSUM = TEMPSUM + QY(KZ)
5290 NEXT KZ
5300 VNOW = TEMPSUM / (POINT2 - POINT1 + 1)
5310 PRINT "AVERAGE VOLTAGE FOR THAT RANGE IS "; VNOW
5320 INPUT "CHANGE V0 "; ANANS$
5330 IF ANANS$ = "N" THEN GOTO 5350
5340 INPUT "NEW V0"; V0
5350 INPUT "CHECK VOLTAGES AGAIN "; ANANS$
5360 IF LEFT$(ANANS$, 1) = "Y" THEN GOTO 5250
5370 INPUT "CHANGE VM "; ANANS$
5380 IF ANANS$ = "N" THEN GOTO 5410
5390 INPUT "NEW VMAX "; VM
5400 VFULL = VM - V0
5410 PRINT "L IS NOW "; L: INPUT "CHANGE L "; ANANS$
5420 IF ANANS$ = "N" THEN GOTO 5440
5430 INPUT "NEW L"; L
5440 PRINT "E IS NOW "; EE: INPUT "CHANGE E "; ANANS$
5450 IF ANANS$ = "N" THEN GOTO 5470
5460 INPUT "NEW E "; EE
5470 LEFF = 2.303 * L * EE: VFULL = VM - V0
5480 QY(516) = V0: QY(517) = VM: QY(518) = L: QY(519) = EE
5490 IF VFULL = 0 OR LEFF = 0 THEN PRINT "BAD CONSTS. ": GOTO 5230
5500 PRINT "V0,VM,VFULL,L,LEFF,E": PRINT V0, VM, VFULL, L; " "; LEFF, EE
5510 FOR I = 1 TO 512
5520 QX(I) = I * PER
5530 CON(I) = -LOG(ABS(((I) - V0) / VFULL)) / LEFF
5540 REM PRINT CON(I)
5550 NEXT I
5560 FLDATA = 2
5570 RETURN
5580 REM *****DISK DIR*****
5590 INPUT "WHICH DRIVE "; DRV$: IF DRV$ = "" THEN DRV$ = "C"
5600 DRV$ = LEFT$(DRV$, 1)
5610 IF DRV$ = "A" OR DRV$ = "B" GOTO 5640
5620 IF DRV$ = "C" OR DRV$ = "D" GOTO 5640
5630 GOTO 5590
5640 MYCALL$ = DRV$ + ":"
5650 FILES MYCALL$
5660 REM OPEN "O", #2, MYCALL$
5665 INPUT "Hit return to go to main menu"; r$
5670 RETURN
5680 INPUT "WHICH DRIVE"; DRV$: IF DRV$ = " " THEN DRV$ = "C"
5690 DRV$ = LEFT$(DRV$, 1)
5700 IF DRV$ = "A" OR DRV$ = "B" GOTO 5730
5710 IF DRV$ = "C" OR DRV$ = "D" GOTO 5730
5720 GOTO 5680

```

```

5730 DRV$ = DRV$ + ":"
5740 INPUT "FILE NAME"; FILENAME$
5750 B$ = DRV$ + LEFT$(FILENAME$, 8)
5760 OPEN "O", #2, B$
5770 FOR I = N TO J STEP 5
5780 PRINT #1, QX(I), ",", OD(I), ","
5790 NEXT I
5800 CLOSE #2
5810 GOTO 1530
5820 PRINT " "
5830 REM ***** CALIBRATION *****
5840 ROUTINE$ = "CAL"
5850 PRINT "Present time delay is "; TDELAY%; INPUT "data points. Do you want to
change it"; B$
5860 PRINT " "
5870 IF B$ <> "Y" THEN 5920
5880 INPUT "New time delay (number of data points 0 to 512)"; TDELAY%
5890 PRINT " "
5900 GOTO 5850
5910 QY(520) = TDELAY%
5920 PRINT "The period is "; PERIOD$: PRINT "The multifact% is "; MULTFACT%
5930 INPUT "do you want to change this"; C$
5940 IF C$ <> "Y" THEN GOTO 5990
5950 PRINT " "
5960 PRINT "Type in the new period, your choices are as follows:"
5970 INPUT "25NS, 100NS, 200NS, 250NS, 500NS, 1US, 2.5US, 25US, 250US)";
PERIOD$
5980 GOTO 5920
5990 IF PERIOD$ = "25NS" THEN PERIOD% = &H0
6000 IF PERIOD$ = "250NS" THEN PERIOD% = &H10
6010 IF PERIOD$ = "2.5US" THEN PERIOD% = &H20
6020 IF PERIOD$ = "25US" THEN PERIOD% = &H30
6030 IF PERIOD$ = "250US" THEN PERIOD% = &H40
6040 IF PERIOD$ = "100NS" THEN PERIOD% = &H0
6050 IF PERIOD$ = "200NS" THEN PERIOD% = &H0
6060 IF PERIOD$ = "500NS" THEN PERIOD% = &H10
6070 IF PERIOD$ = "1US" THEN PERIOD% = &H10
6080 IF PERIOD$ = "25NS" THEN MULTFACT% = 1
6090 IF PERIOD$ = "250NS" THEN MULTFACT% = 1
6100 IF PERIOD$ = "2.5US" THEN MULTFACT% = 1
6110 IF PERIOD$ = "25US" THEN MULTFACT% = 1
6120 IF PERIOD$ = "250US" THEN MULTFACT% = 1
6130 IF PERIOD$ = "100NS" THEN MULTFACT% = 4
6140 IF PERIOD$ = "200NS" THEN MULTFACT% = 8
6150 IF PERIOD$ = "500NS" THEN MULTFACT% = 2
6160 IF PERIOD$ = "1US" THEN MULTFACT% = 4

```

```

6180 IF PERIOD$ = "25NS" THEN PER = 2.5E-08
6190 IF PERIOD$ = "250NS" THEN PER = 2.5E-07
6200 IF PERIOD$ = "2.5US" THEN PER = .0000025
6210 IF PERIOD$ = "25US" THEN PER = .000025
6220 IF PERIOD$ = "250US" THEN PER = .00025
6230 IF PERIOD$ = "100NS" THEN PER = .0000001
6240 IF PERIOD$ = "200NS" THEN PER = .0000002
6250 IF PERIOD$ = "500NS" THEN PER = .0000005
6260 IF PERIOD$ = "1US" THEN PER = .000001
6262 IF PER > 0 THEN GOTO 6270
6263 PRINT " "
6264 PRINT "  ERROR ERROR ERROR ERROR"
6265 PRINT "  ERROR ERROR ERROR ERROR ERROR "
6266 PRINT " "
6267 INPUT "  YOU MUST INPUT PERIOD IN FORM SHOWN!!!"; P$
6270 POSTTRIGCOUNT% = COUNT% * MULTFACT% - TDELAY% *
    MULTFACT%
6280 CONTROL% = &HA00C OR PERIOD%
6290 PRINT " "
6300 PRINT " "
6310 PRINT "          Trigger when ready"
6320 GOSUB 6820
6330 INPUT "Have you triggered for no light"; E$
6340 IF E$ <> "Y" THEN GOTO 6310
6350 START = TRIG - TDELAY% * MULTFACT%      'Pretrig data address
6360 MAX = START + COUNT% * MULTFACT%      'Last data address
6370 Y = 0                                  'Set sum at zero
6380 W = 0
6390 DEF SEG = SEGMENT%                    'define data segment
6410 FOR I = START TO MAX STEP MULTFACT%
6415 W = W + 1
6420 QY(W) = 255 - PEEK(I)                  'Look at data
6430 Y = Y + QY(W)                          'sum data points
6440 NEXT I
6450 V0 = Y / W                            'Average data points
6460 DEF SEG                                'Restore data segment
6470 F$ = "N"
6480 PRINT "Do you want to trigger for full light (note that if there"
6490 PRINT "is a time delay, the full light value will be the average of"
6500 PRINT "all but the last two pre-trigger values (IF THERE IS NO TIME"
6510 INPUT "DELAY YOU MUST DECLARE FULL LIGHT AT THIS POINT)"; F$
6520 VM = 0
6530 IF F$ = "Y" THEN GOTO 6560
6540 IF F$ <> "N" THEN GOTO 6480
6550 GOTO 6750
6560 PRINT "Trigger when ready"

```

```

6570 GOSUB 6820
6580 INPUT "Have you triggered for full light"; E$
6590 IF E$ = "N" THEN GOTO 6560
6600 IF E$ <> "Y" THEN GOTO 6580
6610 START = TRIG - TDELAY% * MULTFACT%      'Pretrig data address
6620 MAX = START + COUNT% * MULTFACT%        'Last data address
6630 FOR I = 1 TO 512: QY(I) = 0: NEXT I
6640 Y = 0                                     'Set sum at zero
6650 W = 0
6660 DEF SEG = SEGMENT%                       'define data segment
6670 FOR I = START TO MAX STEP MULTFACT%
6680 W = W + 1
6690 QY(W) = 255 - PEEK(I)                   'Look at data
6700 Y = Y + QY(W)                           'sum data points
6710 NEXT I
6720 VM = Y / W                               'Average data points
6730 VFULL = VM - V0
6740 DEF SEG                                  'Restore data segment
6750 PRINT : PRINT "Vmax = "; VM; " V0 = "; V0; " L = "; L; "E = "; EE
6760 PRINT "L-Change L", "E-Change E", "N-No Change": B$ = INPUT$(1)
6770 IF B$ <> "L" AND B$ <> "E" AND B$ <> "N" GOTO 6760
6780 IF B$ = "L" THEN INPUT "L = ", L: GOTO 6750
6790 IF B$ = "E" THEN INPUT "E = ", EE: GOTO 6750
6800 LEFF = L * EE * 2.303
6810 RETURN
6820 REM ***** LOAG TRIG OFFSET *****
6830 DEF SEG = SEGMENT%                       'Define waag II segment
6840 OUT PORT3%, &HC0: OUT PORT2%, &H6F      'Enable trigger offset
6850 POKE 0, TOFFSET%                         'Load offset value
6860 OUT PORT3%, &HA0: OUT PORT2%, &H6F      'Reset control register
6870 DEF SEG                                  'Restore data segment
6880 REM ***** DATA ACQUISITION *****
6890 OUT PORT3%, &HA0: OUT PORT2%, &H6F      'Initialize control regs
6900 OUT PORT1%, &HFF: OUT PORT0%, &HFF      'Clear counter
6910 OUT PORT1%, &HFF: OUT PORT0%, &HFF
6920 N% = -(POSTTRIGCOUNT% + &HFF)         'Correct count
6930 OUT PORT1%, FNHIPT(N%): OUT PORT0%, FNLOBT(N%) 'load count
6940 OUT PORT1%, FNHIPT(N%): OUT PORT0%, FNLOBT(N%)
6950 N1% = CONTROL% AND &HBFFC
6960 OUT PORT3%, FNHIPT(N1%): OUT PORT2%, FNLOBT(N1%) 'Start sampling
6970 WAIT PORT2%, 1                          'Wait for busy
6980 OUT PORT3%, &HA0: OUT PORT2%, &H6F      'enable waag II ram
6990 TRIG = 2 * (INP(PORT0%) + (INP(PORT1%) AND &H3F) * 256) 'Read trig value
7000 GOSUB 7020
7010 RETURN
7020 REM ***** GRAPH RAW DATA*****

```

```

7030 CLS
7040 SCREEN (2)
7050 GOSUB 7070
7060 GOTO 7310
7070 LINE (15, 40)-(537, 170), , B
7080 LINE (10, 105)-(20, 105)
7090 LINE (12, 115)-(18, 115)
7100 LINE (12, 125)-(18, 125)
7110 LINE (12, 135)-(18, 135)
7120 LINE (12, 145)-(18, 145)
7130 LINE (12, 155)-(18, 155)
7140 LINE (12, 95)-(18, 95)
7150 LINE (12, 85)-(18, 85)
7160 LINE (12, 75)-(18, 75)
7170 LINE (12, 65)-(18, 65)
7180 LINE (12, 55)-(18, 55)
7190 LINE (12, 45)-(18, 45)
7200 LINE (20, 168)-(20, 172)
7210 LINE (70, 168)-(70, 172)
7220 LINE (120, 168)-(120, 172)
7230 LINE (170, 168)-(170, 172)
7240 LINE (220, 168)-(220, 172)
7250 LINE (270, 168)-(270, 172)
7260 LINE (320, 168)-(320, 172)
7270 LINE (370, 168)-(370, 172)
7280 LINE (420, 168)-(420, 172)
7290 LINE (470, 168)-(470, 172)
7300 RETURN
7310 START = TRIG - TDELAY% * MULTFACT%      'Pretrig data address
7320 MAX = START + COUNT% * MULTFACT%        'Last data address
7330 DEF SEG = SEGMENT%                      'Define data segment
7340 X% = 19                                'Define x
7350 FOR I = START TO MAX STEP MULTFACT%
7360 RAWDAT% = PEEK(I)
7370 X% = X% + 1
7380 Y% = CINT(169 - (RAWDAT% * 128) / 255)
7390 PSET (% , Y%)
7400 IF I = TRIG AND ROUTINE$ = "CAL" THEN GOSUB 7440
7410 NEXT I
7420 DEF SEG
7430 RETURN
7440 CIRCLE (% , Y%), 4
7450 RETURN
7460 REM ***** DATA *****
7470 IF ROUTINE$ <> "CAL" THEN GOTO 7500
7480 PLOTTABLE$ = "NEWDATASOURCE"

```



```

7490 GOTO 7520
7500 INPUT "You have not calibrated. Hit return to go to main menu."; B$
7510 RETURN
7520 FOR I = 1 TO 512                'Clear data points
7530 QY(I) = 0
7540 QX(I) = 0
7550 NEXT I
7560 PRINT " "
7570 PRINT " "
7580 PRINT "      Trigger when ready"
7590 ROUTINES$ = "DATA"
7600 GOSUB 6820                      'Get data and graph it
7610 INPUT "Type T for trigger or S to stop"; G$
7620 IF G$ = "S" THEN GOTO 7640
7630 GOTO 7660
7640 ROUTINES$ = "CAL"
7650 RETURN
7660 IF G$ <> "T" THEN GOTO 7610
7670 ROUTINES$ = "DATA"
7680 START = TRIG - TDELAY% * MULTFACT%      'Pretrig data address
7690 MAX = START + COUNT% * MULTFACT%        'Last data address
7700 Y = 0                                  'Set sum at zero
7710 W = 0
7720 DEF SEG = SEGMENT%                  'define data segment
7730 FOR I = START TO MAX STEP MULTFACT%
7740 W = W + 1
7750 QY(W) = 255 - PEEK(I)              'Look at data
7760 NEXT I                             'Calc. vm
7770 IF VM < 0 THEN GOTO 7860
7780 VMY = 0
7790 X = 0
7810 FOR I = 1 TO TDELAY% - 2
7820 X = X + 1
7830 VMY = VMY + QY(I)
7840 NEXT I
7850 VM = VMY / X
7860 VFULL = VM - V0
7870 ROUTINES$ = "DATA"
7880 REM find maximum and minimum values of y
7890 FOR I = 1 TO 512
7900 IF QY(I) >= QMAXY THEN QMAXY = QY(I)
7910 IF QY(I) <= QMINY THEN QMINY = QY(I)
7920 NEXT I
7930 QMAXX = 0: QMINX = 512 * PER
7940 LEFF = L * EE * 2.303
7950 FOR I = 1 TO 512: QX(I) = I * PER

```

```

7960 IF VM = 0 THEN VM = -3: IF L = 0 THEN L = 39: IF V0 = 0 THEN V0 = -1
7970 CON(I) = -LOG(ABS(((I) - V0) / VFULL)) / LEFF
7980 OD(I) = -LOG(ABS(((I) - V0) / VFULL)) / 2.303
7990 NEXT I
8000 QY(513) = PER: QY(514) = QMAXY: QY(515) = QMINY
8010 QY(516) = V0: QY(517) = VM: QY(518) = L: QY(519) = EE
8020 RETURN
8030 '***** SAVE *****
8040 IF ROUTINES$ = "DATA" THEN GOTO 8170
8050 IF ROUTINES$ <> "LOAD" THEN GOTO 8100
8060 INPUT "This data has been loaded from a file. Save again"; LOADSUB$
8070 IF LOADSUB$ = "Y" GOTO 8170
8080 IF LOADSUB$ <> "N" THEN GOTO 8060
8090 RETURN
8100 IF ROUTINES$ <> "SAVE" THEN GOTO 8150
8110 INPUT "Data has already been saved, save again under another name"; H$
8120 IF H$ = "N" THEN RETURN
8130 IF H$ = "Y" THEN GOTO 8170
8140 IF H$ <> "N" GOTO 8110
8150 PRINT "There is no data to be saved. Returning to menu"
8160 RETURN
8170 INPUT "WHICH DRIVE "; DRV$: IF DRV$ = "" THEN DRV$ = "C"
8180 DRV$ = LEFT$(DRV$, 1)
8190 IF DRV$ = "A" OR DRV$ = "B" GOTO 8220
8200 IF DRV$ = "C" OR DRV$ = "D" GOTO 8220
8210 GOTO 8170
8220 DRV$ = DRV$ + ",."
8225 PRINT "LAST FILE SAVED WAS NAMED:"; TFILENAMES
8230 INPUT "FILENAME "; FILENAMES$
8240 IF FILENAMES$ = "" GOTO 8230
8245 TFILENAMES$ = FILENAMES$
8250 B$ = DRV$ + LEFT$(FILENAMES$, 8)
8255 QY(520) = TDELAY%
8260 OPEN "O", #2, B$
8270 PRINT #2, B$
8280 SIZE = 518
8290 FOR I = 1 TO SIZE STEP 5
8300 PRINT #2, QY(I), QY(I + 1), QY(I + 2), QY(I + 3), QY(I + 4)
8310 NEXT I
8320 CLOSE #2
8330 RETURN
8340 '***** LOAD *****
8360 INPUT "WHICH DRIVE "; DRV$: IF DRV$ = "" THEN DRV$ = "C"
8370 DRV$ = LEFT$(DRV$, 1)
8380 IF DRV$ = "A" OR DRV$ = "B" GOTO 8410
8390 IF DRV$ = "C" OR DRV$ = "D" GOTO 8410

```

```

8400 GOTO 8360
8410 DRV$ = DRV$ + ":"
8420 INPUT "FILENAME"; FILENAME$
8430 B$ = DRV$ + LEFT$(FILENAME$, 8)
8440 OPEN "I", #2, B$
8450 ON ERROR GOTO 3960
8460 PLOTTABLE$ = "FILESOURCE"
8470 SIZE = 518
8475 INPUT #2, B$
8480 FOR I = 1 TO SIZE STEP 5
8490 INPUT #2, QY(I), QY(I + 1), QY(I + 2), QY(I + 3), QY(I + 4)
8500 NEXT I
8510 CLOSE #2
8520 PER = QY(513): QMAXY = QY(514): QMINY = QY(515)
8530 V0 = QY(516): VM = QY(517): L = QY(518): EE = QY(519): TDELAY% =
      QY(520)
8540 PRINT "FILE "; B$; " FOUND."
8550 LEFF = 2.303 * L * EE: VFULL = VM - V0
8560 PRINT "V0,VM,VFULL,L,LEFF,E": PRINT V0, VM, VFULL, L; " "; LEFF, EE
8570 INPUT "WANT TO CHANGE V0,VM,L,OR E "; ANANS$
8580 IF ANANS$ = "Y" THEN GOSUB 5220
8590 LEFF = 2.303 * L * EE: VFULL = VM - V0
8600 FOR I = 1 TO 512
8610 QX(I) = I * PER
8620 CON(I) = -LOG(ABS(((I) - V0) / VFULL)) / LEFF
8630 OD(I) = -LOG(ABS(((I) - V0) / VFULL)) / 2.303
8640 NEXT I
8650 ROUTINE$ = "LOAD"
8660 RHGRFLAG = 1
8670 RETURN
8680 SCREEN (0)
8690 END

```

APPENDIX B  
COMPUTER PROGRAM TO CALCULATE CONCENTRATIONS OF PRINCIPLE  
SPECIES PRODUCED DURING IRRADIATION OF WATER

```

10 REM *****
20 REM * THIS PROGRAM WILL GIVE CONCENTRATIONS FOR THE
    PRODUCTS
30 REM *** OF PULSE RADIOLYSIS OF WATER BASED ON
    A CONCENTRATION ***
40 REM *** OF e-(aq) INPUT BY THE USER BY CRAIG HOAG ***
50 REM *****
65 REM
70 CLS
75 PRINT " ": PRINT " ": PRINT " ": PRINT " "
80 PRINT "CAPSLOCK MUST BE ON FOR THIS PROGRAM TO WORK"
90 PRINT " ": PRINT " ": PRINT " "
100 INPUT "TYPE IN THE DESIRED CONC. OF e-(aq)"; EAQ
120 GEAQ = 2.63: GHPLUS = 2.63: GOH = 2.72: GH = .55: GH2 = .45: GH2O2 = .68
140 GHO2 = .026: GHO2M = .0925: GO2M = .0035
160 HPLUS = EAQ
180 OH = GOH * EAQ / GEAQ
200 H = GH * EAQ / GEAQ
220 H2 = GH2 * EAQ / GEAQ
240 H2O2 = GH2O2 * EAQ / GEAQ
260 HO2 = GHO2 * EAQ / GEAQ
280 HO2M = GHO2M * EAQ / GEAQ
300 O2M = GO2M * EAQ / GEAQ
400 INPUT "DRIVE TO BE SAVED ON"; DRV$
420 IF DRV$ = "" THEN DRV$ = "C"
440 IF DRV$ = "B" THEN GOTO 480
450 IF DRV$ = "A" THEN GOTO 480
460 IF DRV$ = "D" THEN GOTO 480
470 IF DRV$ = "C" THEN GOTO 480
475 GOTO 400
480 DRV$ = DRV$ + ":"
500 INPUT "ENTER FILENAME"; FILENAME$
520 FILNAME$ = DRV$ + FILENAME$
550 OPEN "O", #2, FILNAME$
580 PRINT #2, "EAQ,"; EAQ
590 PRINT #2, "HPLUS,"; HPLUS

```

```
600 PRINT #2, "OH,"; OH
610 PRINT #2, "H,"; H
620 PRINT #2, "H2,"; H2
630 PRINT #2, "H2O2,"; H2O2
640 PRINT #2, "HO2.,"; HO2
650 PRINT #2, "HO2-,"; HO2M
660 PRINT #2, "O2-,"; O2M
680 CLOSE #2
700 INPUT "DO YOU WANT TO CREATE ANOTHER FILE"; CRS
900 IF CRS = "Y" THEN GOTO 10
910 END
```

## BIBLIOGRAPHY

- [1] Gray, H. B.; and Maverick, A. W. "Solar chemistry of metal complexes," *Science*, **1981**, *214*, 1201-1205.
- [2] Eidmen, P. K.; Maverick, A. W.; Gray, H. B. "Production of hydrogen by irradiation of metal complexes in aqueous solution," *Inorganica. Chemica. Acta.*, **1981**, *50*, 59-64.
- [3] Gupta, A. K.; Parker, R. Z.; Hanrahan, R. J. "Solar-assisted production of hydrogen and chlorine from hydrochloric acid using hexachloroiridate (III) and (IV)," *Int. J. Hydrogen Energy* **1993**, *18*, 713-717.
- [4] Parker, R. Z.; Hanrahan, R. J.; Gupta, A. K. "Hydrogen generation and utility load leveling system and the method therefore," U.S. Patent number 5,219,671 issued June 15, 1993.
- [5] Gupta, A. K.; Parker, R. Z.; Keefer, C. E.; Hanrahan, R. J. "Factors affecting quantum yields for chlorine formation in the solar photolysis of acidic chloride solutions containing hexachloroiridate (IV)," *Solar Energy*, **1993**, *51*, 409-414.
- [6] Gupta, A. K.; Parker, R. Z.; Keefer, C. E.; Hanrahan, R. J. "Gas phase formation of hydrogen chloride by a solar-driven chlorine-steam reaction," *Int. J. Hydrogen Energy*, **1992**, *17*, 757-762.
- [7] Gupta, A. K.; Parker, R. Z.; Hanrahan, R. J. "Gas phase formation of hydrogen chloride by thermal driven chlorine steam reaction," *Int. J. Hydrogen Energy* **1991**, *16*, 677-682.
- [8] Lopez, J. P.; Case, D. A. "Relativistic scattered wave calculations of hexachloro- and hexabromoiridate(IV)," *J. Chem. Phys.* **1984**, *81*, 4554-4563.
- [9] Adams, G. E.; Fielden, E. M.; Michael, B. D. "Fast processes in radiation chemistry and biology," John Wiley and Sons, 1973.
- [10] Buxton, G. V.; Sellers, R. M. "The radiation chemistry of metal ions in aqueous solution," *Coord. Chem. Rev.* **1977**, *22*, 195-274.
- [11] Farhataziz; Rodgers, M. A. J. "Radiation chemistry, principles and applications," VCH Publishers, New York, NY, 1987.

- [12] Hoffman, M. Z.; Ross, A. B. "Bibliographies on radiation chemistry: IX. metal ions and complexes part A: cobalt, rhodium, iridium," *Radiat. Phys. Chem.* **1986**, *27*, 477-487.
- [13] Broszkiewicz, R. K. "Pulse radiolysis studies on complexes of iridium," *J. Chem. Soc. Dalton Trans.*, **1973**, 1799-1802.
- [14] Mills, G.; Henglein, A. "Radiation chemistry of  $\text{Na}_3\text{IrCl}_6$  solutions: catalyzed  $\text{H}_2$  formation by radicals and post irradiation reduction of  $\text{IrCl}_6^{3-}$  by Propanol-2," *Radiat. Phys. Chem.* **1985**, *26*, 391-399.
- [15] Adams, G. E.; Broszkiewicz, R. K.; Micheal, B. D. "Pulse radiolysis studies on stable and transient complexes of platinum," *Trans. Faraday Soc.* **1968**, *64*, 1256-1264.
- [16] Broszkiewicz, R. K. "Pulse radiolysis studies on chloro-complexes of hexabromoiridate(IV)," *Int. J. Radiat. Chem.* **1974**, *6*, 249-258.
- [17] Broszkiewicz, R. K. "Pulse radiolysis study on aquochlorocomplexes of Rh(III)," *Radiat. Phys. Chem.* **1977**, *10*, 1-5.
- [18] Broszkiewicz, R. K. "Redox reactions of  $\text{OsCl}_5(\text{H}_2\text{O})^-$  and  $\text{OsCl}_6^{2-}$ , a pulse radiolysis study," *Radiat. Phys. Chem.* **1977**, *10*, 303-307.
- [19] Broszkiewicz, R. K. "Redox reactions of  $\text{RuCl}_6^{3-}$  and  $\text{RuCl}_6^{2-}$ : a pulse radiolysis study," *Radiat. Phys. Chem.* **1980**, *15*, 133-138.
- [20] Li, Z.; Hanrahan, R. J. "Radiolytic oxidation as a measure of stability in solutions of hexachloroiridate(III)," *Radiochimica Acta* **1995**, *64*, 61-65.
- [21] Crawford, C. L.; Gholami, M. R.; Roberts, S. L.; Hanrahan, R. J. "A fast kinetic investigation of the redox chemistry of iridium chloride complexes using pulse radiolysis," *Radiat. Phys. Chem.* **1992**, *40*, 205-212.
- [22] Crawford, C. L. "The pulse radiolysis of sodium tetraphenylborate and sodium hexachloroiridate in aqueous solution," Ph.D. Dissertation, University of Florida, 1992. Available from University Microfilms, Ann Arbor, Michigan.
- [23] Hoag, C. M. "Pulse radiolysis of iridium bromide complexes: role of bromide competition," Master's Thesis, University of Florida, Gainesville, Florida, 1994.
- [24] Brown, R. L. "A computer program for solving systems of chemical rate equations," Document number NBSIR 76-1055, Institute of Materials Research, National Bureau of Standards in Washington, DC, 1976.
- [25] Matheson, M. S.; Rabani, J. "Pulse radiolysis of aqueous hydrogen solutions. I. rate constants for reaction of  $e_{aq}^-$  with itself and other transients. II. The interconvertibility of  $e_{aq}^-$  and  $\text{H}$ ," *J. Phys. Chem.* **1965**, *69*, 1324-1335.

- [26] Buxton, G. V.; Greenstock, C. L.; Hellman, W. P.; Ross, A. B. "Critical review of rate constants for reactions of hydrated electrons, hydrogen atoms and hydroxyl radicals ( $\cdot\text{OH}/\cdot\text{O}$ ) in aqueous solutions," *J. of Phys. Chem. Ref. Data*, **1988**, *17*, 513-886.
- [27] Felix, W. D.; Gall, B. L.; Dorfman, L. M. "Pulse radiolysis studies. IX. reactions of the ozonide ion in aqueous solution," *J. Phys. Chem.*, **1967**, *71*, 384-392.
- [28] Gordon, S.; Hart, E. J.; Matheson, M. S.; Rabani, J.; Thomas, J. K. "Reaction constants of the hydrated electron," *J. Am. Chem. Soc.*, **1963**, *85*, 1375-1377.
- [29] Pagsberg, P.; Christensen, H.; Rabani, J.; Nilsson, G.; Fenger, J.; Nielsen, S. O. "Far-ultraviolet spectra of hydrogen and hydroxyl radicals from pulse radiolysis of aqueous solution. Direct measurement of the rate of  $\text{H} + \text{H}$ ," *J. Phys. Chem.*, **1969**, *73*, 1029-1038.
- [30] Thomas, J. K. "Rates of reaction of the hydroxyl radical," *Trans. Faraday Soc.*, **1965**, *61*, 702-707.
- [31] Hart, E. J.; Anbar, M., "The hydrated electron," Wiley-Interscience, New York, New York, 1970.
- [32] Christensen, H.; Sehested, K.; Corfitzen, H. "Reactions of hydroxyl radicals with hydrogen peroxide at ambient and elevated temperatures," *J. Phys. Chem.* **1982**, *86*, 1588-1590.
- [33] Buxton, G. V. "Radiation chemistry of the liquid state: (1) water and homogeneous aqueous solutions," chapter 10 from "Radiation chemistry: Principles and applications," Farhat Aziz and Rodgers, M. A. J., eds., VCH, New York, New York, 1987.
- [34] Gordon, S.; Hart, E. J.; Thomas, J. K. "The ultraviolet spectra of transients produced in the radiolysis of aqueous solutions," *J. Phys. Chem.* **1964**, *68*, 1262-1264.
- [35] Thomas, J. K. "The rate constants for H atom reactions in aqueous solutions," *J. Phys. Chem.* **1963**, *67*, 2593-2595.
- [36] Sehested, K.; Rasmussen, O. L.; Gricke, H. "Rate constants of OH with  $\text{HO}_2$ ,  $\text{O}_2^-$ , and  $\text{H}_2\text{O}_2^+$  from hydrogen peroxide formation in pulse-irradiated oxygenated water," *J. Phys. Chem.* **1968**, *72*, 626-631.
- [37] Divisek, J.; Kastening, B. J. "Electrochemical generation and reactivity of the superoxide ion in aqueous solutions," *Electroanal. Chem. and Interfacial Electrochem.* **1975**, *65*, 603-621.
- [38] Christensen, H.; Sehested, K.; Logager, T. "Temperature dependence of the rate constant for reactions of hydrated electrons with H, OH and  $\text{H}_2\text{O}_2$ ," *Radiat. Phys. Chem.* **1994**, *43*, 527-531.



- [39] Rabani, J.; Matheson, M. S. "The pulse radiolysis of aqueous solutions of potassium ferrocyanide," *J. Phys. Chem.* **1966**, *70*, 761-769.
- [40] Christensen, H.; Sehested, K.; Bjergbakke, E. "Radiolysis of reactor water: reaction of OH radicals with  $O_2$ ," chapter 34 from "Water Chemistry of Nuclear Reactor System 5," Vol. 1, published for the British Nuclear Energy Society, Thomas Telford Limited, London, 1989.
- [41] Sehested, K.; Holcman, J.; Bjergbakke, E.; Hart, E. J. "Ultraviolet spectrum and decay of the ozonide ion radical,  $O_3^-$ , in strong alkaline solution," *J. Phys. Chem.* **1982**, *86*, 2066-2069.
- [42] Janata, E.; Schuler, R. H. "Rate constant for scavenging  $e_{aq}^-$  in  $N_2O$ -saturated solutions," *J. Phys. Chem.* **1982**, *86*, 2078-2084.
- [43] Matheson, M. S.; Mulac, W. A.; Weeks, J. L.; Rabani, J. "The pulse radiolysis of deaerated aqueous bromide solutions," *J. Phys. Chem.* **1966**, *70*, 2092-2099.
- [44] Zehavi, D.; Rabani, J. "The oxidation of aqueous bromide ions by hydroxyl radicals. A pulse radiolytic investigation," *J. Phys. Chem.* **1972**, *76*, 312-319.
- [45] Ruasse, M.; Aubard, J.; Galland, B.; Adenier, A. "Kinetic study of the fast halogen-trihalide ion equilibria in protic media by the raman-laser temperature-jump technique. A non-diffusion-controlled ion-molecule reaction," *J. Phys. Chem.* **1986**, *90*, 4382-4388.
- [46] Allen, A. O. "The Radiation Chemistry of Water and Aqueous Solutions," D. Van Nostrand Company, Inc., New York (1961).
- [47] Buxton, G. V. "Pulse radiolysis studies of aqueous solutions," chapter 17 from "Pulse Radiolysis," edited by Tabata, Y., CRC Press, Inc., Boca Raton, Florida, 1991.
- [48] Saito, E.; Belloni, J. "All-silica cell for pulse radiolysis studies of liquid crystals with low-energy (600 KeV) electrons," *Rev. Sci. Instrum.* **1976**, *47*, 629-630.
- [49] Durrum Instrument Corporation, "Operation and maintenance manual; Durrum stopped-flow spectrophotometer Model D-110," Durrum Instrument Corporation, Palo Alto, CA, 1972.
- [50] Kenney-Wallace, G. A.; Shaede, E. A.; Walker, D. C.; Wallace, S. C. "Nanosecond pulse radiolysis techniques for the study of liquids using a 600 keV Febetron," *Int. J. Radiat. Phys. Chem.* **1972**, *4*, 209-225.
- [51] Hewlett-Packard, "Model 706 System Instruction Manual," McMinnville Division, McMinnville, OR, 1969.

- [52] Chatterjee, A. "Interaction of ionising radiation with matter," chapter 1 from "Radiation chemistry: Principles and applications," Farhatziz and Rodgers, M. A. J., eds., VCH, New York, New York, 1987.
- [53] Buxton, G. V. "Basic radiation chemistry of liquid water," chapter 16 from "The study of fast processes and transient species by electron pulse radiolysis," edited by Baxendale, J. H., and Busi, F., D., Reidel Publishing Company, 1981.
- [54] Jonah, C. D.; Miller, J. R.; Matheson, M. S. "The reaction of the precursor of the hydrated electron with electron scavengers," *J. Phys. Chem.* **1977**, *81*, 1618-1622.
- [55] Draganic, I. G.; Draganic, Z. D. "The Radiation Chemistry of Water," Academic Press Inc., New York, 1971.
- [56] Schuler, R. H.; Hartzell, A. L.; Behar, B. "Track effects in radiation chemistry. Concentration dependence for the scavenging of OH by ferrocyanide in N<sub>2</sub>O-saturated aqueous solutions," *J. Phys. Chem.* **1981**, *85*, 192-199.
- [57] Kravtsov, V. I.; Tsventarnyi, E. G.; Chamaeva, N. B. "Influence of doubly-charged cations on the rate of aquation of hexabromo-complexes of iridium(III)," *Rus. J. Inorg. Chem.* **1971**, *16*, 1332-1334.
- [58] Dwyer, F. P.; McKenzie, H. A.; Nyholm, R. S. "The chemistry of bivalent and trivalent iridium. Part IV. The oxidation-reduction potential of the bromiridate-bromiridite system," *J. and Proc. Royal Soc. of New South Wales* **1947**, *81*, 216-220.
- [59] Melvin, W. S.; Haim, A. "Reductions of hexabromoiridate(IV) by chromium(II) and by pentacyanocobaltate(II). Evidence for bromide-bridged intermediates," *Inorg. Chem.* **1977**, *16*, 2016-2020.
- [60] DeFelippis, M. R.; Murthy, C. P.; Faraggi, M.; Klapper, M. H. "Pulse radiolytic measurement of redox potentials: The tyrosine and tryptophan radicals," *Biochemistry* **1989**, *28*, 4847-4853.
- [61] Fergusson, J. E.; Rankin, D. A. "The chloro and bromo complexes of iridium(III) and iridium(IV). I. Preparation," *Aust. J. Chem.* **1983**, *36*, 863-869.
- [62] Kravtsov, V. I.; Tsventarnyi, E. G.; Tsayun, G. P.; Yusupove, V. A. "Influence of the cations of the background on the rate of the aquation of hexachloro-complexes of tervalent iridium," *Rus. J. Inorg. Chem.* **1970**, *15*, 42-43.
- [63] Ramette, R. W.; and Palmer, D. A. "Thermodynamics of tri- and pentabromide anions in aqueous solution," *J. of Sol. Chem.* **1986**, *15*, 387-395.
- [64] Popov, A. I. "Polyhalogen complex ions," from "Halogen Chemistry," edited by Viktor Garmane, Vol. 1, Academic Press Inc., New York, 1967.

[65] Raphael, L. "The UV spectra of bromine, chlorine, and bromine chloride in aqueous solution," chapter 13 from, "Bromine Compounds," edited by Price, D., Iddon, B., and Wakefield, B. J., Elsevier, New York (1988).

[66] Pelizzetti, E.; Mentasti, E.; Pramauro, E. "Outer-sphere oxidation of ascorbic acid," *Inorg. Chem.* **1978**, *17*, 1181-1186.

[67] Scurlock, R. D.; Gilbert, D. D.; DeKorte, J. M. "Oxidation of ascorbic acid by aquopentabromoiridate (IV): An assessment of the effect of aquation on rates of oxidation by bromo- and chloroiridium (IV) complexes," *Inorg. Chem.* **1985**, *24*, 2393-2397.

[68] Mussini, T.; Longhi, P. "Bromine," chapter 3 from "Standard Potentials in Aqueous Solution," edited by Bard, A. J., Parsons, R., and Jordan, J., Marcel Dekker, Inc., New York and Basel, 1985.

[69] Malone, S. D.; Edicott, J. F. "The photochemical behavior of cobalt complexes containing macrocyclic ( $N_4$ ) ligands. Oxidation-reduction chemistry of dihalogen radical anions," *J. Phys. Chem.* **1972**, *76*, 2223-2229.

[70] Thornton, A. T.; Laurence, G. S. "Kinetics of oxidation of transition-metal ions by halogen radical anions. Part II. The oxidation of cobalt(II) by dichloride ions generated by flash photolysis," *J. Chem. Soc., Dalton Trans.* **1973**, *16*, 1632-1636.

[71] Henglein, A. "Energetics of reactions of  $O_{aq}^-$  and of  $O^-$ -transfer reactions between radicals," *Radiat. Phys. Chem.* **1980**, *15*, 151-158.

[72] Woodruff, W. H.; Margerum, D. W. "Thermochemical parameters of aqueous halogen radicals," *Inorg. Chem.* **1973**, *12*, 962-964.

[73] Surdhar, P. S.; Armstrong, D. A. "Redox potentials of some sulfur-containing radicals," *J. Phys. Chem.* **1980**, *90*, 5915-5917.

[74] Frank, A. J.; Graetzel, M.; Henglein, A.; Janata, E. "Kinetics of the heterogeneous electron transfer reaction of triplet pyrene in micelles to  $Br_2^-$  radicals in aqueous solution," *Int. J. Chem. Kinet.* **1976**, *8*, 817-824.

[75] Laurence, G. S.; Thornton, A. T. "Kinetics of oxidation of transition-metal ions by halogen radical anions. Part III. The oxidation of manganese (II) by dibromide and dichloride ions generated by flash photolysis," *J. Chem. Soc., Dalton Trans.* **1973**, *16*, 1637-1644.

[76] Nadezhdin, A.; Dunford, H. B. "Horseradish peroxidase. XXXIV. Oxidation of compound II to I by periodate and inorganic anion radicals," *Can. J. Biochem.* **1979**, *57*, 1080-1083.

- [77] Schwarz, H. A.; Dodson, R. W. "Equilibrium between hydroxyl radicals and thallium (III) and the oxidation potential of OH(aq)," *J. Phys. Chem.* **1984**, *88*, 3643-3647.
- [78] Von Sontag, C. "The Chemical Basis of Radiation Biology," Taylor and Francis, London, 1987
- [79] Benson, S. W. "The Foundations of Chemical Kinetics," McGraw-Hill Book Company, Inc., New York, 1960.
- [80] Weeks, J. L.; Rabani, J. "The pulse radiolysis of deaerated aqueous carbonate solution I. Transient optical spectrum and mechanism; II. pK for OH-radicals," *J. Phys. Chem.* **1966**, *70*, 2100-2106.
- [81] Behar, D.; Czapski, G.; Duchovny, I. "Carbonate radical in flash photolysis and pulse radiolysis of aqueous carbonate solutions," *J. Phys. Chem.* **1970**, *74*, 2206-2210.
- [82] Eriksen, T. E.; Lind, J.; Merenyi, G. "On the acid-base equilibrium of the carbonate radical," *Radiat. Phys. Chem.* **1985**, *26*, 197-199.
- [83] Lilie, J.; Henglein, A.; Hanrahan, R. J. "O<sup>-</sup> transfer reactions of the carbonate radical anion," *Radiat. Phys. Chem.* **1978**, *11*, 225-227.
- [84] Laidler, K. J. "Chemical Kinetics," 3<sup>rd</sup> edition, HarperCollins Publishers, Inc., New York, NY, 1987.

## BIOGRAPHICAL SKETCH


Craig M. Hoag was born in the Dallas-Fort Worth area of Texas on February 26, 1960. He grew up near Denver, Colorado, graduating from Nederland High School in 1978.

He spent 3 years on tour of duty with the Marine Corps. For the majority of time while in the Marine Corps, he was assigned to Reconnaissance, from which special operations in support of the division were carried out; he was also assigned for a brief period of time to STA (Search, Target, Acquisition) platoon, where special operations in direct support at the battalion level were carried out. He received an honorable discharge in February, 1983.


After leaving the Marine Corps, Craig Hoag worked and attended college, earning a Bachelor of Science degree in chemistry from Metropolitan State College of Denver in May, 1990. In May, 1994, he received his Master's degree from the University of Florida, in Gainesville, Florida. The title of his Master's Thesis was "Pulse radiolysis of iridium bromide complexes: role of bromide competition." He then immediately began working on the research discussed in this document, attending graduate school at the University of Florida until the present time.

In 1998, he married Huong Thi Ngoc Phu. During the summer of 1999, his daughter, Windy Linh Hoag, was born. Finally, during the summer of 2000, he finished this work, graduating with a Doctorate of Philosophy from the University of Florida.

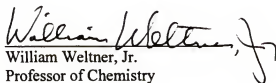
I certify that I have read this study and that in my opinion it conforms to acceptable standards of scholarly presentation and is fully adequate, in scope and quality, as a dissertation for the degree of Doctorate of Philosophy.

  
Robert J. Harrahan, Chairman  
Professor of Chemistry

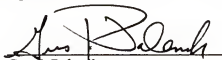
I certify that I have read this study and that in my opinion it conforms to acceptable standards of scholarly presentation and is fully adequate, in scope and quality, as a dissertation for the degree of Doctorate of Philosophy.

  
M. Luis Muga  
Professor of Chemistry

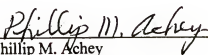
I certify that I have read this study and that in my opinion it conforms to acceptable standards of scholarly presentation and is fully adequate, in scope and quality, as a dissertation for the degree of Doctorate of Philosophy.

  
William Weltner, Jr.  
Professor of Chemistry

I certify that I have read this study and that in my opinion it conforms to acceptable standards of scholarly presentation and is fully adequate, in scope and quality, as a dissertation for the degree of Doctorate of Philosophy.

  
Gus J. Palenik  
Professor of Chemistry

I certify that I have read this study and that in my opinion it conforms to acceptable standards of scholarly presentation and is fully adequate, in scope and quality, as a dissertation for the degree of Doctorate of Philosophy.



Phillip M. Achey  
Professor of Microbiology  
and Cell Science

This dissertation was submitted to the Graduate Faculty of the College of Liberal Arts and Sciences and to the Graduate School and was accepted as partial fulfillment of the requirements for the degree of Doctorate of Philosophy.

August, 2000

---

Dean, Graduate School